OPTIMIZATION OF ADVANCED FILTER SYSTEMS

OPTION I PROGRAM - BENCH-SCALE TESTING
FOR THE RESOLUTION OF TECHNICAL ISSUES

FINAL REPORT

Reporting Period: August 20, 1997 - June 30, 2002

By

R. A. Newby, Program Manager
M. A. Alvin
G. J. Bruck
T. E. Lippert
E. E. Smeltzer
M. E. Stampahar

June 2002

DOE Award Number: DE-AC26-97FT33007

OPTIMIZATION OF ADVANCED FILTER SYSTEMS

OPTION I PROGRAM - BENCH-SCALE TESTING
FOR THE RESOLUTION OF TECHNICAL ISSUES

ABSTRACT

Two advanced, hot gas, barrier filter system concepts have been proposed by the Siemens Westinghouse Power Corporation to improve the reliability and availability of barrier filter systems in applications such as PFBC and IGCC power generation. The two hot gas, barrier filter system concepts, the inverted candle filter system and the sheet filter system, were the focus of bench-scale testing, data evaluations, and commercial cost evaluations to assess their feasibility as viable barrier filter systems.

The program results show that the inverted candle filter system has high potential to be a highly reliable, commercially successful, hot gas, barrier filter system. Some types of thin-walled, standard candle filter elements can be used directly as inverted candle filter elements, and the development of a new type of filter element is not a requirement of this technology. Six types of inverted candle filter elements were procured and assessed in the program in cold flow and high-temperature test campaigns. The thin-walled McDermott 610 CFCC inverted candle filter elements, and the thin-walled Pall iron aluminide inverted candle filter elements are the best candidates for demonstration of the technology. Although the capital cost of the inverted candle filter system is estimated to range from about 0 to 15% greater than the capital cost of the standard candle filter system, the operating cost and life-cycle cost of the inverted candle filter system is expected to be superior to that of the standard candle filter system. Improved hot gas, barrier filter system availability will result in improved overall power plant economics. The inverted candle filter system is recommended for continued development through larger-scale testing in a coal-fueled test facility, and inverted candle containment equipment has been fabricated and shipped to a gasifier development site for potential future testing.

Two types of sheet filter elements were procured and assessed in the program through cold flow and high-temperature testing. The Blasch, mullite-bonded alumina sheet filter element is the only candidate currently approaching qualification for demonstration, although this oxide-based, monolithic sheet filter element may be restricted to operating temperatures of 538°C (1000°F) or less. Many other types of ceramic and intermetallic sheet filter elements could be fabricated. The estimated capital cost of the sheet filter system is comparable to the capital cost of the standard candle filter system, although this cost estimate is very uncertain because the commercial price of sheet filter element manufacturing has not been established. The development of the sheet filter system could result in a higher reliability and availability than the standard candle filter system, but not as high as that of the inverted candle filter system. The sheet filter system has not reached the same level of development as the inverted candle filter system, and it will require more design development, filter element fabrication development, small-scale testing and evaluation before larger-scale testing could be recommended.

TABLE OF CONTENTS

LIST OF TABLES

LIST OF FIGURES

1. INTRODUCTION

The current, state-of-the-art, barrier filter system for hot gas particulate removal is subject to several technical concerns relating to its effective use in pressurized fluidized bed combustion (PFBC) and integrated gasification combined cycle (IGCC) power generation applications. Two advanced, hot gas, barrier filter systems, the "inverted candle" filter system and the "sheet filter" filter system, have been proposed to overcome these technical concerns. The advanced concepts have been previously described and evaluated at a conceptual, commercial level during the Base Period for this program (Newby et al., 1998). In the Option I Phase of this program, the subject of this report, the two advanced, hot gas, barrier filters systems were evaluated through testing at bench scale to assess their feasibility and to resolve their technical issues. This introductory section describes the Siemens Westinghouse Power Corporation (SWPC) standard candle filter system features and identifies its major technical concerns. The introduction section also describes the two advanced, hot gas, barrier filter concepts that were the subject of testing in the Option I Program, it reviews the results and conclusions from the previously reported Base Program, and it defines the objectives and scope of the Option I, bench-scale test program.

1.1 STANDARD CANDLE HOT GAS FILTER SYSTEM DESCRIPTION

The SWPC commercial, standard candle, hot gas filter design, schematically shown in Figure 1.1, consists of stacked arrays of filter elements supported from a common tube sheet structure. In this design, the arrays are formed by attaching individual candle elements (Item 1) to a common plenum section (Item 2). All the dirty gas filtered through the candles comprising this single array is collected in the common plenum section and discharged through a pipe to the clean side of the tube sheet structure. Each array of filter elements is cleaned from a single pulse nozzle source. The individual plenum assemblies (or arrays) are stacked vertically from a common support structure (pipe), forming a filter cluster (Item 3). The individual clusters are supported from a common, high alloy, uncooled tube sheet structure and expansion assembly (Item 4) that spans the pressure vessel and divides the vessel into its "clean" and "dirty" gas sides. Each cluster attaches to the tube sheet structure by a specially designed split ring assembly. The cluster is free to expand downward at operating temperatures. The plenum discharge pipes ducting the filtered gas to the clean gas side of the tube sheet structure are contained within the cluster support pipe and terminate at the tube sheet. Each discharge pipe contains an eductor section. Separate pulse nozzles are positioned over each eductor section. The eductors assist pulse cleaning. During cleaning, the pulse gas is contained within and ducted down the discharge pipe and pressurizes the respective plenum section.

The plenum assembly and cluster (stacked plenums) form the basic modules needed for constructing large filter systems that meet utility power generation requirements. The scale-up approach is:
- Increasing plenum diameter (more filter elements per array),
- Increasing the number of plenums per cluster,
- Increasing the vessel diameter to hold more clusters.

In general, vessel diameter will be limited by the uncooled tube sheet structure and the desire to shop fabricate the pressure vessel.
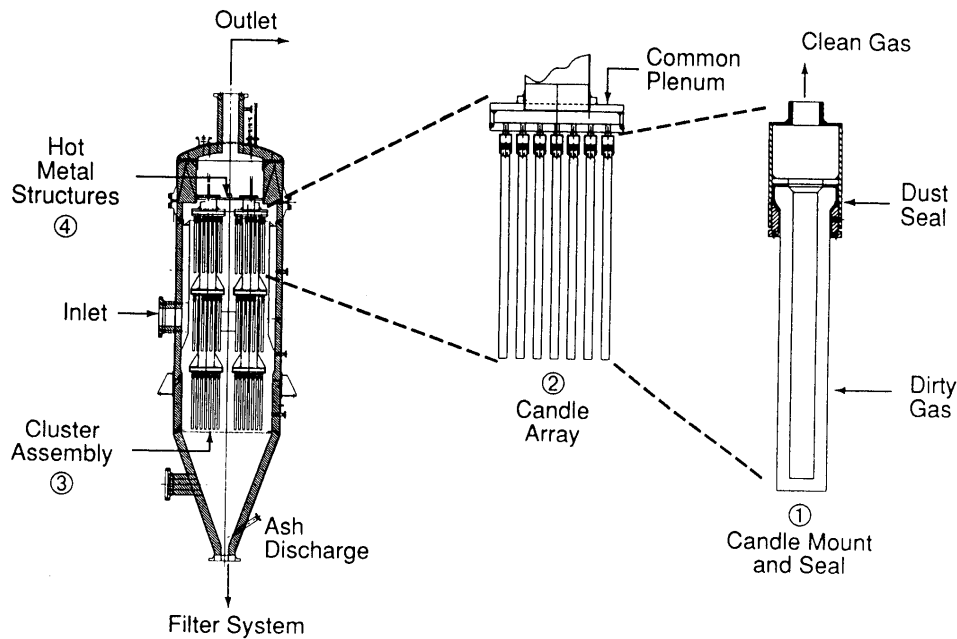
Figure 1.1 - SWPC Standard Candle Filter Cluster Configuration

Standard candle dimensions are used, 1.5 m length, 60 mm outer diameter, and wall thickness of 10 to 15 mm. A variety of ceramic candle materials are available or are under development. Clay-bonded silicon carbide (SiC) candle filters are commercially available. The structure of these candle elements is mainly a coarse-grained SiC bonded by a clay-based binder. Each element is provided with a fine grained SiC or aluminosilicate fiber outer skin that serves as the filtration surface.

Alternate, oxide-based ceramic materials are also being developed for barrier filter application. Candle filter elements have been constructed using a homogeneous structure that is an alumina/mullite matrix containing a small percentage of amorphous (glass) phase. Over the past several years, SWPC working with DOE and various suppliers, have helped to develop and qualify alternative, advanced ceramic filter materials and candle elements. This development has included both dense and lightweight monolithic, vapor infiltrated and Sol-Gel fiber reinforced and filament wound constructions. Laboratory and field evaluations of these and other materials are being conducted to identify, characterize and compare their respective chemical and thermal stability for IGCC and PFBC applications. The status of testing of commercial and advanced ceramic candle filters has been recently reviewed (Alvin et al., 1997; Alvin, 2001).

1.2 STANDARD CANDLE FILTER SYSTEM TECHNICAL CONCERNS

Potential technical concerns associated with the standard candle, hot gas filter system exist in several areas, many of which are sensitive to the nature of the feedstock and the application:

- Performance
  - pressure drop control
  - outlet dust penetration
  - pulse gas consumption
- Operating procedures
  - startup: heatup rate; residual carbon combustion; condensation; filter element deposits
  - shutdown: cooling rate; gas purge; residual carbon combustion; condensation, corrosion
- Reliability
  - filter element long-term properties degradation
  - filter element short-time failure (e.g., mechanical failure from ash bridging, from falling objects, from vibrations, or process upsets that cause severe thermal or flow excursions)
  - gasket degradation
  - degradation of uncooled metal structures
  - ash hopper drainage failure (ash hopper bridging or nozzle plug resulting from failed filter element)
  - ash handling system failure (conveyor equipment failure or jamming by failed filter element)
  - filter subsystem component failure (e.g., loss of pulse valves or pulse gas compressor)
- Availability
  - fail-safe device for minimum unscheduled shutdowns due to filter element leak
  - redundant critical component features (e.g., pulse valves and pulse gas compressor)
- Maintenance
  - easy access to filter elements
  - on-line access to critical subsystem components
- Cost Effectiveness
  - filter element costs (initial and replacement candles)
  - element support structure high alloy material costs
  - minimum number of shop fabricated, shop insulated, and road shippable pressure vessels
  - associated, connecting hot gas piping and ash handling systems
  - impact of filter system availability on power plant availability

Many of these concerns have been resolved through good engineering practice and innovation. Other concerns require the development of new features through testing and design evolution. The reliability concerns, and in particular, the filter element short-time reliability issues (e.g., mechanical failure from ash bridging, from falling objects, from vibrations, or process upsets that cause severe thermal or flow excursions) are ranked as the most critical, and represent the key focus of the Option I Program.

1.3 ADVANCED, HOT GAS BARRIER FILTER CONCEPTS

The results and experience gained from previous hot gas barrier filter laboratory studies and field testing form the basis for the two advanced, hot gas barrier filter system concepts and their testing approaches. Two advanced, hot gas barrier filter concepts are evaluated in this report that have the potential, in principle, to significantly mitigate the occurrence of short-term filter element failure events and improve filter system reliability. The advanced, hot gas barrier filter concepts are described here in terms of the geometric properties of their basic filter elements and the configuration of their support structures for the filter elements, and these are related to their potential performance advantages.

Filter Element Types

Two advanced, barrier filter element configurations have been conceived:

- "inverted candle" filter elements -- thin-walled, candle-like, elements using inside-surface filtering,
- "sheet" filter elements -- simple, flat-walled, filter elements.

The general features of these advanced filter elements are illustrated in Figure 1.2. The possible range of element dimensions are shown in the figure, and these dimensions have been treated as parameters in evaluations. The inverted candle filter elements are essentially standard candle elements that are operated in reverse, with dirty-gas flow into the candle bore, through the inside surface area, and with clean gas exiting through the larger, outside surface area. While inverted candle filter element lengths up to 2 m, and outer diameters (OD) to 110 mm have been considered, the standard candle filter element size (1.5 m long and 60 mm OD) is favored at this time because it is a commercially-available size. The inverted candle filter element may need an inside-surface membrane coating to prevent fine particle penetration into the filter matrix.

Sheet filter elements are relatively simple structures, being two, parallel flat plate filtering surfaces that are closed on the edges, except for one flanged edge. The filter element is designed to be rugged with respect to IGCC and PFBC environments. As shown in Figure 1.2, a large range of sheet filter element dimensions have been considered, but a basic 0.3 m by 0.3 m (1 ft by 1 ft) size is currently favored. This results in a sheet filter element surface area slightly smaller than a conventional candle filter element, but the sheet filter element design is very amiable to achieving very high surface area packaging. The use of lightweight ceramics and/or ceramic composites offers the potential for developing light-weight sheet elements that enhance economics and maintainability. The details of the sheet filter element construction (materials, thicknesses, need for internal ribs) were considered in this Option I Program.
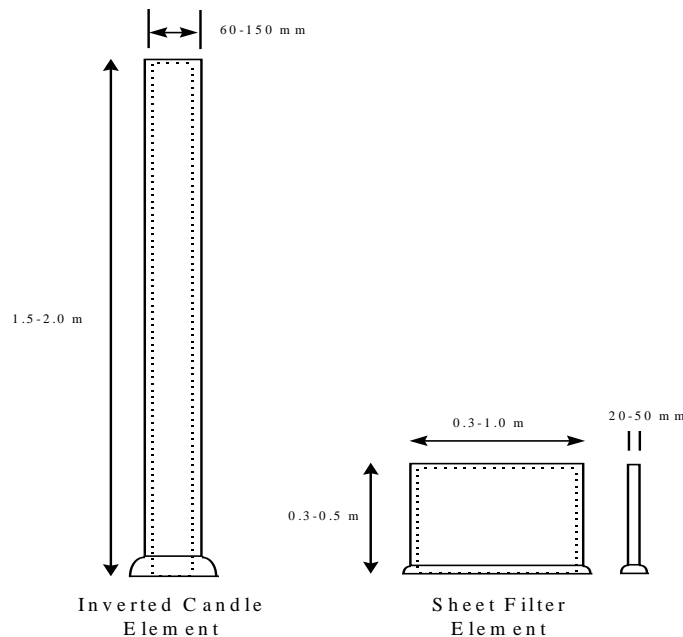
Figure 1.2 - Inverted Candle and Sheet Filter Element Geometries

The projected pressure drop behavior of standard candles, inverted candle filter elements, sheet filter elements, and two types of channel filter elements are shown in Figure 1.3. These projections have resulted from a SWPC model that has been established through laboratory and field data. The curves are for a typical, high-dust-loading condition and filter cake permeability representative of IGCC barrier filter systems, with all of the filter elements operating with the same face velocity of 2.4 cm/sec (4.8 ft/min). The face velocity is based on the filter element surface area in contact with the dirty gas. At these conditions, both cross-flow (Lippert et al., 1993) and CeraMem (Bishop and Raskin, 1996) channel filter designs show an asymptotic pressure drop behavior that would be unacceptable in practice. Acceptable pressure drop behavior can be achieved with both the inverted candle and the sheet filter element concepts.

The channel filter elements, having channel dimensions that are comparable to typical filter cake thicknesses, show a dramatic pressure drop rise as the available gas flow channel decreases in size. They have, in some cases, exhibited unrecoverable channel plugging in laboratory and field testing. The channel elements have a minimum pulse cleaning frequency for any given set of conditions (face velocity and dust loading) based on their filling rate, and they must be pulse-cleaned at a higher rate than this minimum to maintain acceptable pressure drop. While channel filter elements offer a large surface area-to-volume ratio that suggests compact barrier filter systems, the reality of these elements is that: (1) the channels result in nonlinear increase in pressure drop as they accumulate filter cake, resulting in very high pressure drops and high pulse cleaning rates that require operating at low face velocity, and (2) the channels can not operate reliably with fly ashes that are prone to deposits or bridging.
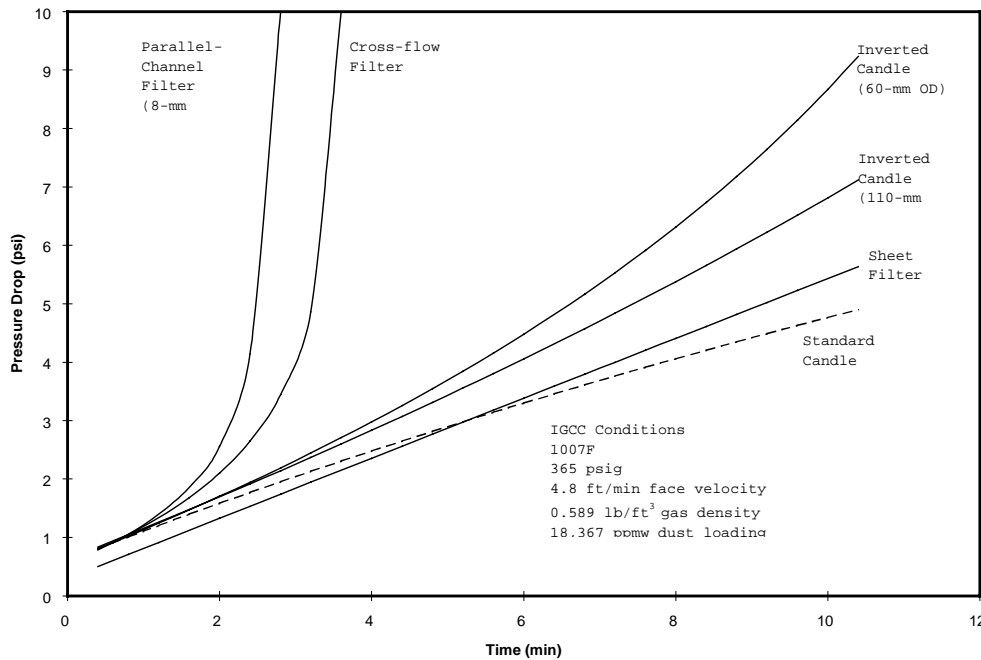
Figure 1.3 - Barrier Filter Element Pressure Drop Characteristics

The inverted candle filter element has a large bore relative to typical, maximum filter cake thickness, and ash plugging is not likely. The inverted candle filter element, though, builds a filter cake with decreasing gas-cake interface and increasing gas velocity through the cake as it thickens. This results in the accelerated pressure drop behavior shown in Figure 1.3. Thinner inverted candle filter element walls and larger bore diameters improve the pressure drop behavior.

The sheet filter element concept eliminates the accelerated pressure drop behavior and plugging potential of small flow channels, but it maintains a relatively high surface packaging potential. Its flat filtering surfaces result in a pressure drop characteristic close to that of the standard candle filter element.

Filter System Configuration Concepts

Filter element support-configuration concepts have been identified for each of the advanced ceramic filter elements that potentially provide excellent filter system reliability at competitive cost:

- The inverted candle filter elements are supported on a multi-plenum, cluster structure similar to that used for the SWPC standard candle filter elements, as shown in Figure 1.4
- The sheet filter elements are supported on a pipe-header structure, as shown in Figure 1.5.

In the inverted candle filter concept, dirty gas is filtered on the inside surface of each candle-type filter element. Each individual inverted candle filter element is contained in a metal housing that protects the filter element from cantilevered ash bridging and vibration. Each inverted candle filter element is fixed at the bottom end and guides are used to maintain the candle in fixed position within the housing. The holders are designed to allow removal of the inverted candle filter element from beneath the plenum, into the dirty-side of the vessel.
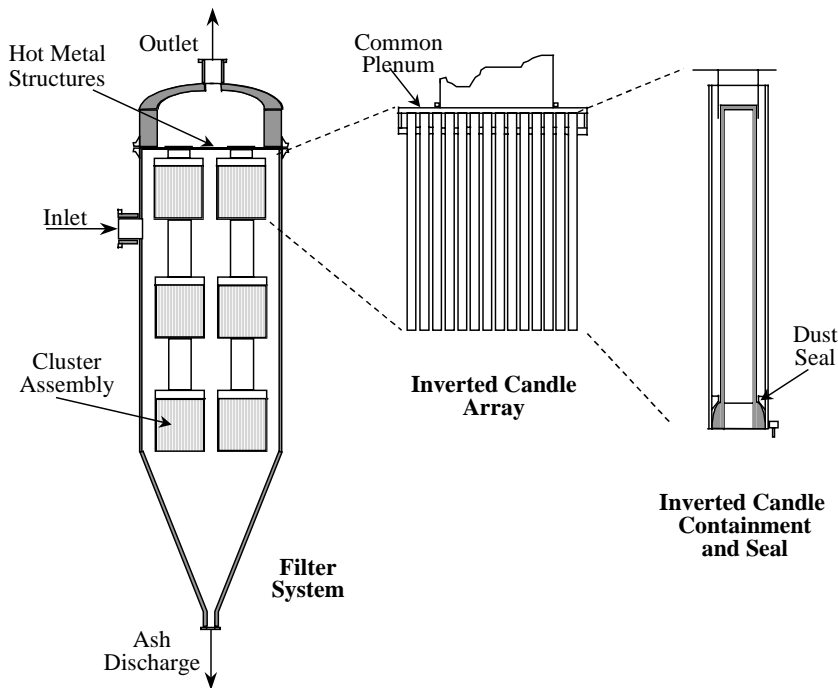
Figure 1.4 - Inverted Candle Filter System Configuration Concept

Two major advantages of this configuration are that all of the filter elements are directly accessible without removal of any equipment or neighboring filter elements, and they are free from the possibility of ash bridging and the potential damage caused by bridging. Because of this, the inverted candle filter elements may be as closely packed as is mechanically feasible.

Furthermore, with the inverted candle filter system concept, should an element crack or fail, it is almost certain to stay contained in its housing, possibly still providing partial filtering. The inverted candle filter elements cannot drop out of their position if they are fractured, so cannot damage other filter elements, plug the ash drain nozzle, or jam the ash removal system. The configuration is also more rugged to process upsets, like sudden excursions in inlet gas temperature or ash flow, or over-filling of the vessel with ash.

Based on the previous Base Program results, the key developmental aspects of the inverted candle filter system concept are to ensure cake pulse discharge (effective pulse cleaning) without plugging, and to demonstrate the durability of thin-walled filter elements, with inside membranes if needed. The capital cost of the inverted candle filter support structure may be higher than that of the standard candle filter support structure, but the life cycle cost of the inverted candle filter system should be superior.

The sheet filter system configuration concept is shown in Figure 1.5. The sheet filter elements are placed on parallel, vertical, clean-gas pipe manifolds, or clusters. The sheet filter elements are arranged to have uniform, face-to-face spacing, and to provide clear pathways for released ash agglomerates to drop to the vessel hopper. The opportunity for ash bridge formation is minimized by the unobstructed path for ash cake discharge. The parallel clusters in the filter vessel are arranged so that each sheet filter element is accessible for maintenance and inspection. The configuration is potentially compact, increasing the filtration surface area within a given filter vessel substantially above that of a conventional candle hot gas filter configuration.
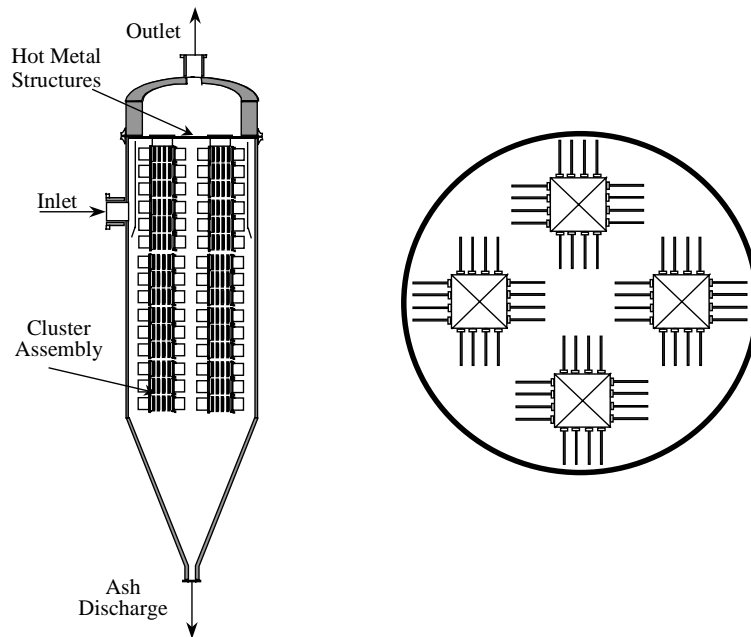
Figure 1.5 - Sheet Filter System Configuration Concept

The key development aspects of the sheet filter system concept are the demonstration of durable and leak-free sheet filter element and gasketing-holder designs, sheet filter element fixing to the plenum pipe so that it will not drop off if damaged, and the development of a packaging configuration that provides a reliable filter system with ease of maintenance. Both capital cost reduction and improved operating cost relative to the standard candle filter system should result.

1.4 BASE PROGRAM SUMMARY AND CONCLUSIONS

The Optimization of Advanced Filter Systems Base Program was conducted to conceptually evaluate the two advanced, hot gas, filter system designs. In the Base Program (Newby et al., 1998), SWPC developed conceptual designs of the two advanced barrier filter systems to assess their performance, availability and cost potential, and to identify technical issues that may hinder the commercialization of the technologies.

Two advanced, coal-fired power generation applications were considered in the evaluation: integrated gasification combined cycle (IGCC) and pressurized fluidized-bed combustion (PFBC). The specific IGCC and PFBC applications selected for the evaluation were those most challenging to the barrier filter systems. A 314 MWe, first-generation PFBC power plant, with barrier filter temperature of 871°C (1600°F) was selected because of its high volumetric gas flow and high operating temperature. A 406 MWe, air-blown, fluid bed gasification IGCC power plant having a barrier filter temperature of 542°C (1007°F) was selected because of its high volumetric fuel gas flow and high filter operating temperature compared to alternative IGCC fuel gas filtration conditions.

A well-defined design basis was established for the barrier filter systems. Barrier filter system operating conditions, design conditions, performance requirements, and design constraints were defined based on the advanced power plant needs and standard engineering practice. Cost premises were also selected. The scope of the barrier filter system equipment supply included the filter vessels, the filter elements, all of the filter vessel internals, the pulse gas control skids, and the pulse gas compressor skids. Costs were also estimated for the connecting hot gas piping, and the filter ash handling equipment (water-cooled screw conveyors and lock hoppers) to properly account for the overall cost and reliability impacts of multiple filter vessel systems.

Several assumptions were also developed and designated for the conceptual design activities, the key assumptions being:
- the PFBC and IGCC filter cake properties and behavior were selected from pilot test experience,
- the costs of the advanced filter elements were assumed to be identical to those of conventional ceramic candle elements on the basis of dollars per unit of dirty-side filter area,
- the advanced, barrier filter systems were assumed to function as configured: the inverted candle filter elements were assumed non-plugging, effectively pulse cleaned, and free from ash bridging; the sheet filter elements were assumed effectively pulse cleaned, free from ash bridging and mechanically/thermally stable and unable to drop from their positions.

8

A procedure was devised for estimating relative hot gas filter system reliability, and the reliability estimates were performed for operating conditions that were conducive to ash bridging and ceramic filter element failures in the standard candle, hot gas filter system.

PFBC Filter System Conclusions

The two advanced barrier filter systems evaluated for the PFBC application showed the potential to provide hot gas particulate removal with comparable operating performance (pressure drop, pulse cleaning frequency, pulse gas consumption) and slightly lower-to-comparable capital cost to the standard candle filter system. With difficult ashes that are prone to bridging, sintering, and poor vessel hopper flow, the advanced barrier filter systems have the potential for significantly improved filter system reliability and availability, with easier maintenance and lower operating costs.

The major parameters considered were the advanced filter element dimensions, alternative support arrangements for the filter elements, number of filter vessels and number of filter clusters in each vessel. In the PFBC application, inverted candle filter elements having wall-thickness of 5 mm, outer diameter of 60 mm, and lengths of 1.5 and 2.0 m were used. Inverted candle filter element cluster configurations with each inverted candle filter element enclosed in a container is favored due to its higher potential availability over housing all of the inverted candle elements in a single container. A single geometry for the sheet filter element was used, with a 0.3 m x 0.3 m (1 ft by 1 ft) sheet dimension and about 25 mm (1 inch) thickness. Larger sheet filter elements were found to have little cost benefit and are expected to be more difficult to manufacture.

The standard candle filter system cost was estimated to be about 10% of the projected, future, optimized PFBC power plant cost, a significant cost component of the PFBC power plant. The capital cost of the inverted candle filter system was estimated to be about 6% higher than the standard candle filter system. The inverted candle configuration using 2.0 m long inverted candle elements has the greatest cost-reduction potential. The sheet filter system evaluated had about a 5% capital cost advantage over the standard candle filter system. The advanced filter elements by themselves represented a cost of about 10-12% of the total capital cost of the advanced filter system.

The reliability and availability of the inverted candle filter systems are potentially much higher than that of the standard candle filter system, especially if difficult ashes that are prone to bridging, sintering, and poor vessel hopper flow are characteristic of the PFBC application. The sheet filter system potential availability is not expected to be quite as high as that of the inverted candle filter system. The potential improvements in the barrier filter system availability with the advanced barrier filter systems could have a great impact on the PFBC power plant performance and cost, depending on the availability performance of the other major components in the plant.

IGCC Filter System Conclusions

The two advanced barrier filter systems evaluated for IGCC application show the potential to provide hot gas particulate removal with comparable performance, but with comparable, to slightly higher, capital cost compared to the standard candle filter systems. With difficult ashes that are prone to bridging, and poor vessel hopper flow, the advanced barrier filter systems have the potential for significantly improved filter system availability and provide easier maintenance. In IGCC, the total capital cost of the standard candle filter system is a small

fraction of the projected, future, optimized power plant cost -- about 3% or less for the air-blown gasification case considered in this evaluation, and even lower for oxygen-blown gasification cases. The barrier filter system design emphasis should be placed on improved availability and ease of maintenance rather than on capital cost reduction.

The major parameters considered were the advanced filter element dimensions, alternative support arrangements for the filter elements, number of filter vessels and number of filter clusters in each vessel. In the IGCC application, inverted candle filter elements having wall-thickness of 5 mm, outer diameter of 60 mm and 110 mm, and lengths of 1.5 and 2.0 m were used. A larger-diameter inverted candle filter element was considered for the IGCC application because of the significantly lower permeability of the IGCC filter cake and the large impact of this on the maximum acceptable face velocity in the inverted candles. A single geometry for the sheet filter element was used, with a 0.3 m x 0.3 m (1 ft by 1 ft) sheet dimension and about 25 mm (1 inch) thickness, and a single sheet filter cluster design was defined.

The inverted candle filter system evaluated was comparable-to-higher in capital cost (0 to 23%) than the standard candle filter system. The inverted candle filter system using 2.0 m long inverted candles, has the greatest cost potential, being comparable in cost to the standard candle filter system. The sheet filter system evaluated has almost identical capital cost to the standard candle filter system.

The reliability and availability of the inverted candle filter systems are potentially much higher than that of the standard candle filter system, especially if difficult ashes that are prone to bridging, and poor vessel hopper flow are characteristic of the IGCC application. The sheet filter system availability is not quite as high as the inverted candle filter system. The potential improvements in the filter system availability with the advanced barrier filter systems could have a great impact on the IGCC power plant performance and cost depending on the availability of the other major components in the IGCC plant.

1.5 OPTION I PROGRAM OBJECTIVES AND SCOPE

In the Option I Program, "Bench-Scale Testing for the Resolution of Technical Issues", the subject of this report, development activities focussed on the key issues for the two advanced barrier filter concepts, the inverted candle and the sheet filter systems, that have been identified in the Base Program. The Option I Program consisted of engineering activities related to inverted candle filter element and sheet filter element design and manufacturing, seals and element fixing, fail-safe/regenerator adaptation to the advanced filter configurations. Testing focused on the advanced filter element key issues. The testing was conducted under simulated PFBC conditions, utilizing existing filter test facilities.

Filter element manufacturing is a key consideration in the development of advanced barrier filter concepts. Suppliers were identified and chosen based on both the particular ceramic/intermetallic matrix(s) they can process and on the actual process used. The manufacturing process must produce a product that meets the specified configuration requirements and is inspectable, reproducible and cost effective. Inverted candle filter elements that do not require an inside membrane can be manufactured by methods identical with those of standard candle filter elements, but the desirability of thin-walled inverted candle filter elements means that only selected materials and fabrication processes will be acceptable. The inverted candle filter element materials that require an inside membrane, and the sheet filter elements,

both require the development and qualification of new processing techniques. Suppliers capable of manufacturing the advanced filter elements and meeting specified requirements were identified for the Option 1 test program.

Key feasibility issues considered in the program, grouped into "engineering issues" and "performance issues subject to testing" are listed below. In the category of <u>engineering issues</u>:

Inverted candle filter element
- flange design and inside membrane skin specification,
- gasket and holder design,
- candle placement guide design located at candle tip,
- manufacturing feasibility and cost for inverted candle filter elements 60 mm OD; less than 5 mm wall thickness; 1.5 m and 2 m length, with inside membrane if needed,
- manufacturing feasibility and cost for large-diameter inverted candle filter elements, up to 110 mm OD; less than 10 mm wall thickness; 1.5 m length.

Sheet filter element
- sheet filter element body features (wall thickness, internal support ribs),
- sheet filter element durable flange design,
- gasket and holder design,
- fixture design to keep sheet filter "locked" in position if it fails,
- manufacturing feasibility and cost in a size expected to be acceptable, 0.3 m x 0.3 m (1 ft by 1 ft).

In the category of <u>performance issues subject to testing</u>:

Inverted candle filter element

- filtration and pulse cleaning performance,
- candle plugging and plug recovery performance,
- ash re-entrainment,
- filter element and gasket short-term durability,
- filter element self-sealing performance – that is, the ability of a fracture in the element to plug with dust.

Sheet filter element
- filtration and pulse cleaning performance,
- close-packed filter elements resistance to ash bridging,
- filter element and gasket short-term durability,
- ability of fixture to keep filter element locked in position if the element is damaged.

2. EXECUTIVE SUMMARY

Two advanced, hot gas, barrier filter concepts have been proposed by the Siemens Westinghouse Power Corporation to improve the reliability and availability of barrier filter systems in applications such as PFBC and IGCC power generation. The two hot gas, barrier filter concepts, the "inverted candle" filter system and the "sheet" filter system, were the focus of bench-scale testing, data evaluation, and commercial cost evaluation to assess their feasibility as viable barrier filter systems.

The inverted candle filter element is a standard candle operated in reverse, with dirty gas entering the bore of the candle. The inside surface acts as the filtering surface, and pulse gas periodically dislodges the filter cake from the candle bore as a jet of ash agglomerates. The inverted candle filter system configuration houses each inverted candle filter element within a metal containment pipe that isolates it and minimizes the effects of many hot gas filter failure modes. It is expected that the inverted candle filter system configuration has the potential to minimize forced outages resulting from ash bridging, filter element vibration, filter element elongation and deformation, cascading filter element damage, ash nozzle plugging, ash handling equipment damage, vessel ash overfilling, and various process upsets. The sheet filter element has a simple, flat-plate construction with one flanged end that may be easily manufactured. The sheet filter elements can be supported in a pipe-header cluster structure that provides compact packaging in a filter system. The sheet filter system is configured so that ash that is pulse dislodged from the sheet element surfaces has a clear drop path to fall to the vessel ash hopper, thus minimizing the possibility of ash bridging.

Six types of inverted candle filter elements were procured from various manufactures and their performance was assessed through cold flow and high-temperature test campaigns. Cold flow tests were performed with a set of three Coors inverted candles to observe the inverted candle pulse cleaning mechanism and to produce some basic inverted candle pressure drop data. Inverted candle filter test plenums were designed and fabricated to hold 4 inverted candles in a high-temperature, high-pressure filter test rig. All six types of inverted candle filter elements were tested in test runs conducted at temperatures ranging from 538 to 843°C (1000 to 1550°F). More than 300 hours of ash exposure time was accumulated in the test program, looking at pulse cleaning performance, short-term inverted candle durability, and observing the filter internals for evidence of ash bridging potential. Notably, the high-temperature testing showed that:

- increased operating temperature results in a reduction in residue permeability, and the need for more frequent pulse cleaning, this trend being identical for both inverted candles and standard candles,
- evidence of plugging of the inverted candle bore, or excessive ash re-entrainment was not found with the inverted candles,
- the inverted candles all were durable at the severe test conditions, except for the monolithic, oxide-based inverted candles (Coors and Ensto), which fractured,
- broken inverted candles were retained within their containment pipes, and the potential for cascading damage to other filter elements in the array was eliminated.

The test results were applied to make commercial cost estimates and overall feasibility evaluations for the inverted candle filter system in PFBC and IGCC applications. The thin-walled McDermott 610 CFCC inverted candle filter element would be the most suitable filter element for high-temperature PFBC application, while the thin-walled McDermott 610 CFCC,

12

and the Pall iron aluminide inverted candle filter elements could both be suitable for IGCC application. These filter elements could be manufactured in both 1.5 m and 2 m lengths.

For PFBC applications, the hot gas filter system cost is a substantial portion of the total plant cost, and it is desirable to minimize the hot gas filter capital investment. The use of inverted candles having 2-m length, coupled with the improved availability of the PFBC plant resulting from the inverted candle configuration, should improve the overall PFBC power plant cost-of-electricity significantly.

In IGCC, the barrier filter system cost is a relatively small portion of the total plant cost. Thus, in IGCC, the capital investment for the barrier filter system is not as sensitive a factor as it is in PFBC. Depending on the inverted candle filter element cost and the vessel maintenance configuration, the inverted candle filter system investment can be comparable to the standard candle filter system capital investment. The improved IGCC power plant availability of the inverted candle filter system will result in lower IGCC power plant cost-of-electricity.

Overall, the results show that the inverted candle filter system has high potential to be a reliable, commercially successful, hot gas, barrier filter system. It is recommended for continued development testing at a coal-fueled test facility. Fifty-five inverted candle containment pipes have been fabricated and shipped to the Southern Company Services, Power Systems Development Facility for testing with a developing, transport coal gasifier.

Two types of sheet filter elements were procured and assessed in the program through cold flow and high-temperature testing, Blasch, mullite-bonded alumina, and IF&P recrystallized SiC sheet filter elements. The IF&P recrystallized SiC sheet filter elements failed in cold flow testing and were deemed not suitable for application. About 150 ash-exposure hours at temperatures ranging from 538 to 760°C (1000 to 1400°F) were completed with the Blasch, mullite-bonded alumina sheet filter elements. The major conclusions from the testing are:
- the filter cake pulse cleaning performance is very good, with almost 100% pressure drop recovery at very low pulse intensities, with a significant reduction in pulse gas consumption compared to the standard candle filter system,
- the filter cake release phenomena appears relatively gentle and should be effective for limiting bridge formation that might result from released ash,
- testing with filter cake thickness up to 0.5-inches show no signs of bridge formation and results in no pulse cleaning difficulties,
- two broken Blasch sheet filters occurred during HTHP testing at 1400°F,
- flanges on all of the Blasch sheet filter elements subjected to 1400°F were cracked,
- pulse cleaning distribution on the plenums used in the high-temperature testing was found to favor the cleaning of the bottom element position at the low pulse gas supply pressures used.

The estimated capital cost of the sheet filter system is comparable to the capital cost of the standard candle filter system, although this cost estimate is very uncertain because the commercial price of sheet filter element manufacturing has not been established. The sheet filter system has the potential, in principle, to result in a higher reliability and availability than the standard candle filter system, but not as high as that of the inverted candle filter system. The sheet filter system has not reached the same level of development as the inverted candle filter system, and it will require significantly more design development, filter element fabrication development, and small-scale testing before larger-scale testing could be recommended.

3. INVERTED CANDLE HOT GAS FILTER

This section reviews the inverted candle hot gas filter engineering and test work completed in the program. It discusses the inverted candle filter element procurement activities, the hardware development and fabrication, the cold flow and high-temperature testing, and the test data evaluation and interpretation.

3.1 INVERTED CANDLE FILTER ELEMENT PROCUREMENT

Several candidate vendors for the supply of inverted candle filter elements were identified. The types of inverted candle filter element materials considered were oxide-based ceramics, non-oxide-based ceramics, and intermetallics. Discussions were held with the vendors to assess the manufacturing feasibility of the inverted candle filter elements in the sizes conceived:

- standard size: 60 mm OD with 1.5 m length,
- increased length: 60 mm OD with 2 m length,
- increased diameter: 110 mm OD with 1.5 m length,
- inside membrane, if required to make the filter media surface impermeable to fine particle penetration.

Inverted candle filter element specifications were prepared, including flange design and inside membrane skin specification, based on current experience with standard candle filter elements. Requests for cost-quotations were submitted to the eleven suppliers listed in Table 3.1 for production of 5 candle filter elements fabricated with a 60 mm OD, as well as a 110 mm OD. These were all of standard candle length (1.5 m long). It was understood from the Base Program evaluation that thin-walled inverted candle filter elements (wall thickness of 5 mm or less) were economically critical to the inverted candle hot gas filter system feasibility, but thicker-walled inverted candle filter elements were also procured for testing purposes.

Table 3.1 lists each vendor's candle filter element material, nominal wall thickness, and need for an inside membrane. Bids for the supply of inverted candle filter elements were received from all vendors except Specific Surface, who couldn't meet the specifications, and Schumacher.

Acceptable bids were received from, and orders were placed with, Ensto, IF&P, Pall (326 SiC and iron aluminide materials), and McDermott for 5, 60 mm OD inverted candle filter elements, and with Ensto for 5, 110 mm OD inverted candle filter elements. This selection provided a wide range of inverted candle filter element materials (alumina mullite, mullite-bonded alumina, recrystallized silicon carbide, clay-bonded silicon carbide, iron aluminide, and oxide-based CFCC), as well as a range of fabrication techniques and wall thicknesses. Only the McDermott 610 CFCC and the Pall iron aluminide inverted candle filter elements could be considered thin-walled. The set of 110 mm OD inverted candle filter elements were ordered from Ensto for the purpose of establishing fabrication feasibility, knowing that the test equipment fabricated for the high-temperature, high-pressure (HTHP) testing would not accommodate these larger filter elements. Five standard Coors alumina/mullite candles (60 mm OD, 40 mm ID, 1.5 m long) were also identified for the cold flow testing and for the initial high-temperature, high-pressure (HTHP) testing.

Table 3.1- Potential Inverted Candle Filter Element Vendors and Materials

Supplier	Matrix material	Nominal wall thickness (mm)	ID membrane required
Coors	P-100A-1 Alumina/Mullite	10	No
Ensto	Mullite-Bonded Alumina	10	No
Blasch	Mullite-Bonded Alumina	10	No
Specific Surface	Alumina	10	No
	Mullite		No
	Cordierite		No
	Iron Aluminide		No
IF&P	Recrystallized Silicon Carbide (REECER)	10	No
Pall	Clay Bonded Silicon Carbide 326	10	Yes
	Clay Bonded Silicon Carbide 181	10	Yes
	Iron Aluminide	2	No
Schumacher	Clay Bonded Silicon Carbide F20	10	Yes
Ultramet	CVI-SiC Reticulated Foam	10	Yes
Allied Signal Composites	Filament Wound PRD-66	7	Yes
Albany Int. Techniweave, Inc.	Oxide-Based CFCC	2	No
McDermott	Oxide-Based CFCC	5	No

After receipt, the inverted candle filter elements were inspected. Inspection comments are tabulated below, in Table 3.2. Room temperature gas flow resistance measurements were conducted on a maximum of two elements selected from each filter manufacturer's production lot. The gas flow resistance for the standard 60 mm OD, Pall FeAl, Pall 326 clay bonded silicon carbide, Coors P-100A-1 alumina/mullite, Ensto mullite-bonded alumina, McDermott 610 CFCC, and IF&P REECER recrystallized SiC filter elements, based on the ID filtration surface area, was generally less than 2.5 kPa (10 in-wg) at a face velocity of 0.05 m/s (10 ft/min), meeting the specification. In contrast, a significantly higher gas flow resistance of about 9.0 - 9.7 kPa (36-39 iwg), based on ID filtration surface area, was measured for the thicker-walled, 110 mm OD, Ensto mullite-bonded alumina inverted candle filter elements. This exceeds SWPC's gas flow resistance tolerance for as-manufactured candle filter elements. In addition, the Ensto 110 mm OD inverted candle filter element length was less than 1 m and its excessive thickness resulted in a very heavy filter element that would lead to difficult installation.

A photograph of the procured inverted candle filter elements is shown in Figure 3.1. The six standing candles are, from left to right, Pall iron aluminide, McDermott 610 oxide-based CFCC, IF&P (REECER) recrystallized SiC, Ensto mullite-bonded alumina (110 mm OD), another McDermott oxide-based CFCC, and Pall 326 clay-bonded SiC. The two inverted candle filter elements on their sides are an Ensto mullite-bonded alumina (110 mm OD), and a McDermott oxide-based CFCC element.

The inside diameters were measured for several of the procured inverted candle filter elements. The calculated wall thicknesses, based on a 60-mm outside diameter, are shown in Table 3.3.

Table 3.2 - Inverted Candle Filter Element Inspection Comments

IF&P REECER™ -- no ID membrane	• Acceptable installation of insert along flange ID, to accommodate gasketing and mounting • Calcine/firing material may be present along several areas of the filter body
McDermott -- no ID membrane	• Rough OD surface on all elements • One element has a small, dark defect area • Strong smell of acetone

Pall
  Clay Bonded SiC 326
    -- ID membrane coated
	• Very irregular top flange surface for sealing and mounting due to the inclusion of the ID membrane coating
	• No membrane coating applied to the OD surface

Iron Aluminide -- no ID membrane	• No comments

Ensto
  60 mm OD
    -- no ID membrane
	• Irregular OD surface (ripply) on the 60 mm OD elements
	• Some calcine/firing material along OD as remnant from high firing

110 mm OD -- ID membrane coated	• 110 mm OD elements < 1 m long • Bottom end cap OD — 108 mm (4-1/4 in) • Wall thickness 15 mm

Figure 3.1 - Procured Inverted Candle Filter Elements

Table 3.3 - Wall Thicknesses of Inverted Candle Filter Elements

Inverted candle type	Inside Diameter (mm)	Wall Thickness (mm)
Coors alumina-mullite	40.4	9.8
Ensto	36.4	11.8
McDermott 601 CFCC	49.6	5.2
Pall Clay-bonded SiC	38.9	10.6
IF&P Recrystallized SiC	43.1	8.4
Pall Iron Aluminide	55.4	2.3

The inverted candle filter element has geometry and manufacturing form closely related to the standard candle, and its manufacturing feasibility is not an issue. The larger diameter (110 mm OD) and longer (2 m) inverted candle filter elements have an uncertain manufacturing feasibility and require further development effort. The manufacturing feasibility of the inside membrane on the inverted candle filter elements is possibly the largest manufacturing issue for the 60 mm OD, 1.5 m long inverted candle filter elements, for those materials that require such a membrane. The McDermott 610 CFCC and Pall Iron Aluminide inverted candles have the greatest merits of all of the inverted candle filter elements -- the thinnest walls, no need for inside membrane, and best potential to manufacture at 2 m length.

3.2 INVERTED CANDLE TEST HARDWARE

The inverted candle filter element gasket and holder designs were reviewed based on standard candle filter experience. The design of the inverted candle containment pipe, placement guides and fail-safe regenerators were also conceptually evaluated. Confidence is high that the flange, gasketing, holder, and fail-safe designs for the inverted candle filter elements are a direct extrapolation of the techniques used for the conventional candle filter elements. An initial, general configuration for the inverted candle hardware, its gasketing, holder and fail-safe device was defined in the Base Program. This general configuration was applied in the Base Program evaluation and there is currently no indication that the general configuration proposed needs to be modified. A sketch of the inverted candle containment pipe showing the flanged top and bottom end is provided in Figure 3.2.
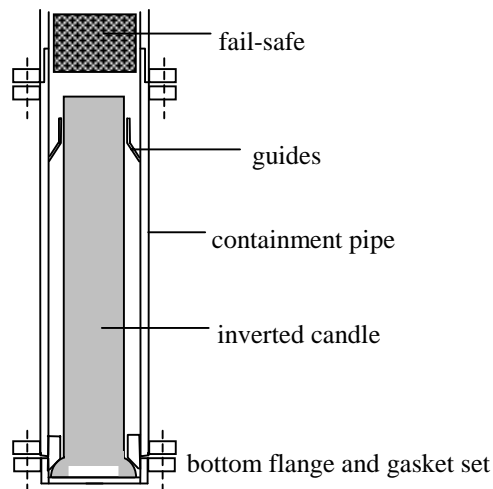
Figure 3.2 - Inverted Candle Containment Pipe and Holder Concept

The inverted candle hot gas filter commercial configuration might place a flange at the top of the containment pipe to allow inverted candle filter element insertion and removal by simultaneous removal of the containment pipe. Alternatively, there might be no top flange, with the containment pipe being welded to the plenum, and with inverted candle filter element removal from the bottom of the containment pipe only. Having the containment pipe with a top flange means less maintenance space is required in the vessel and the vessel will be shorter than in the case of the bottom withdrawal method. The top flange also means an additional set of nuts & bolts are required for each inverted candle filter element.

For the cold flow testing of the inverted candle filter elements, four inverted candle containment pipes had already been constructed prior to this contract for in-house testing. These four containment pipes were compatible for installation on the existing cold flow filter test unit, and could be used in the HTHP test unit, using conventional gasket sets. Fail-safe elements were not included in any of the inverted candle testing.

Two, new and independent plenums were needed to provide independent pulse cleaning of two sets of inverted candle filter elements for HTHP testing. These plenums were designed and fabricated with prototypic features and are pictured in Figure 3.3. The left photograph shows one of the plenums, with two pipe nozzles on the base to couple to a pair of inverted candle containment pipes, and a large nozzle on the top to couple to the vessel tube sheet. The photograph on the right is a view looking into the containment pipe nozzles. Sealing surfaces and gas discharge holes can be seen within each pipe nozzle.
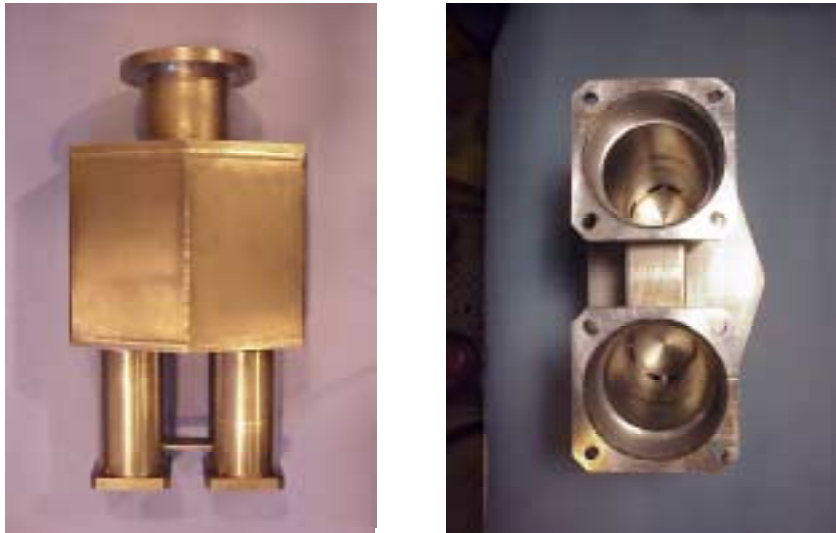
Figure 3.3 - Inverted Candle Plenum Hardware for HTHP Testing

As part of this program, a total of 55 of the inverted candle filter containment pipes have been fabricated and shipped to the Southern Company, Power System Development Facility (PSDF), in Wilsonville, Alabama. An inverted candle configuration will be tested at this site in the future, with the number of inverted candles installed on an existing SWPC filter cluster ranging from four, up to a full plenum of 55. The testing will subject the inverted candle configuration to a fuel gas generated by a pilot-scale, air-blown or oxygen-blown, transport gasifier and will complement the testing under oxidizing conditions that has been conducted in this program.

3.3 EXPERIMENTAL - INVERTED CANDLE COLD FLOW TEST

Test Program Objectives and Scope

A series of cold flow tests were conducted to visually observe inverted candle filter element ash accumulation and pulse cleaning phenomena, as well as to generate basic pressure drop data. The tests were conducted in an existing barrier filter, cold flow, Plexiglas test rig that had been previously used for both cross flow filter element and standard candle filter element cold flow testing. The test facility is pictured in Figure 3.4, showing the Plexiglas vessel, 79 cm (31 inch) ID, with 1.9 cm (3/4 inch) wall thickness, and 460 cm (15 ft) tall. The ash feed pressure vessel, the pulse cleaning system, and instrumentation and data acquisition equipment are also seen in the photo. A set of three Coors inverted candle filter elements (60 mm OD, 10 m wall thickness, 1.5 m long) were installed on the vessel tube sheet using the existing inverted candle holders and containment fixtures. The Coors inverted candle filter elements were the only inverted candles tested in the cold flow unit because procurement of the alternative inverted candles had not been completed at the time of this testing.

Figure 3.4 - The Inverted Candle Cold Flow Test Facility

The cold flow test conditions are displayed in Table 3.4. Two major test segments are identified: 1) tests focussed on the performance of 60 mm OD inverted candles, and 2) tests simulating the performance of 100 mm inner diameter (ID) inverted candle filter elements by

dimensionally-scaling 60 mm OD, 40 mm ID Coors inverted candle filter elements. The face velocities were selected to have relatively high values, >4.6 cm/s (9.1 ft/min) based on commercial studies reported in the Base Program final report. Variations in the trigger pressure drop and the pulse cleaning intensity were considered in the testing, with selected tests to also simulate a completely plugged inverted candle's ability to recover. Additional tests were performed in the test program, looking at pulse cleaning with no simultaneous gas "forward" flow, and testing standard candles for direct performance comparison with inverted candles. Most of the tests were performed with simultaneous pulsing of all three inverted candles, and efforts to modify the equipment for independent candle pulse cleaning were generally unsuccessful.

Table 3.4 - Inverted Candle Cold Flow Test Conditions

	60 mm OD, 40 mm ID, 1.5 m long inverted candles	Simulation of 100 mm ID, 1.5 m long inverted candles
Temperature, °C (°F)	21 (70)	21 (70)
Pressure, kPa (atm)	122 - 132 (1.2 - 1.3)	132 (1.3)
Filter type	Coors	Coors (with 60% of the ID surface blocked)
Number filters installed	3	3
Face velocity, cm/s (ft/min)	4.1 - 5.1 (8 - 10)	4.6 - 5.6 (9 - 11)
Filter bore inlet velocity, m/s (ft/s)	5.5 - 7.3 (18 - 24)	2.7 - 3.4 (9 - 11)
Gas flow, m^3/min (acfm)	1.3 - 1.6 (45 - 57)	0.60 - 0.7 (21 - 24)
Ash type	Karhula Lakeland	Karhula Lakeland
Ash flow, kg/hr (lb/hr)	1.8 - 2.7 (4 - 6)	1.8 - 2.7 (4 - 6)
Ash flow (ppmw)	13,000 - 25,000	31,000 - 55,000

Note the high inverted candle bore inlet velocity for the 60 mm OD candles. This high inlet velocity was a conceptual concern for the inverted candle performance since it could potentially hinder the cleaning pulse gas and/or could result in excessive ash re-entrainment. This was one of the performance issues focussed on with the cold flow testing.

Video records of selected pulse cleaning events were combined with pressure drop measurements to assess performance. Test parameters were the accumulated ash load in the candles, and the pulse cleaning intensity, as controlled by the pulse gas source pressure. A completely plugged inverted candle condition was also tested, and inverted candles were removed after ash loading in some runs, and weighed to determine their ash content. The uniformity and nature of the filter cake accumulation within the inverted candle was also observed in several test runs, there being a conceptual issue that the bore inlet region of the inverted candle might tend to preferentially plug.

The 100 mm ID inverted candle simulation tests were conducted to show the influence of the inverted candle "bore" inlet velocity on the pulse cleaning performance. The dimensional-scaling of the Coors, 40 mm ID inverted candles was done by stuffing cloth material into the candle bore to shut off the upper portion of the inverted candle filter element. This allowed

testing at the reference face velocity, with the appropriate bore inlet velocity, and L/D of a 100 mm ID inverted candle.

All of the tests used ash obtained from a Foster Wheeler PFBC test facility in Karhula, Finland, and this ash had been previously characterized in field filter tests and laboratory tests. The ash was generated in support of the Lakeland PFBC Clean Coal Demonstration Project using an Eastern Kentucky coal (Beach Fork) and a Florida Limestone (Gregg Mine).

Description of Testing

The cold flow inverted candle filter element testing runs were performed at the reference face velocity using the Karhula Lakeland filter ash. A range of inlet dust loadings were first tried, ranging from greater than 100,000 ppmw down to about 25,000 ppmw. Due to the large vessel free-space relative to the three inverted candles, and the fact that the gas and dust mixture was injected at a relatively high velocity, impinging on the ash shed structure, it is estimated that only about 20-25% of the inlet ash at the highest inlet loading was deposited on the inverted candle filtering surfaces. At the lower inlet ash loadings, this increased to about 50%. The lower rates were selected for continued testing because they resulted in less frequent refilling of the ash feed pressure vessel and more efficient use of the PFBC ash. Various modifications were made to the instrumentation and the equipment configuration to improve the system performance and the quality of the test data during the initial, trial testing.

Figure 3.5 shows a view of the interior of the cold flow filter vessel, looking through the Plexiglas wall. The three inverted candle containment pipes and a central flow pipe and dust shed are seen in the photo. The central flow pipe was not used for air flow in these tests, but it was left in the vessel because it did simulate the commercial internals geometry in the vessel.

Following the preliminary testing, a series of tests recorded the inverted candle pressure drop as a function of time, leading up to a total filter cake pressure drop of 7.5 - 10.0 kPa (30-40 iwg). After each filter cake accumulation, the ash feed was shut off and pulse cleaning was performed, starting at low pulse tank pressures, and increasing the pulse gas delivery pressure in subsequent runs. A forward gas flow was maintained during pulse cleaning in these tests, and all three of the inverted candles were pulsed simultaneously. Tank pressures of 345-517 kPa (50 and 75 psig) were tested, corresponding to relatively low pulse intensities. Pulse valve open times were set at 0.3 to 0.5 seconds during the tests. Two replicates of each test were also conducted to determine the repeatability of the tests. The inverted candle total pressure drop was found to increase linearly with time over the 7.5-10.0 kPa (30-40 iwg) filter cake DP range, not yet approaching the region where exponential pressure drop increase occurs. The filter cake maximum thicknesses during these tests were estimated to be about 0.5 cm (0.2 inch).

Pulsing at the low intensities resulted in only partial cleaning of the filter elements, and it was estimated that the maximum pulse air delivery rate to each filter element was about 0.023-0.036 kg (0.05 - 0.08 lb). The first pulse in each test resulted in about 65% pressure drop recovery, but this corresponded to an estimate of only 30% of the filter cake removal. A second pulse resulted in about 85% pressure drop recovery, with an estimated 50% of the remaining filter cake being removed. Little ash re-entrainment was observed on the first two pulses. Two subsequent pulses, used to reach a low pressure drop and clean filter condition for the following test, showed definite evidence of dust re-entrainment – visually, the ejected ash from the last two pulses formed a much dustier condition in the vessel, and the pressure drop record showed a rapid increase in pressure drop following the initial recovery.

Figure 3.5 - Cold Flow Vessel Interior

Visually, the pulse gas cleaning phenomena with simultaneous pulsing of all of the inverted candles, was seen as a transient jet of gas carrying entrained ash agglomerates that issued from each inverted candle bore and spread at a normal jet angle of about 30 degrees. This pulse flow completely stopped the forward flow of process gas through the filter vessel. The pulse gas velocity issued from the candle bore was 3 to 10 times the forward gas velocity into the bore. Following completion of the pulse event, with the forward gas flow still on, a rush of gas quickly entered the inverted candle bores to re-establish the forward flow through the filter elements. The extent of ash re-entrainment depended on the quantity of unagglomerated ash issued from the inverted candles during the pulse.

The testing was continued with increased pulse tank pressures up to about 862 kPa (125 psig), nearly the maximum capability of the facility. A test simulating "plugged" inverted candles was also conducted to measure the pulse cleaning behavior under these highly loaded conditions, with the inverted candle pressure drop being the maximum value the cold flow vessel could safely tolerate. A borescope inspection of a loaded inverted candle was attempted to observe the profile of the filter cake in the element. No indication of an ash cake restriction at the bore entrance was found, but it was difficult to see further into the bores.

Next, the "plugged" inverted candle testing was conducted. The cold flow filter, with the three Coors inverted candles, was operated with PFBC ash for a long time period, increasing the pressure drop up to the limit of the cold flow equipment, a value of about 28 kPa (4 psi)

22

candle pressure drop at a reduced gas flow rate. This condition represented an extreme in inverted candle filter system operation; equivalent to a loss in pulse cleaning capability with continued filter system operation. Following maximum loading of the inverted candles, the three inverted candles were removed from the vessel and from their enclosures to be visually examined, photographed and weighed. Examination showed that some ash leakage had occurred around the rubber gaskets on the inverted candle enclosures at these very high pressure drop conditions and these gaskets were improved for continued testing. These gasket leaks are expected to have had little impact on the previous test results.

Visually, the filter cakes looked slightly different in the entrance region of each inverted candle where ash impaction occurred under differing conditions depending on the inverted candle location relative to the vessel gas inlet. Several diameters up the inverted candle bores, the filter cakes assumed a common appearance. It appeared that a central "tunnel", having a diameter of about 1.3 cm (0.5 inch) ran the full length of each candle, with the filter cake thickness being about 1.3 cm (0.5 inch). The weight of ash accumulated on each inverted candle was almost identical at about 1.4 kg (3 lb), and the bulk density of the filter cake was estimated to be 640-800 kg/m^3 (40-50 lb/ft^3). The filter cake may have been compressed in the testing since previous bulk density estimates with this ash have been 480-560 kg/m^3 (30-35 lb/ft^3).

The candles were reinstalled in the cold flow rig for pulse cleaning to verify that recovery from this loaded condition could be achieved. The plugged inverted candles were pulse cleaned with a 862 kPa (125 psig) pulse source pressure, but without normal forward airflow during the pulse cleaning event. The pulse cleaning duration (the time that significant ash was seen being ejected from the inverted candle) was observed to continue for a relatively long period of time (on the order of 1-2 seconds). The inverted candles were removed and weighed, and it was found that more than 99% of the ash cake had been removed with a single pulse. Subsequently, the cleaned inverted candles were reinstalled, and pressure drop measurement showed that they had been cleaned extremely well with the single pulse. This test implied that ash re-entrainment carried with the forward gas flow into the inverted candle had been the reason that the prior series of pulse cleaning tests had taken 2 to 3 pulses for substantial cleaning. On the other hand, all of the inverted candles in the cold flow model were pulsed simultaneously with no bypass, and in a real filter system, only a portion of the inverted candles would be pulsed at any one time. Thus, the forward flow would be diverted to other elements and might make cleaning more effective than measured in the cold flow unit.

Some cold flow unit equipment modifications were made so that a single inverted candle could be pulse cleaned without simultaneous cleaning the neighboring inverted candles, so that pulse cleaning performance could be observed under more representative conditions. The tests conducted under this condition showed a definite improvement in the pulse cleaning performance of the inverted candle, although the neighboring inverted candles could not be pulse cleaned and repeated cycles resulted in heavy accumulation of ash and non-representative conditions. The inverted candles were again inspected to determine the internal ash distribution following a single pulse event. It was clear that the hot filter testing to be conducted in the future must incorporate the capability to pulse clean individual elements to achieve a representative simulation.

Since the effectiveness of the pulse gas cleaning system on the cold flow unit was not known, it was decided to also perform tests with three standard candles mounted in the same positions as the inverted candle filter elements and loaded with dust at the same gas flow rate. It was expected that pulsing the standard candles at the same pulse conditions as the inverted

candle filter elements would demonstrate if the pulse cleaning system or the inverted candle geometry was controlling the pulse cleaning behavior observed. Preparations were made to test the cold flow unit with three standard candles (the same three Coors candles) placed in the same locations. This provided a relative check on the pulse gas injection system and a relative measure of the pulse cleaning behavior of inverted candles (1.5 m long, 40 mm ID) and standard candles. Several cycles of ash accumulation and pulse cleaning of all of the standard candles were simultaneously performed. Cleaning was very effective and showed very little of the re-entrainment behavior observed with the inverted candles, although, as will be shown in Section 3.4, the pulse source pressure had a distinct impact on the pulse cleaning performance. This testing confirmed the effectiveness of the cold flow unit pulse cleaning equipment and provided a relative measure of the hindered pulse cleaning of inverted candles.

Next, the testing was focused on the simulation of the 1.5 m long, 100 mm ID candles. The Coors inverted candles were stuffed with material (rag) to the appropriate depth to block the upper 60% portion of the candle bores and provide the appropriate L/D-ratio. Inverted candle cold flow testing at the same face velocity and inlet dust loading as that completed earlier was performed, with all inverted candles pulsed simultaneously. The inverted candle bore inlet velocity was reduced by a factor of more than 2 under these conditions. Video recordings of some of the pulse cleaning events were made. The data suggests that imperfect pulse cleaning still persisted, though better than found for the 60 mm OD inverted candle testing. Re-entrainment of ash into the inverted candle, laying down a uniform cake layer, is evidently the cause of the imperfect cleaning.

Test data for a total 33 tests were recorded during these test campaigns, although several other tests were also conducted for preliminary planning, test data reproducibility evaluation, and general observations. All of the cold flow test data is compiled in Appendix A, and key performance factor calculations are listed.

3.4 RESULTS AND DISCUSSION - INTERPRETATION OF INVERTED CANDLE COLD FLOW TEST DATA

Quantitative assessment of the cold flow unit data collected from all of the inverted candle test runs was conducted and results are presented in Table 3.5. Three test segments are listing: 1) 3, 60 mm OD inverted candles simultaneously pulse cleaned and having a forward gas flow during pulse cleaning; 2) 3, 60 mm OD standard candles simultaneously pulse cleaned and having a forward gas flow during pulse cleaning; 3) 3, simulated, 100 mm ID inverted candles simultaneously pulse cleaned and having a forward gas flow during pulse cleaning. Results are not shown for tests CI-13 through CI-20, which were filter cake accumulation runs for the plugged inverted candle test. Results are also not listed for CI-21, which was an inverted candle test where pulse cleaning was performed without a simultaneous forward gas flow. The tabulated results show the test conditions and the pulse cleaning performance of the inverted candles (60 mm OD and 100 mm ID simulation) relative to standard candles.

The pulse cleaning test results are plotted in Figure 3.6, showing a clear trend. The first-pulse pressure recovery is plotted against the pulse gas source pressure for standard candles, for 60 mm OD inverted candles, and for 100 mm ID simulated inverted candles. Pulse source

Table 3.5 - Summary of Inverted Candle Cold Flow Testing

3, 60-mm Inverted Candles -- forward gas flow during pulse cleaning

Run number:	CI-1	CI-2	CI-3	CI-4	CI-5	CI-6	CI-7	CI-8	CI-9	CI-10	CI-11	CI-12	CI-22	CI-23
Maximum pressure drop (iwg):	39	42	41	53	51	51	51	52	53	86	54	74	58	56
Ash delivered to candle (lb):	1.9	1.9	1.9	1.8	2.1	2.6	2.4	2.4	2.3	1.6	4.9	2.1	2.5	2.4
Mean face velocity (ft/min):	9.6	9.6	9.6	9.4	9.5	9.5	9.5	9.5	9.4	9.2	9.4	9.2	8.9	9.5
Pulse pressure (psi):	50	50	50	75	75	75	100	100	100	100	125	125	125	125
Ash released on 1st pulse (% of total fed):	43.4	48.5	46.6	61.6	60.2	54.9	61.6	68.2	63.3	54.9	68.4	70.0	63.2	66.0
Ash released after 2nd pulse (% of total fed):	66.7	84.3	81.0	95.2	86.0	83.0	84.4	88.9	86.1	87.7	93.6	91.7	89.0	
Pressure recovery after 1st pulse (%):	48.4	53.3	51.6	67.5	66.3	61.3	67.5	73.4	69.1	66.6	73.8	77.5	69.5	71.6
Pressure recovery after 2nd pulse (%):	71.0	86.7	83.9	96.3	88.8	86.3	87.5	91.1	88.9	92.0	95.0	94.2	69.5	

3 Standard Candles -- forward gas flow during pulse cleaning

Run number:	CI-28	CI-29	CI-30
Maximum pressure drop (iwg):	58	58	58
Ash delivered to candle (lb):	9.6	10.0	11.0
Mean face velocity (ft/min):	6.3	5.8	5.6
Pulse pressure (psi):	50	75	100
Ash released on 1st pulse (% of total fed):	78.9	98.0	100.0
Ash released after 2nd pulse (% of total fed):	95.2	103.9	105.6
Pressure recovery after 1st pulse (%):	74.1	97.4	100.0
Pressure recovery after 2nd pulse (%):	93.8	105.3	107.7

3, 110-mm Inverted Candles -- forward gas flow during pulse cleaning

Run number:	CI-31	CI-32	CI-33
Maximum pressure drop (iwg):	63	62	60
Ash delivered to candle (lb):	0.9	0.9	0.9
Mean face velocity (ft/min):	10.3	10.4	10.6
Pulse pressure (psi):	75	100	100
Ash released on 1st pulse (% of total fed):	73.1	82.1	80.4
Ash released after 2nd pulse (% of total fed):	106.4		95.3
Pressure recovery after 1st pulse (%):	77.5	85.4	83.8
Pressure recovery after 2nd pulse (%):	105.0		95.0

pressures of 345, 517, 690, and 862 kPa (50, 75, 100, and 125 psig) were used in the cold flow testing. The standard candles cleaned fairly well even at the lower source pressures, requiring 517 kPa (75 psig) for effective pulse cleaning. The 60 mm OD inverted candles cleaned with greater difficulty due to ash re-entrainment, while the 100 mm ID inverted candles cleaned more effectively. Extrapolating the test data suggests that the 100 mm ID inverted candles would clean effectively in a single pulse with a source pressure of about 1200 kPa (175 psi) above the filter operating pressure, while the 60 mm OD inverted candles might require about 2068-2758 kPa (300-400 psi). The Siemens Westinghouse hot gas filter pulse pressure is typically set greater than 2758 kPa (400 psi) above the operating pressure, thus the inverted candle filter system pulse cleaning performance is expected to be acceptable at commercial conditions.

Each individual test is evaluated in each of the Appendix A tables (Tables A1 through A21). Here, test data are listed, assumed filter cake and filter element properties are listed, and performance calculations are used to extract performance parameters. In making these calculations for inverted candles, the following relationships have been applied:

- Filter radius = $r_f = d_i / 2 = (d_o - 2 t_w) / 2$

where d_i is the inverted candle inside diameter, d_o is the inverted candle outside diameter, and t_w is the inverted candle wall thickness.

- Air mass flow $= F_A = N_c \ A_{dc} \ U_f \ \rho$

where N_c is the number of inverted candles, A_{dc} is the dirty-side surface area of each inverted candle, U_f is the filter face velocity based on the dirty-side surface area, and ρ is the gas density.

- Air velocity into candle bore $= U_{cb} = A_{dc} \ U_f \ / \ [\pi \ r_f^2]$.

- Clean element pressure drop $= DP_c = U_f \ \mu \ r_f \ Ln\{(r_f + t_{w-})/ r_f \}/ [k_v \ g_c]$

where μ is the gas viscosity, k_v is the filter cake volumetric permeability, and g_c is the gravitational constant.

- Ash feed rate = $F_d = A \ / t_a$

where A is the mass of ash fed during the test, and t_a is the time of ash feeding during the test.

- Feed dust loading $= l_d = F_d \ / \ F_A$.

- Dust-to-filter element efficiency (%) $= \eta_f = m_d \ N_c \ 100 / A$

where m_d is the mass of ash loaded on the inverted candle before the initial pulse, as estimated in a following relationship.

- Effective dust loading $= l_{de} = l_d \ \eta_f \ / \ 100$.

- Loaded cake thickness $= t_c$

  $= (r_f - t_r) [1 - 1/ Exp\{(DP^* - DP^o) \ k_v \ g_c / [U_f \ \mu \ r_f] \}]$
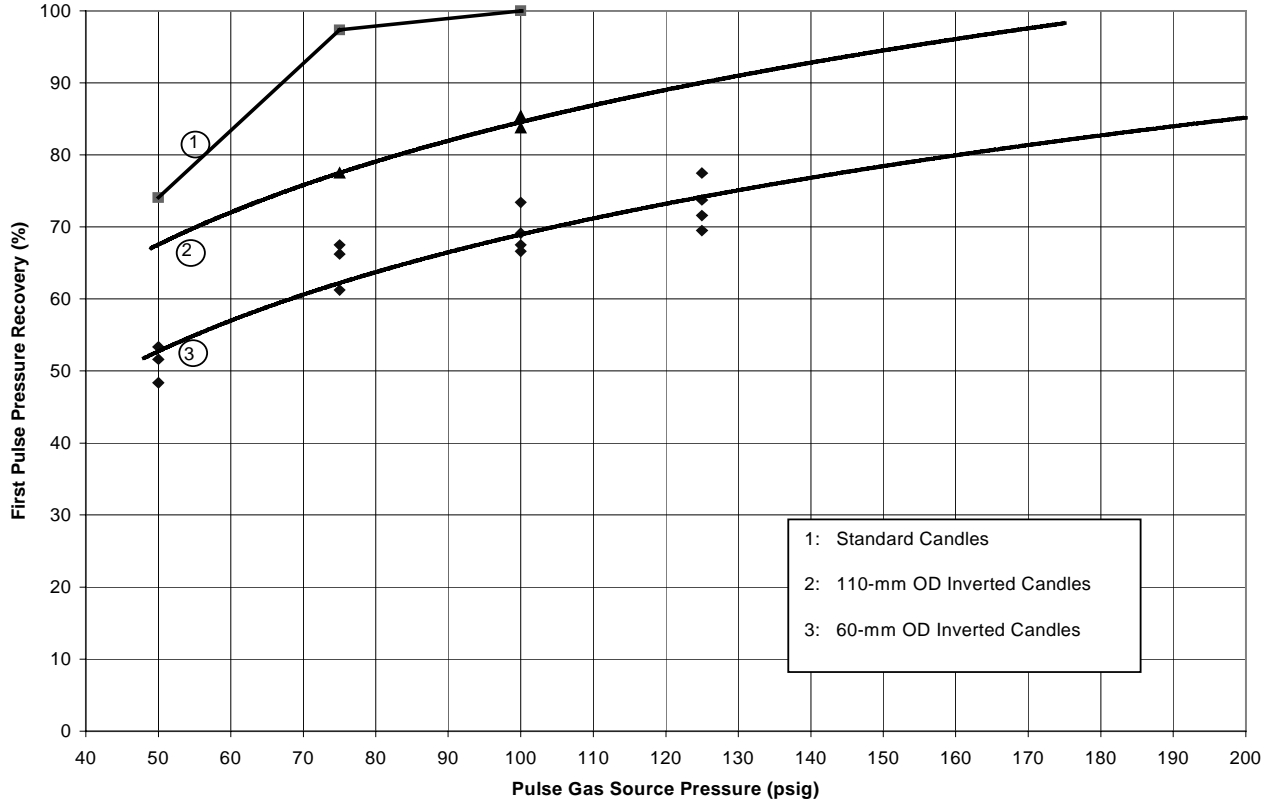
Figure 3.6 - Inverted Candle Cold Flow Pulse Cleaning Performance Results

where t_r is the thickness of the residual filter cake on the candle (as estimated in a following relationship), DP^* is the pressure drop across the loaded inverted candle, and DP^o is the pressure drop across the pulse-cleaned inverted candle.

- Loaded cake mass = $m_d = \pi \, L_f \; \rho_b \, [\; (r_f - t_r)^2 - (r_f - t_r - t_c)^2]$

where L_f is the length of the inverted candles, ρ_b is the filter cake bulk .

- Residue layer thickness = t_r

    = $r_f \, [1 - 1/\, Exp\{(DP^* - DP_c) \, k_{vr} \; g_c \, / \, [\; U_f \; \mu \; r_f \,] \; \} \;]$

where k_{vr} is the volumetric permeability of the residual cake layer.

- Fraction remaining cake removed = $f_r = (m_d^* - m_d^o) \, / \, m_d^*$

where m_d^* is the mass loading on a single candle when loaded, and m_d^o is the ash mass loading on the candle following a pulse cleaned event.

- Candle bore outlet pulse velocity = $U_{cb} = F_p \, \eta_p \, / \, [N_c \; t_v \; \pi \, (\, r_f - t_r - t_c)^2 \,]$

28

where F_p mass of pulse gas supplied by the pulse system, η_p is the efficiency of the pulse control system (mass of pulse gas supplied by the system over the mass of pulse gas delivered).

- Pulse face velocity = $U_{pf} = F_p\ \eta_p\ /\ [\ N_c\ t_v\ \rho\ A_{dc}\ 100]$

where t_v is the pulse valve open time.

- Cake pulse DP = DP_{cp}

  $= U_{pf}\ \mu\ r_f\ Ln\{(r_f - t_r)\ /\ (r_f - t_r - t_c\ )\}\ /\ [\ k_v\ g_c\ ]$

Tests with standard candles replacing the inverted candles have been characterized with the following relationships, showing only the relationships that differ from those above:

- $r_f\ =\ d_o\ /\ 2$,

- $t_c = (r_f + t_r\ )\ [\ Exp\{(DP^* - DP^o\ )\ k_v\ g_c\ /\ [\ U_f\ \mu\ r_f\ ]\ \}- 1\ ]$,

- $m_d = \pi\ L_f\ \rho_b\ [(r_f + t_r + t_c\ )^2 - (r_f + t_r\ )^2]$,

- $t_r\ =\ r_f\ [\ Exp\{(DP^* - DP^o\ )\ k_{vr}\ g_c\ /\ [\ U_f\ \mu\ r_f\ ]\ \}- 1\ ]$,

- $DP_{cp} =\ U_{pf}\ \mu\ r_f\ Ln\{(\ r_f + t_r + t_c\ )\ /\ (r_f + t_r)\ \}\ /\ [\ k_v\ g_c\ ]$.

Test data from low-pressure testing is difficult to assess quantitatively because the filter gas density is highly variable during a test -- the unit exhaust pressure is fixed and the pressure within the filter enclosure is a variable that changes with time as the pressure drop changes. In high-pressure environments, the gas density is nearly constant within the filter enclosure, independent of the filter pressure drop.

The inverted candle testing occurred at very high face velocities of 0.046-0.056 m/s (9-11 ft/min), with forward gas flow during the pulses, and with all of the inverted candles being pulsed simultaneously. It was shown in the testing that if the forward gas flow was shut off during the pulse cleaning, the inverted candles cleaned as effectively as standard candles, and if the candles were not pulsed simultaneously, they cleaned more effectively. Thus, the cleaning performance of the inverted candles is expected to be acceptable in practice.

The test results have been used to make high-pressure, PFBC commercial condition projections of pressure drop performance and these are shown in Figures 3.7 and 3.8. The figures considering 10 mm and 5 mm inverted candle wall thicknesses. Figure 3.7, showing the pressure drop behavior of inverted candles having 10 mm wall thickness, illustrates that the 60 mm OD inverted candle pressure drop starts to rise dramatically far earlier than with the 110 mm OD inverted candle. For example, with the standard candle being pulsed 2 times per hour, the 60 mm inverted candle must be pulse cleaned 4 times per hour and the 110 mm OD inverted candle must be pulsed 2.7 per hour, for the same pressure drop.

Figure 3.8 illustrates the significant performance improvement in reducing the 60 mm OD inverted candle wall thickness from 10 mm to 5 mm wall thickness. The improvement in the performance of the 110 mm OD inverted candle is, in contrast, smaller. Again, if the standard
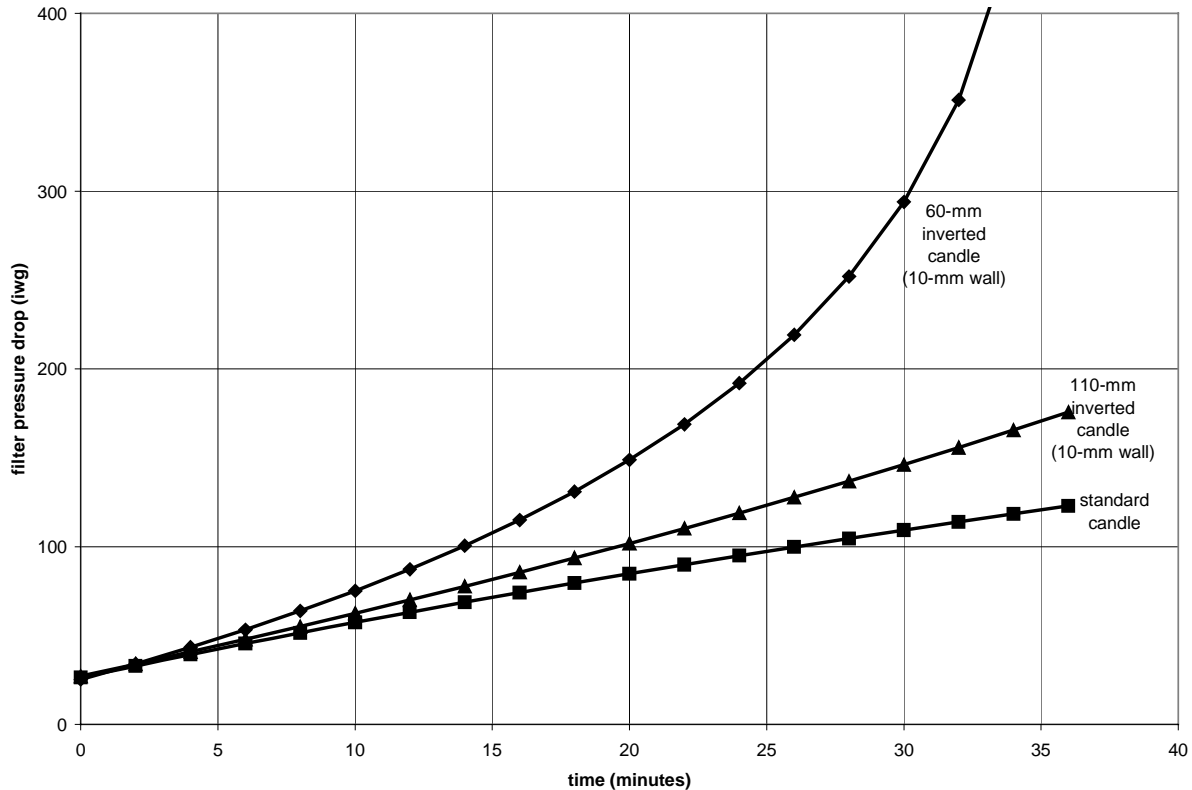
Figure 3.7 - Projected Inverted Candle Pressure Drop Performance with 10-mm Wall Thickness (conditions: face velocity 4.1 cm/s, dust loading 10,500 ppmw)

candle is pulse cleaned 2 times per hours, then the 60 mm inverted candle would be cleaned 2.9 times per hour and the 110 mm OD inverted candle would be pulsed 2.5 times per hour. Thus, there are four factors influencing the economic and performance feasibility of inverted candle filter system relative to standard candle filter system:

1) The number of inverted candles needed in a filter system to yield the same face velocity as in a standard candle system is d_o / d_i , where the inverted candles and standard candles have the same length.

2) Because of the constricting nature of ash accumulation in inverted candles, versus the expanding nature of the ash cake on standard candles, smaller inverted candle inner diameters results in higher pressure drops and more frequent pulse cleaning.

3) Larger diameter inverted candles will pack less effectively in a filter system than smaller diameter inverted candles, probably resulting in higher investment costs for larger diameter inverted candles.

4) The thickness of the inverted candle wall becomes less significant as the inverted candle diameter is increased.

The cold flow testing overall conclusions are:

- Thin-walled inverted candles, having wall thickness of 5 mm or less, are desirable when using 60 mm OD candles.

- It may be desirable for the inverted candle ID to be larger than 50 mm (as large as 90 to 100 mm), especially for IGCC applications where the filter cakes are less permeable, in order to reduce the pulse cleaning frequency and promote pulse cleaning effectiveness. This selection must be made based on the specific conditions and requirements of each application because of the cost impacts of packing effectiveness of larger diameter inverted candles.
- Walls less than 10 mm diameter are not needed for larger diameter, say 100 mm ID diameter inverted candles.
- Acceptable, single-pulse cleaning is expected for inverted candles when commercial pulse intensities are provided and when pulse cleaning is distributed among several independent plenums.
- Inverted candle plugging and excessive re-entrainment are not expected to be characteristic of inverted candle operation.
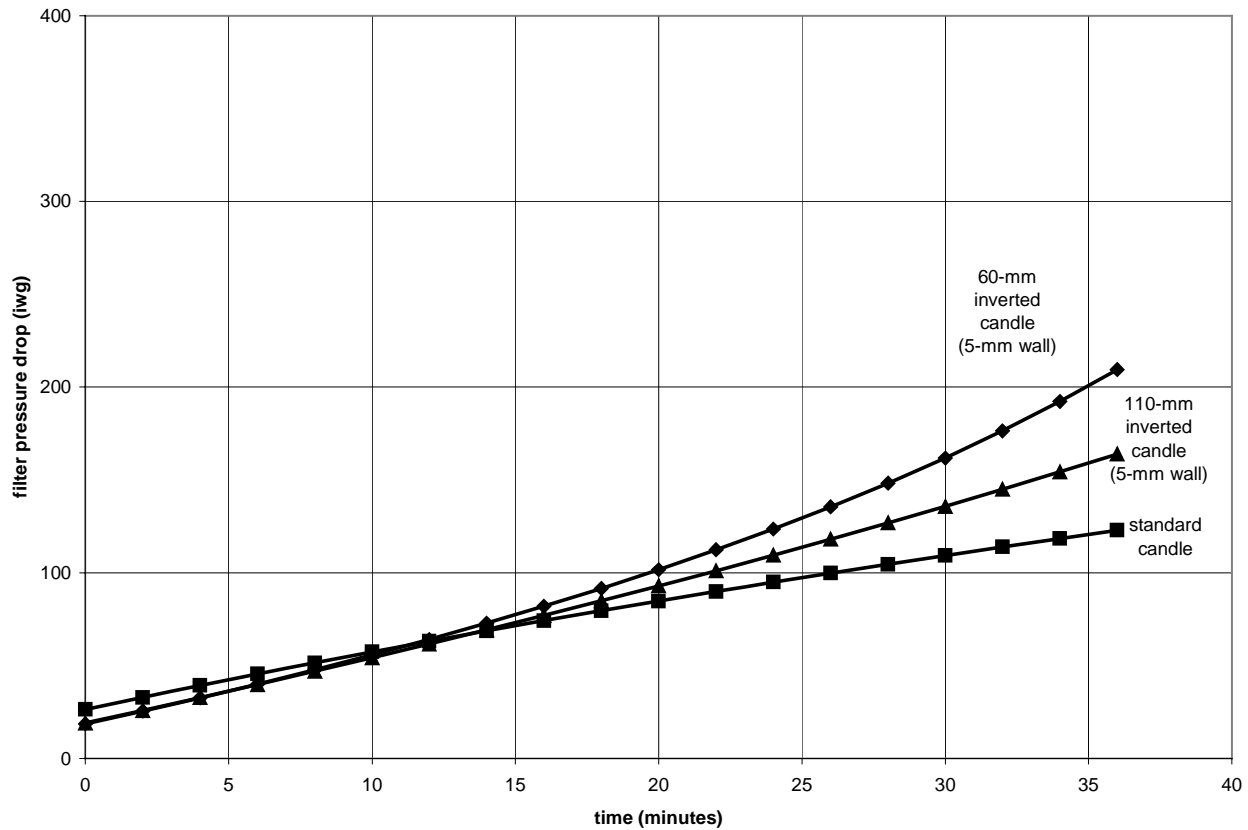
Figure 3.8 - Projected Inverted Candle Pressure Drop Performance with 5-mm Wall Thickness (conditions: face velocity 4.1 cm/s, dust loading 10,500 ppmw)

3.5 EXPERIMENTAL - INVERTED CANDLE HIGH-TEMPERATURE TESTS

In the bench-scale, high-temperature, high-pressure (HTHP) test program, the overall operating performance of the inverted candle filter system was assessed in terms of:

- filtration effectiveness of the inverted candle filter system,
- conditioned inverted candle filter element pressure drop,
- baseline pressure recovery,
- elimination of ash plugs within the bore of the inverted candle **filter element**s,
- pulse cleaning requirement (gas quantity and supply pressure),
- short-term durability of the filter body and flange (i.e., absence of crack formations; retention of the as-manufactured dimensional tolerances),
- reliability and durability of the gasket seal and mounting configuration,
- self-sealing, fail-safe capability of damaged inverted candle **filter element**s.

No post-test characterizations of the inverted candle filter element material strength were performed because the testing was of a short-term nature and did not represent materials tests so much as performance testing.

The HTHP test conditions are summarized in Table 3.6. A series of tests with the five sets of inverted candle filter elements procured were conducted in the modified HTHP barrier filter test rig. The tests were run primarily to address filtration performance for the inverted candles (pressure drop behavior, pulse cleaning performance, and operability). Much of the testing was performed at PFBC temperatures and with face velocities representative of commercial filter operation for economical PFBC application, about 4.6 - 5.1 cm/s (9 - 10 ft/min). Lower face velocities and temperatures, more representative of IGCC, were also included.

Simulation of 100 mm ID inverted candle filter elements performance was not addressed in the testing because in was conclusively dealt with in the cold flow testing and was difficult to perform in the HTHP testing. Since no vendor had been able, or willing, to fabricate a full-length, 110 mm OD inverted candle filter element (Ensto fabricated 110 mm OD inverted candles having less than 1 m length and having excessively thick walls), this test simulation would not have had significant purpose. Damaged inverted candle self-sealing performance was also considered in the testing through observation of broken candle performance when they occurred, but was not specifically simulated.

The outlet dust loading from the HTHP barrier filter test vessel was monitored by isokinetic outlet sampling during the testing to determine if any major ash leaks had developed during the testing. The outlet dust loading was also monitored to assess the self-sealing performance of damaged inverted candle filter elements.

The testing was carried out on a daily, 5-day per week, test schedule, starting up the unit in the morning, heating the unit until the test temperature and gas flow rate were achieved, and switching on the PFBC ash feed. Test data were collected during the remainder of the day, and the gas flow was switched off at the end of the day. The unit would remain warm overnight, but would cool thoroughly over a weekend.

Table 3.6 - Inverted Candle High-temperature Test Conditions

Temperature, °C (°F)	538 - 871 (1000-1600)
Pressure, kPa (psia)	1034 (150)
Filter types	6
Number of filter elements installed	4
Face velocity, cm/s (ft/min)	3 - 5 (6 - 10)
Bore inlet velocity, m/s (ft/s)	3.0 - 7.3 (10 - 24)
Gas flow, m^3/s (acfm)	1.6 - 2.2 (56 - 79)
Ash type	Karhula Lakeland
Ash flow, kg/hr (lb/hr)	About 0.9 (2)
Ash flow, ppmw	About 2,000 - 4,000
Pulse source pressure, kPa (psia)	1724 and 3447 (250 and 500)

The existing HTHP filter vessel tube sheet was adapted for two-plenum pulsing. The fabrication of two small plenums, each holding two inverted candles, was completed, and the plenums were installed in the HTHP test rig. Figure 3.9 shows the inverted candle plenums assembled in the tube sheet.

Figure 3.9 - Initial Installation of Inverted Candle Plenums

Four Coors inverted candles, used previously in the cold flow testing, were installed for initial shakedown of the unit. Figure 3.10 shows the plenums with the attached containment pipes holding the Coors inverted candle filter elements.

Figure 3.10 - Plenums with Inverted Candles Installed

Monitoring of the HTHP filter vessel outlet dust content indicated that a significant dust leak was present from the start of the test sampling, and only two cleaning cycles were completed before the test was halted. Inspection of the unit showed that a tube sheet weld had failed. The tube sheet was removed, a repair plan was formulated, and the tube sheet was repaired and re-installation into the HTHP unit.

The four Coors inverted candles were re-installed for continued shakedown testing. After a short test period, it was discovered that the water-cooled exhaust gas piping had developed a leak and a significant quantity of water had accumulated in the HTHP filter vessel during shutdown. The piping was disassembled and the water leak location was identified. A section of defective piping was removed and sent out for repair. The section was reinstalled and the unit readied for continued testing.

Final preparations were made for the continued inverted candle HTHP testing. Modifications were made to the pulse cleaning nozzles to improve pulse cleaning performance. The inverted candle HTHP rig internals were again installed. HTHP shakedown testing was continued with the Coors inverted candle filter elements that had been used earlier. The testing showed that the pulse cleaning system was functioning properly. The testing at high temperature, up to 843°C (1550°F) and with no fail-safe/regenerator in place was too severe for the monolithic, oxide-based Coors inverted candle filter elements and they all fractured. The fractured candle pieces were completely contained within the inverted candle containment pipes, as intended with the design to prevent collateral damage to other filter elements and plugging of the vessel ash drain, demonstrating this aspect of the inverted candle concept. Significant dust, though, did leak through the fractured filter elements, and they showed no tendency to self-seal.

IF&P Recrystallized SiC Inverted Candle Testing

Four of the IF&P recrystallized silicon carbide inverted candles were installed in the HTHP barrier filter test unit for testing of their pressure drop characteristics and pulse cleaning performance. The IF&P recrystallized SiC inverted candles had standard candle dimensions and a wall thickness of about 10 mm, yielding an inside surface area of only about 0.054 m^2 (1.9 ft^2) per candle. The test conditions were very uniform throughout the campaign and were representative of PFBC conditions, with a pressure of 1034 kPa (150 psia), a temperature of about 760-843°C (1500 to 1550°F), and a face velocity of 4.6 - 5 cm/s (9-10 ft/min), in an oxidizing gas atmosphere, using an injected PFBC flyash ("Lakeland" flyash).

Testing was conducted during eleven days. A total of about 47 hours of testing were completed (defined as the time ash was being fed to the HTHP unit). During the testing, a total of 70 cleaning pulses were performed. The total ash fed during the testing was about 41 kg (90 lb). A typical day of pressure drop measurements are shown in Figure 3.11. This was the ninth day of testing in the campaign.
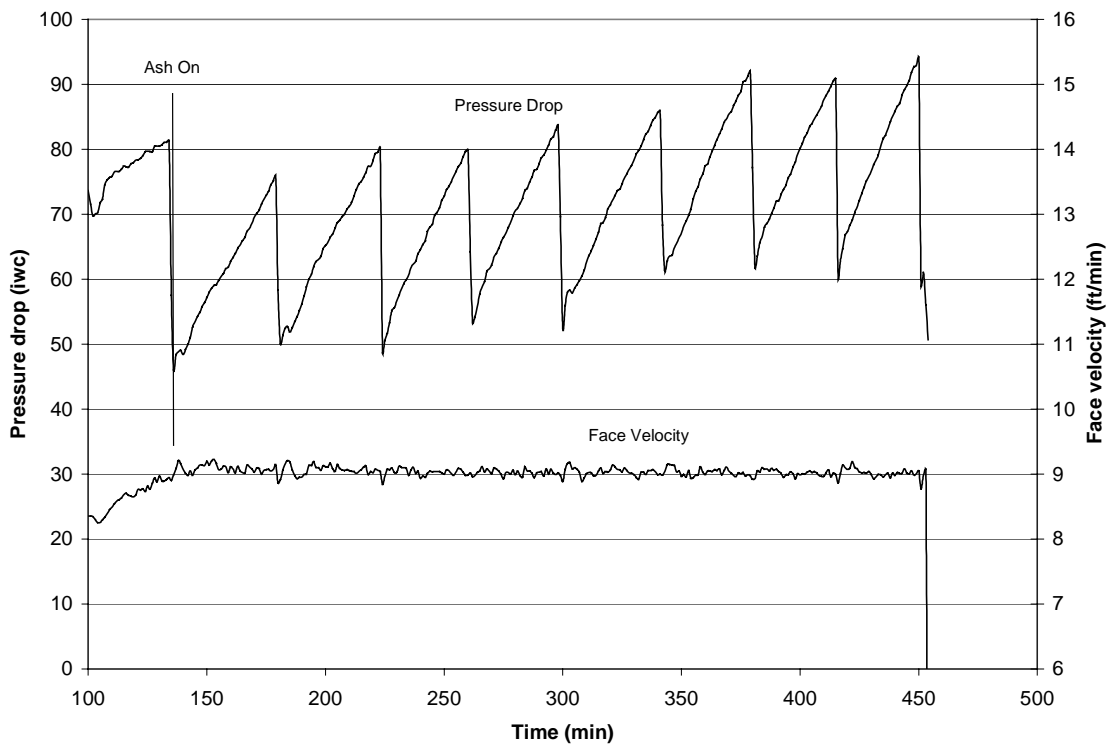
Figure 3.11 - IF&P Recrystallized SiC Inverted Candle Test Data for Day 6/29/2000

The time axis in Figure 3.11 represents the time from the start of the unit heating. The figure shows that during the unit startup, the pressure drop increases due to the deposition of carbon on the elements resulting from the combustion of natural gas into the cool vessel. An initial pulse cleaning is applied to eliminate this pressure drop buildup. This cleaning, plus the effects of overnight cooling, usually drops the filter pressure drop to a slightly lower level than existed at the end of the previous test day.

A series of eight pressure-drop rises, as ash accumulated on the inverted candle filter elements, and eight pressure-drop reduction spikes, as the candles are pulse cleaned, are seen on the figure. The face velocity is also plotted in the figure and is relatively uniform during the day, but tends to become slightly lower as the day progresses and the filter pressure drop increases. Typically, the trigger pressure drop and the baseline pressure drop increases during the test day, leveling out toward the days end.

In these tests, the trigger pressure drop was controlled to be about 7.5 kPa (30 iwg) above the baseline pressure drop. Over all of the IF&P recrystallized SiC inverted candle testing, the trigger pressure drop ranged from 448 to 710 kPa (65 to 103 iwg) and the baseline pressure drop ranged from 262 to 503 kPa (38 to 73 iwg). The general trend was for a gradual increase in the residual, baseline pressure drop over the test period.

All pulse cleaning was performed using a pulse source pressure of 250 psia, the highest that the facility could supply without using bottled air. Dust penetration monitoring during the tests showed very little dust leakage, indicating no inverted candle damage resulting from the severe thermal shock conditions, and no gasket degradation occurred.

Pall 326 SiC Inverted Candle Testing

A new set of 4 Pall 326 SiC inverted candle filter elements were inserted in the test unit for testing. Similar, relatively fixed, test conditions and the same testing procedures used for the IF&P recrystallized SiC inverted candles were used in the testing of the Pall 326 SiC inverted candle filter elements. Testing was conducted during seven days. A total of about 53 hours of testing were completed. During the testing, a total of 115 cleaning pulses were performed. The total ash fed during the testing was about 48 kg (105 lb). A typical day of testing pressure drop measurements are shown in Figure 3.12. This was the fourth day of testing in the campaign.

A series of nineteen pressure-drop rises, as ash accumulated on the inverted candles, and nineteen pressure-drop reduction spikes, as the candles were pulse cleaned, are seen on the figure. The face velocity is also shown in the figure and is relatively uniform during the day at about 5 cm/s (10 ft/min), but tends to become slightly lower as the day progresses and the filter pressure drop increases. Typically, the trigger pressure drop and the baseline pressure drop increases during the test day, leveling out toward the days end. Over all of the Pall 326 SiC testing, the trigger pressure drop ranged from 359 to 641 kPa (52 to 93 iwg) and the baseline pressure drop ranged from 165 to 483 kPa (24 to 70 iwg). All pulse cleaning was performed at a pulse source pressure of 1724 kPa (250 psia).

The test campaign proceeded with the Pall 326 SiC inverted candles, showing good pulse cleaning performance throughout, but with indications of a gradual increase in the residual, baseline pressure drop. Again, no dust leakage was detected.
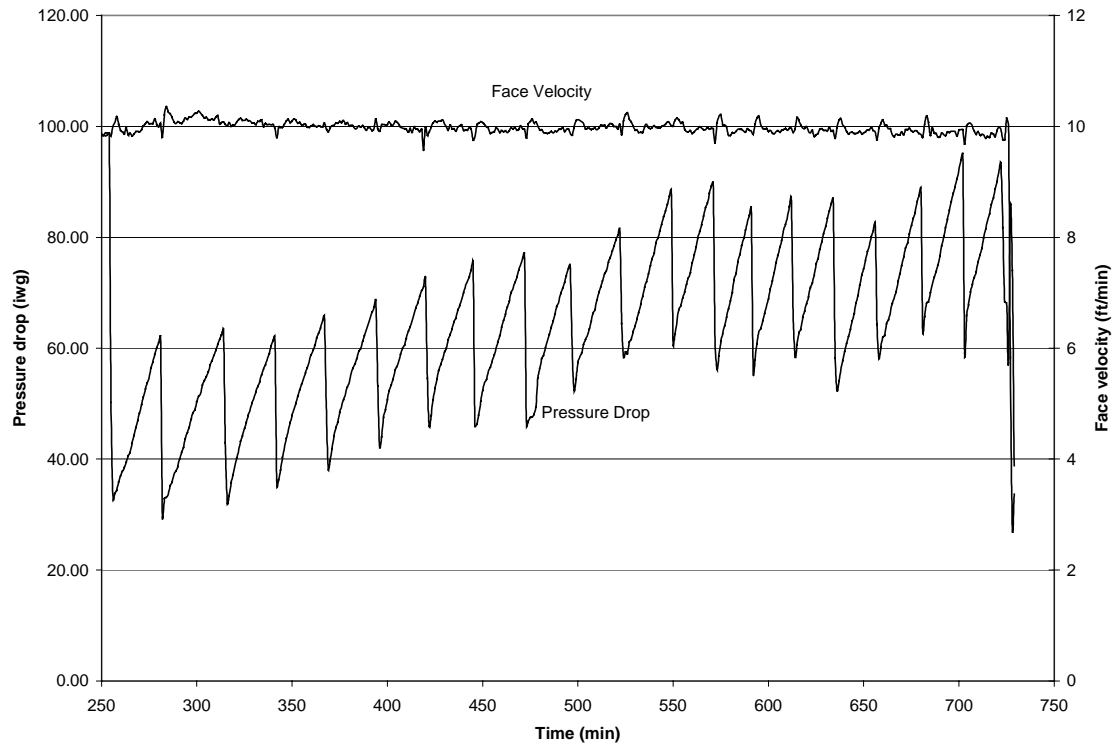
Figure 3.12 - Pall 326 SiC Inverted Candle Test Data for Day 8/03/2000

Ensto Mullite-bonded Alumina Inverted Candle Testing

Four of the Ensto mullite-bonded alumina inverted candle filter elements were installed for testing, following a sequence of testing similar to the last campaign. A P-bank of high-pressure air was installed in the pulse system to allow much higher pulse gas pressures to be used in these tests to see if the pulse cleaning performance of the inverted candles could be improved. The thermal shock exposure was very severe in these tests, with a 815°C (1500°F) operating temperature and no thermal regenerator to preheat the pulse gas. During the testing, all four of the Ensto mullite-bonded alumina candles fractured. Figure 3.13 pictures one of the fractured inverted candle filter elements. The cracking indicates that the pulse-induced thermal stresses contributed strongly to the failures. All of the inverted candle fractured material remained in the inverted candle containment pipes following the failures, demonstrating one benefit of the containment pipe. Dust leakage did occur following the fractures, and sufficient self-sealing behavior was not observed.

Figure 3.13 - Fractured ENSTO Inverted Candle

McDermott 610 CFCC Inverted Candle Testing

The McDermott 610 CFCC inverted candle filter elements were tested over a wide range of temperatures, gas flows and pulse cleaning pressures, in contrast to the previous test campaigns. The thin-walled McDermott inverted candle filter elements are representative of the actual construction needed for commercial inverted candle filter elements and they performed extremely well. Testing was conducted during seventeen, nonconsecutive days with the face velocity ranging from 3.3 - 4.8 cm/s (6.5 - 9.5 ft/min), and the vessel temperature ranging from 538-815°C (1000 to 1500°F). Pulse cleaning was conducted with pulse source pressures of 1724 and 3447 kPa (250 and 500 psia).

A total of more than 117 hours of testing were completed (defined as the time ash was being fed to the HTHP unit). During the testing, 94 cleaning pulses were performed. The total ash fed during the testing was about 109 kg (240 lb). The test data indicates that the McDermott inverted candle cleaning was very good, with the baseline pressure drop being recovered consistently, even when using the lower pulse cleaning pressure, until the gas temperature exceeded 760°C (1400°F). Above this temperature, the baseline pressure drop gradually increased with time. This is probably due to the sintering nature of the specific PFBC ash being tested.

Pall Iron Aluminide Inverted Candle Testing

The testing of the Pall iron aluminide (FeAl) inverted candle filter elements were completed, following a broad test sequence similar to that completed for the McDermott 610 CFCC inverted candle filter elements. Six test days were completed. Again, the thin-walled Pall FeAl inverted candles are representative of the actual construction needed for commercial inverted candles and their pulse cleaning performance was very good.

About 47 hours of test time were accumulated, with 41 pulse cleaning events. Two ranges of test conditions were conducted:

- 3.8 cm/s (7.5 ft/min) face velocity, with vessel temperature ranging from 788 to 815°C (1450 to 1500°F), and pulse cleaning pressures of 1724 and 3447 kPa (250 and 500 psia);
- 4.1 - 4.3 cm/s (8.0 - 8.5 ft/min) face velocity, with vessel temperature of 538-649°C (1000 to 1200°F), and pulse cleaning pressure of 1724 kPa (250 psia).

No dust leakage was detected during the testing. The Pall FeAl inverted candle filter elements would probably be limited to lower temperatures in commercial practice, such as those in IGCC of less than 538°C (1000°F).

Standard Candle Tests

A series of eight test points with standard, ceramic candle filter elements were performed to be used for direct comparison with the HTHP inverted candle tests. About 52 hours of test time was accumulated, with 24 pulse cleaning events. Two ranges of test conditions were conducted:

- 3.3 - 3.8 cm/s (6.5 - 7.5 ft/min) face velocity, with vessel temperature of 538 to 788°C (1000 to 1450°F), and pulse cleaning pressure of 1724 kPa (250 psia);

- 3. 3 cm/s (6.5 ft/min) face velocity, vessel temperature of 760 to 815°C (1400 to 1500°F), and pulse cleaning pressure of 3447 kPa (500 psia).

Inverted Candle Post Test Examinations

Following each testing sequence, the inverted candle filter array was inspected to assess the:

- evidence of potential ash bridges within either the inner bore of the candles, or within various locations of the plenum array,
- nature of dust cake remaining on the inverted candle filtration surface,
- durability and effectiveness of the gasket seals,.
- durability of the inverted candle body and flange sections.

In general, no potential ash bridging was found on the internals and the inverted candle filter element bores showed no signs of plugging. The nature of the ash cake in the bore of the inverted candles was much smoother and more uniform in appearance than the ash cakes seen on standard candle filter elements. The inverted candle filter elements should be completely free from phenomena such as "patchy" cleaning, "elephant feet", candle-to-candle bridges, elongation or bending seen by standard candle filter elements, and this was confirmed by the examinations. This reflects the nature of the pulse cleaning and the method of support seen by the respective filter element configurations. The inverted candle gasket seals performed very well, showing infrequent signs of ash leakage, and they should perform comparably to standard candle gaskets. The inverted candle filter elements, other than the monolithic, oxide-based ceramics as noted above, showed no cracking or elongation under these high-temperature, severe thermal shock test conditions. Some photographs illustrating these points are presented below.

Figure 3.14 shows the tube sheet and inverted candle internals being lifted from the pressure vessel following testing of the Pall FeAl inverted candles. Soft ash piles had accumulated on the bolt regions of the upper and lower flanges of each containment pipe. Thin, smooth layers of ash were attached to all of the vertical metal surfaces. No deformation of the metal containment pipes was found.

Figure 3.14 - Pall FeAl Inverted Candle Internals Following Testing

Photographs of typical inverted candle gaskets following testing are shown in Figures 3.15 and 3.16 for the Pall FeAl and McDermott inverted candles, respectively. They were quite free of ash, and were not degraded by the high-temperature, severe thermal shock exposures or mechanical stresses.

The IF&P recrystallized SiC inverted candle filter elements were removed from the HTHP rig following pulse cleaning of only one of the two plenums and the filter cakes were examined. The thin filter cakes in the candle bores from both plenums were uniform in thickness and slightly wavy over the whole length of the candles and were only slightly thicker and smoother in texture in the un-pulsed inverted candles. While the interior of the bore is difficult to photograph, Figure 3.17 pictures the entrance zone to an inverted candle, the first section being the metal flange, followed by the inlet of the candle bore with deposited ash cake.

The standard candle internals, being withdrawn from the vessel are shown in Figure 3.18. Soft ash was piled on the metal flange region that couples the standard candle filter element to the plenum, and thin, smooth ash layers were attached to vertical metal surfaces. The candles had typical PFBC ash cake appearance, with non-uniform thickness and texture, and regions of patches where the ash cake was very thin.

Figure 3.15 - Condition of Pall Inverted Candle Gaskets Following Testing

Figure 3.16 - Condition of McDermott Inverted Candle Gasket Following Testing

Figure 3.17 - Ash Cake on the Bore of an Inverted Candle Following Testing

Figure 3.18 - Standard Candles Following Testing

3.6 RESULTS AND DISCUSSION - INTERPRETATION OF INVERTED CANDLE HIGH-TEMPERATURE TESTING

The test results from the sub-scale, inverted candle filter system, the measured pressure drop and pulse cleaning performance, and the component durability observations, are assessed in this section. A direct way of assessing the inverted candle test filter system performance is by comparison with standard candle filter system performance measured under similar test conditions. The relative durability of the inverted candle filter elements and their associated components are also judged.

IF&P Recrystallized SiC Inverted Candle Testing

The test results for the IF&P inverted candle test filter system are summarized in four figures. The first, Figure 3.19, shows the residue pressure drop trend during the total test period, plotted as a function of the ash exposure time. The residue pressure drop is the difference in the baseline pressure drop following a pulse event and the "clean" filter element pressure drop that would exist at the test velocity and temperature. The residue pressure drop tendency is to rise during each test day, to level off during some days, and then to drop again before the next test day (this being due to overnight or weekend cooling and startup effects). The overall trend appears to be an increase in the residue pressure drop over the entire test period. The fact that all of this testing was at temperatures greater than 760°C (1400°F) and the pulse gas source pressure was only 1724 kPa (250 psia) probably contributed strongly to the behavior observed.

The second figure, Figure 3.20, shows the fraction of deposited ash removed during each pulse event, or the "pressure drop recovery". A pressure drop recovery, or "fraction of filter cake removed" of unity means that the baseline pressure drop after two successive pulse events were identical and all of the ash deposited was removed by the pulse. The pressure drop recovery jumps around significantly during the testing, ranging from 0.5 to 1.4, but the trend-line shows that the average pressure drop recovery ranges from 0.9 to 0.97 and is approaching unity more closely as the testing progresses. The trend line, having a value less than unity, but approaching unity with increased time, indicates a continual increase in residue pressure drop over the testing, but a trend toward a steady condition.

The third summarizing figure, Figure 3.21, shows the mass permeability of the filter cake over all of the testing and compares this to the average value of filter cake mass permeability extracted from previous PFBC testing at the Karhula facility. The mass permeability is defined as

$$k_m \ = \ \mu \ U \ m_c \ / \ DP_c$$

where μ is the gas viscosity, U is the filter face velocity, m_c is the mass of filter cake per unit area of the filter, and DP_c is the pressure drop across the filter cake. While the test permeability jumps around significantly during testing, it appears to be fairly representative of the Karhula value, which itself showed a large variation over the Karhula testing. Part of the fluctuation in the mass permeability results from the rough model that is used to represent the inverted candle filter element in this data evaluation, and does not adequately account for the gas velocity profile through the inverted candle filter cake. Another significant factor is that the flyash is periodically replaced in the feed vessel and may not be uniform in its properties over the entire test program.

The final summarizing figure for the IF&P recrystallized SiC inverted candles, Figure 3.22, plots the residue permeance over the tests. The residue permeance is defined as

$$K = \mu \, U \, / \, DP_R$$

where DP_R is the residue pressure drop. The temperature range over each day of testing is also indicated in the Figure. The residue permeance is a meaningful indicator of the buildup of flow resistance on the inverted candle filter elements, and it tends to decrease slightly over the duration of each test day, but only decreases slightly over all the tests.

Pall 326 SiC Inverted Candle Testing

The test results are summarized in four figures. The first, Figure 3.23, shows the residue pressure drop as a function of ash exposure time. In this figure, it is seen that the residue pressure drop tends to increase during each day of testing, but over all of the tests, it appears to get smaller. The Pall 326 SiC testing was at a slightly higher face velocity and higher temperatures than the IF&P recrystallized SiC testing. Comparing Figure 3.23 to Figure 3.19 indicates that the Pall 326 SiC inverted candle filter element residue pressure drop fell to lower values at the start of each test day, but rose more abruptly during each test day than did the IF&P recrystallized SiC inverted candle filter elements. The second figure, Figure 3.24, shows the fraction of deposited ash removed during each pulse event, or the pressure drop recovery. The pressure drop recovery jumps around significantly during the testing, ranging from 0.7 to 1.4, but the trend-line shows that the average pressure drop recovery is about 0.95 and is approaching unity more closely as the testing progresses.

The third summarizing figure, Figure 3.25, shows the mass permeability of the filter cake over all of the testing and compares this to the average value of filter cake mass permeability extracted from previous PFBC testing at the Karhula facility. The test permeability jumps around significantly during test testing, and it appears to be significantly lower than the Karhula value until the end of the test campaign.

The final summarizing figure, Figure 3.26, shows the residue permeance over the tests. The residue permeance is a meaningful indicator of the buildup of flow resistance in the inverted candle filter elements. In the Pall 326 SiC inverted candle testing, the residue permeance drops very abruptly over each test day, but it's minimum value also tends to increase slightly over these tests. It generally reaches a value somewhat higher than in the IF&P recyrstallized SiC inverted candle tests.

McDermott 610 CFCC Inverted Candle Testing

The test results are summarized in three figures. The first, Figure 3.27, shows the residue pressure drop as a function of ash exposure time. The mean operating conditions over each test period are also indicated (face velocity, temperature, pulse pressure) because the test conditions were much broader than in the previous tests. In this figure, it is seen that the residue pressure drop tends to increase slowly initially during the low temperature testing, but seems to accelerate as the temperature increases. The residue pressure drop is also seen to drop as the pulse pressure increases.

The second figure, Figure 3.28, shows the fraction of deposited ash removed during each pulse event, or the pressure drop recovery. The pressure drop recovery jumps around significantly during the testing, ranging from 0.6 to 1.4. No trend-line is shown because of the

great alteration in test conditions between each test day. The several initial test days show very good pressure drop recovery, but this performance falls as the temperature is increased and the pulse pressure is decreased.

The final summarizing figure, Figure 3.29, shows the residue permeance over the tests. The temperature range and pulse source pressure are indicated on the figure for each set of data points. A clear trend for lower residue permeance, as the gas temperature increases and as the pulse pressure decreases, is seen.

Pall Iron Aluminide Inverted Candle Testing

The test results are summarized in three figures. The first, Figure 3.30, shows the residue pressure drop as a function of ash exposure time. The mean operating conditions over each test period is also indicated (face velocity, temperature, pulse pressure) because the test conditions were broad and altered after each test period. In this figure, it is seen that the residue pressure drop tends to increase initially during the first, relatively high-temperature, testing period, but seems to accelerate in the second test period as the pulse pressure decreases. The residue pressure drop then falls in the last two low-temperature test periods.

The second figure, Figure 3.31, shows the fraction of deposited ash removed during each pulse event, or the pressure drop recovery. The pressure drop recovery jumps around significantly during the testing, ranging from 0.7 to 1.4. No trend-line is shown because of the great alteration in test conditions on each test day. The several initial, high-temperature test days show poor pressure drop recovery, this being worse during the second test period having lower pulse pressure. This pressure recovery performance becomes good on the last two, low-temperature test periods.

The final summarizing figure, Figure 3.32, shows the residue permeance over the tests. This is a semi-log plot of the data in contrast to the earlier plots. The temperature range and pulse source pressure are indicated on the figure for each set of data points. The residue permeance drops sharply during the first two, high-temperature test periods. It then becomes nearly constant during the last two, low-temperature test periods.

Standard Candle Testing

A significant question is raised by the inverted candle filter testing: are the performance trends found for the inverted candle filter testing different from the trends characteristic of standard candle filter testing, or are these trends a function of the ash properties more than the geometry and cleaning phenomena associated with the filter elements? Evidence is provided by the testing done with standard candle filter elements.

The baseline and trigger pressure drops, and the residue pressure drops measured for the inverted candle filter elements tested are comparable to the values for these parameters measured in the Karhula PFBC tests with standard candle filter elements using the Lakeland feedstocks. For example, in the 10/21/1997 Karhula test, with a face velocity of 4.0 cm/s (7.8 ft/min), the trigger pressure drop was about 552 kPa (80 iwg) and the baseline pressure drop was about 455 kPa (66 iwg). The estimated residue pressure drop was about 303 kPa (44 iwg), and at a face velocity of 5.1 cm/s (10 ft/min) this residue pressure drop would have been about 393 kPa (57 iwg). Thus, the inverted candle filter elements appear to have comparable capabilities to standard candle filter elements, except that their pulse cleaning frequency may need to be greater.

The test results for the standard candle filter elements are summarized in three figures. The first, Figure 3.33, shows the residue pressure drop as a function of ash exposure time. The mean operating conditions over each test period are also indicated (face velocity, temperature, pulse pressure) because the test conditions were broad and altered each test period. In this figure, it is seen that the residue pressure drop tends to increase very slowly during the first three, relatively low-temperature, testing periods. It then increases greatly in the fourth, higher temperature test period, at the same pulse pressure. The residue pressure drop then falls in the last test period having increased pulse pressure.

The second figure, Figure 3.34, shows the fraction of deposited ash removed during each pulse event, or the pressure drop recovery. The pressure drop recovery for the standard candle filter elements jumps around significantly during the testing, ranging from 0.7 to 2.1. No trend-line is shown because of the great alteration in test conditions on each test day. The several initial, low-temperature test periods show good pressure drop recovery, this becoming worse during the fourth test period having higher temperature. This performance becomes good again over the last test periods when the pulse pressure is increased.

The final summarizing figure for the standard candles, Figure 3.35, shows the residue permeance over the tests. The temperature range and pulse source pressure are indicated on the figure for each set of data points. The residue permeance shows the same trends seen before for inverted candle filter elements -- lower residue permeance as the temperature is increased, and higher residue permeance as the pulse pressure in increased. The magnitude of the residue permeance with the standard candle filter elements shown in the figure appears to be slightly larger than that of the inverted candle filter elements, but this is not conclusive.

Compilation of the Test Data

It is evident from the test data that the residue permeance is a function of time as well as temperature and pulse pressure. To compare all of the test data on a consistent basis, it was assumed that the lowest value of the residue permeance during each test day, the "minimum residue permeance", was equal to the eventual steady value the residue permeance would achieve. The test data are plotted in Figure 3.36 for all of the inverted candle tests and the standard candle tests, plotting the "minimum residue permeance" versus the "maximum test point temperature". The "maximum test point temperature" is the highest temperature reached during the corresponding test period. The types of filter elements corresponding to the data are indicated in the figure. All of the data points shown having an associated pulse pressure of 250 psia, unless they have a "box" around them. The boxed data points have an associated pulse pressure of 500 psia. The plot shows a trend toward lower minimum residue permeance as the maximum test point temperature increases, but there is still significant scatter in the data. The boxed data points, having higher pulse source pressures, tend to have higher residue permeance, indicting improved cleaning with increased pulse pressure.

It is also seen from the test data that a high temperature exposure results in a residue pressure drop that is not completely reversible by subsequently reducing the temperature or increasing the pulse pressure. In a second plot of all of the test data, Figure 3.37, the minimum residue permeance is plotted against the "maximum exposure temperature", that is, the maximum temperature that the filter element has experienced during the entire test campaign. The scatter in the test data is greatly reduced in the figure, and the data trend appears quite clear. Note that the trend for reduced residue permeability appears linear with increased operating temperature, and there is no sudden increase in this behavior above some critical temperature, such as 760°C

(1400°F). In standard candle filter systems, increased temperature may also result in increased ash sintering and bridge formation that may result in non-linear increases in system pressure drop.

Inverted Candle Test Conclusions

The test results for the inverted candle filter system tested are very promising. The specific conclusions drawn from the HTHP inverted candle filter system testing are:

- Dust penetration measured during most of the testing was at normal levels for standard candles, indicating no unusual leak paths during the tests.

- The inverted candle filter elements all were durable at the test conditions (high-temperature with severe thermal shock events), other than the monolithic, oxide-based inverted candle filter elements (Coors and Ensto), which fractured.

- The inverted candle gaskets were taken directly from standard candle practice and were durable at the test conditions, showed no signs of significant ash leaks.

- The filter cake pressure drop and pulse cleaning frequency was consistent with theoretical expectations - - that is, the pressure drop increases faster than it would using standard candles, and the pulse cleaning frequency is then greater. Thin-walled inverted candle filter elements minimize this effect.

- A greater pulse gas source pressure, at least 2400 kPa (350 psi) above the filter vessel pressure, improves the cleaning performance, reduces the pulse cleaning frequency and ensures that a stable baseline pressure drop is achieved.

- Plugging of the inverted candle filter element bore, and excessive ash re-entrainment are not expected with the inverted candle hot gas filter.

- All of the inverted candle filter elements appear to have similar performance trends, but the thin-walled McDermott and Pall FeAl candles provide the greatest performance and cost advantages.

- The residue pressure drop is independent of the filter element geometry, and is influenced most strongly by the nature of the ash, the operating temperature, and the pulse cleaning source pressure.

- Increasing temperatures result in much higher residue pressure drop, and the associated need for more frequent pulse cleaning, equally for both inverted candles and standard candles.

- Broken inverted candle filter elements are retained within their containment pipes, and the standard candle filter cascading damage done to other filter elements in the array, with the potential plugging of the ash outlet nozzle, is eliminated.

- The filter cake permeabilities extracted from the test data are consistent with previous dust cake permeability estimates made from Karhula test data with this filter cake material.
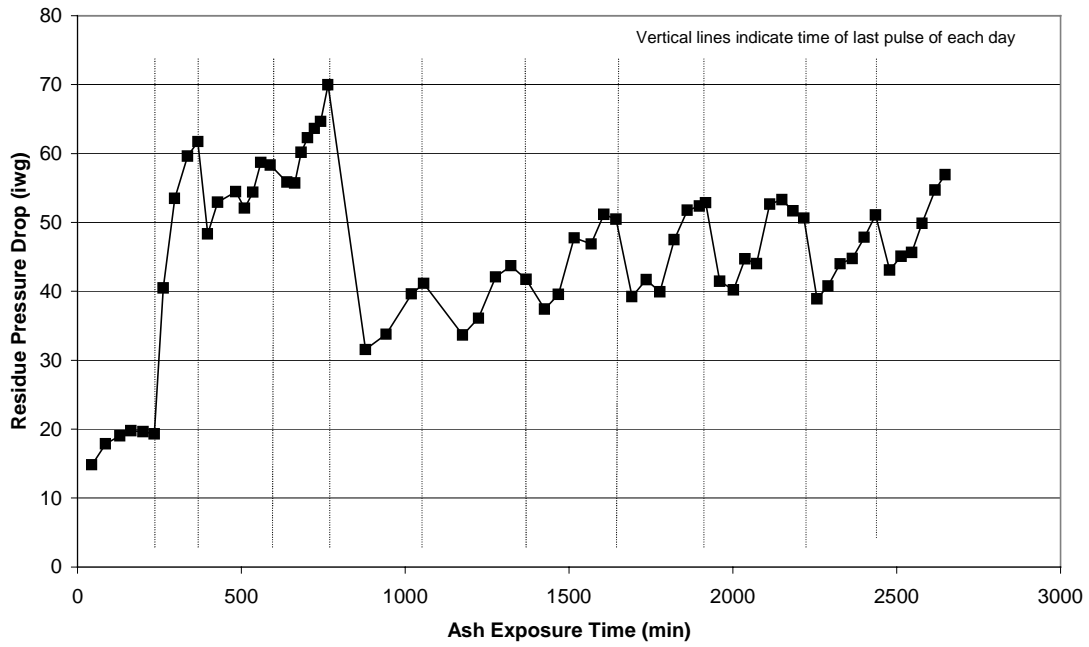
Figure 3.19 - IF&P Recrystallized SiC Inverted Candle Residue Pressure Drop
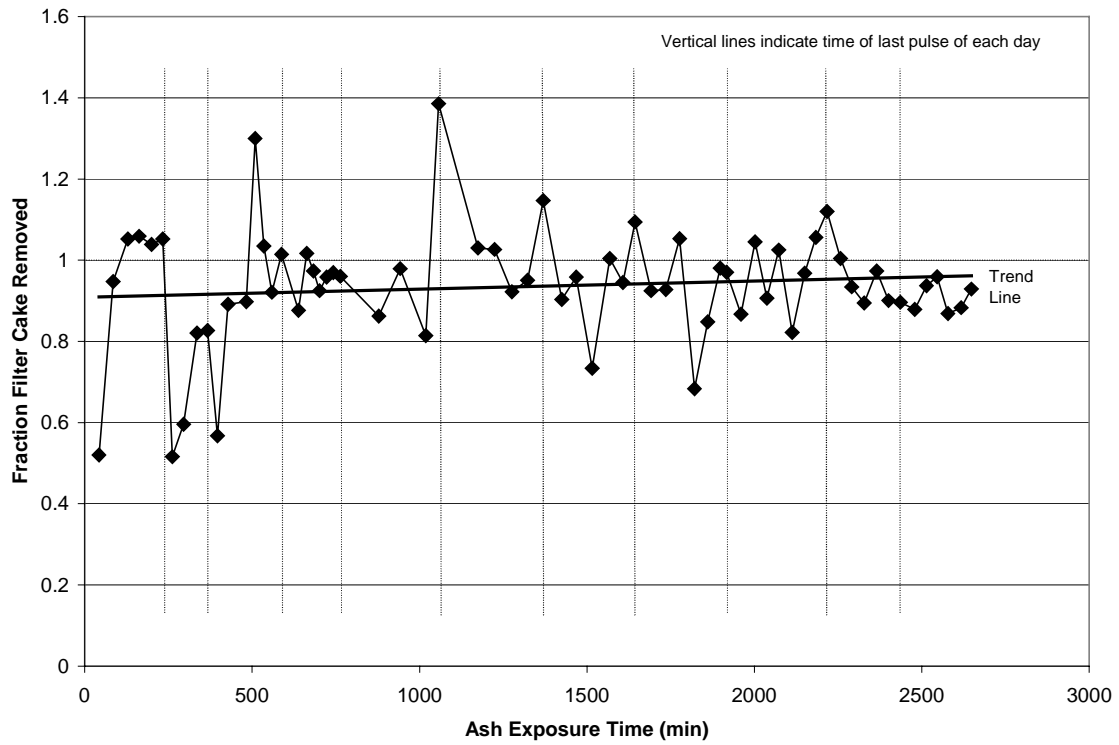
Figure 3.20 - IF&P Recrystallized SiC Inverted Candle Pressure Drop Recovery
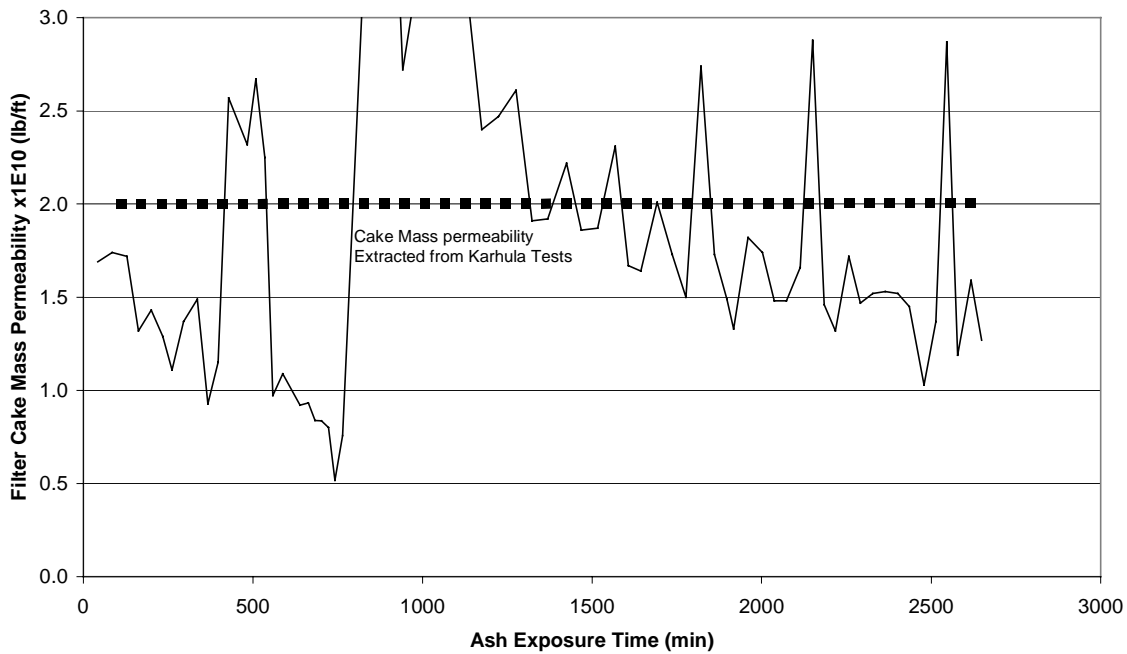
Figure 3.21 - Filter Cake Mass Permeability During IF&P Recrystallized SiC Inverted Candle Testing
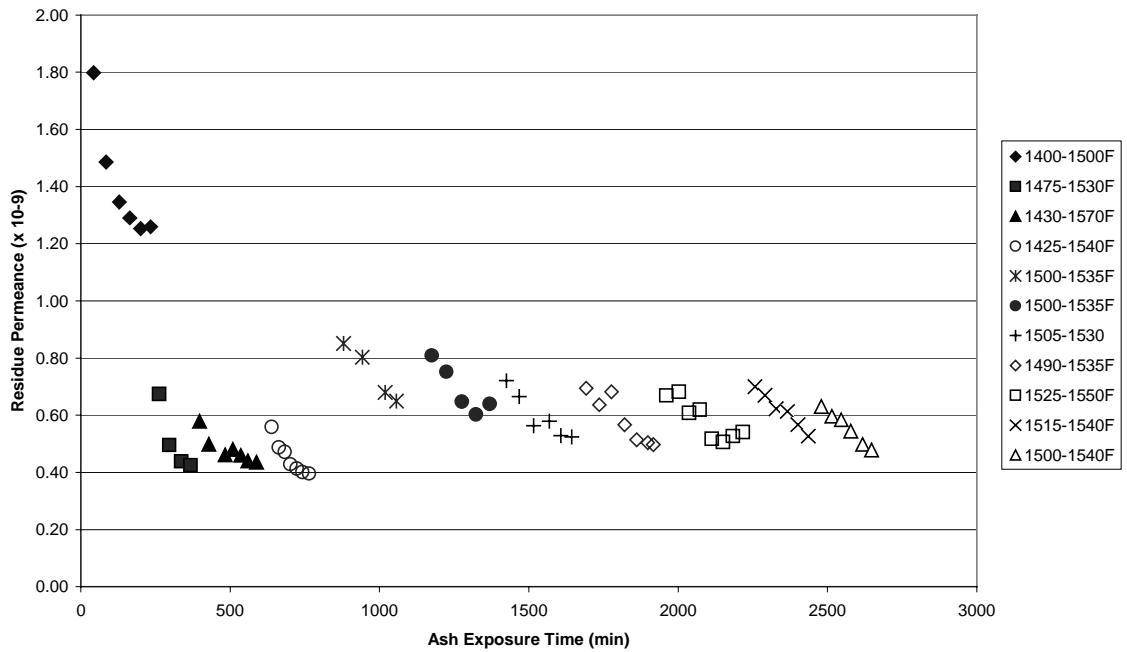
Figure 3.22 - IF&P Recrystallized SiC Inverted Candle Testing Residue Permeance
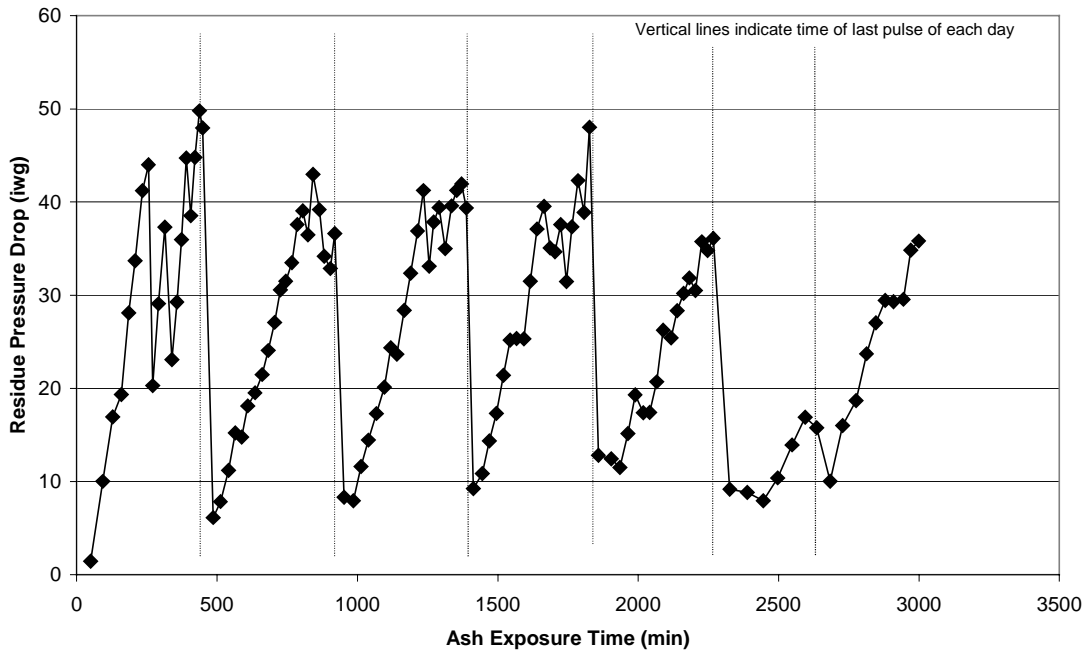
Figure 3.23 - Pall 326 SiC Inverted Candle Residue Pressure Drop
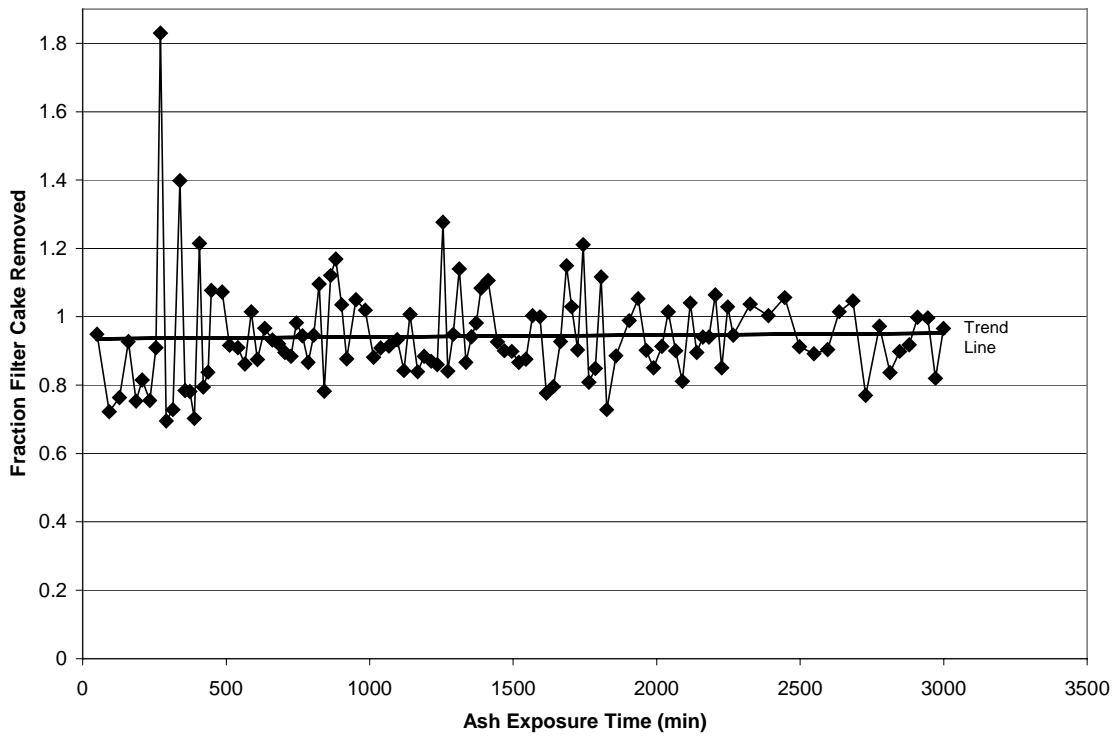
Figure 3.24 - Pall 326 SiC Inverted Candle Pressure Drop Recovery
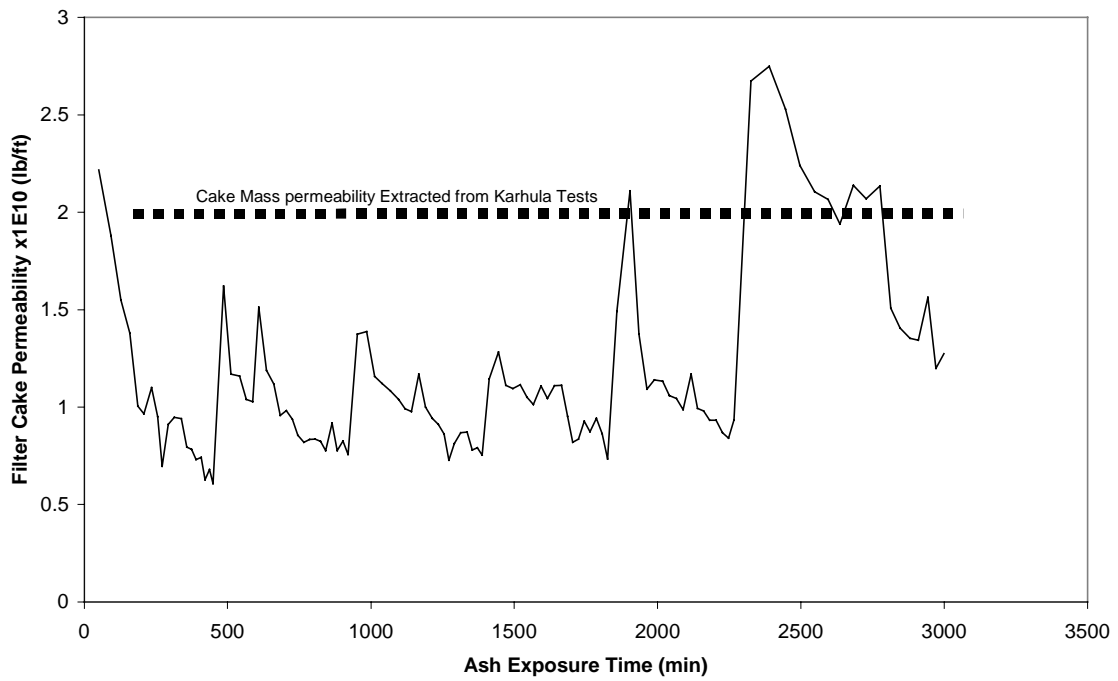
Figure 3.25 - Cake Mass Permeability During Pall 326 SiC Inverted Candle Testing
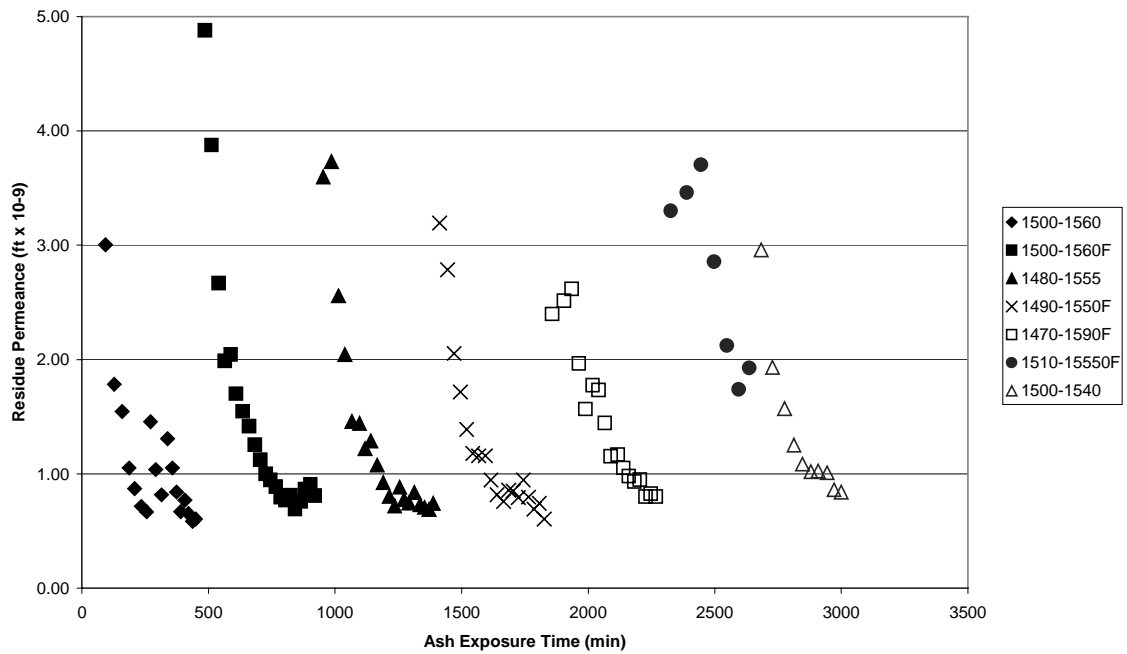
Figure 3.26 - Residue Permeance During Pall 326 SiC Inverted Candle Testing

51
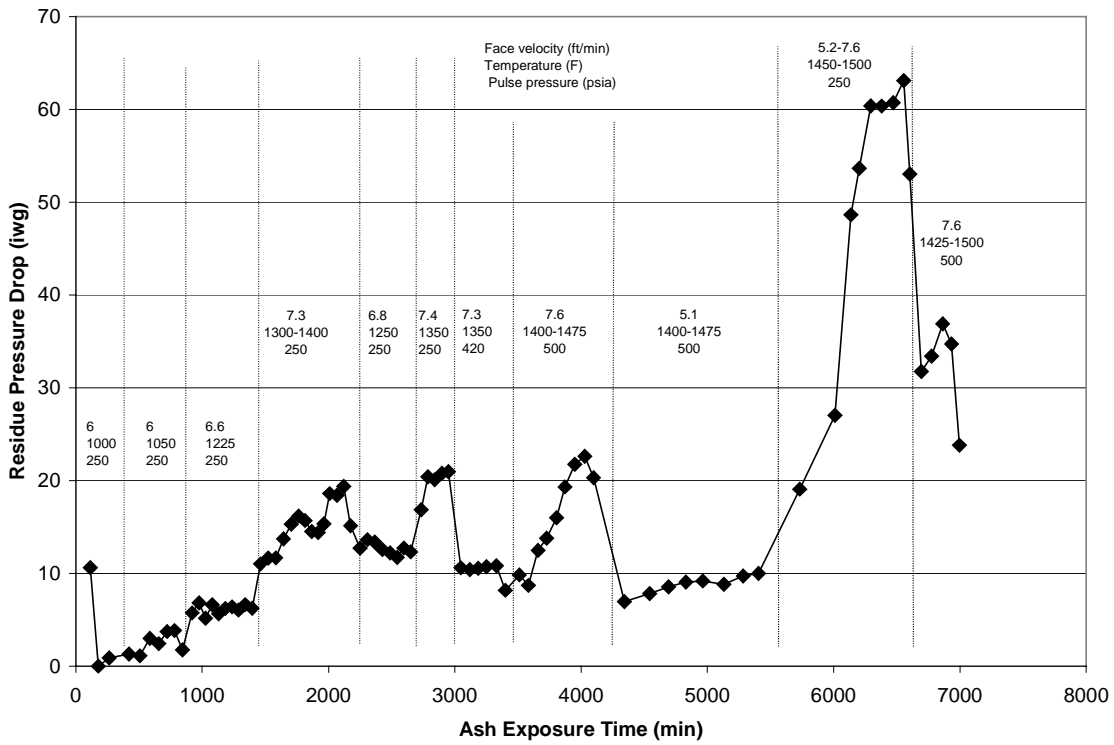
Figure 3.27 - McDermott 610 Inverted Candle Residue Pressure Drop
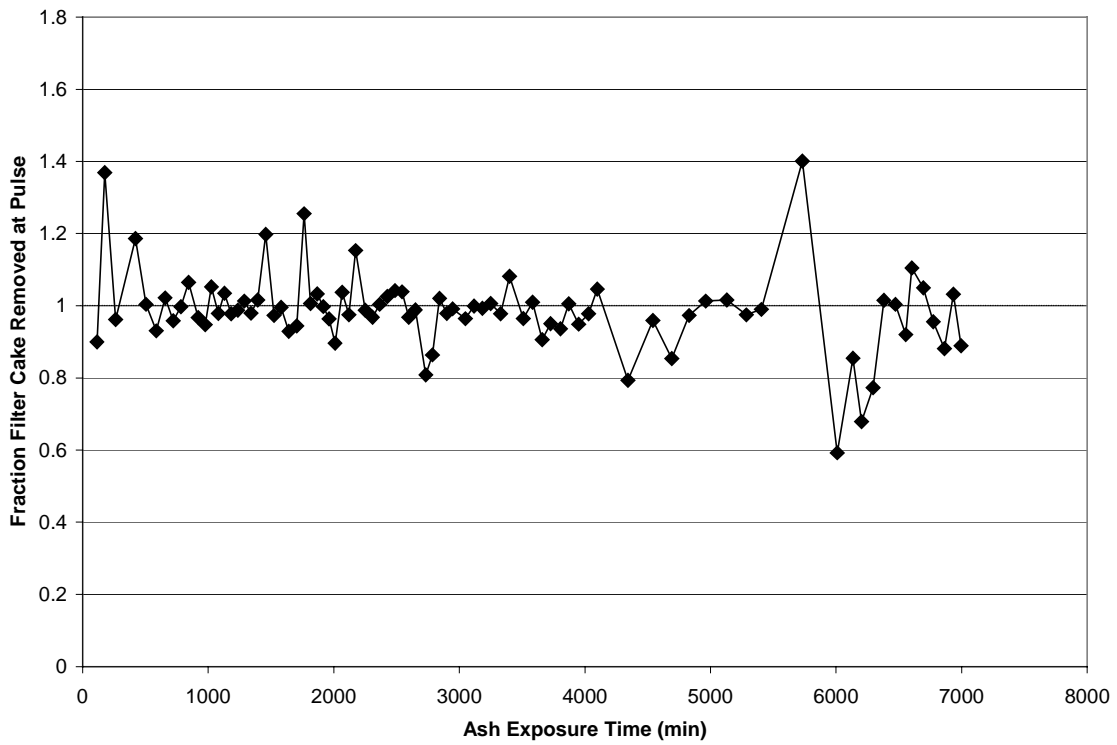
Figure 3.28 - McDermott 610 Inverted Candle Pressure Drop Recovery
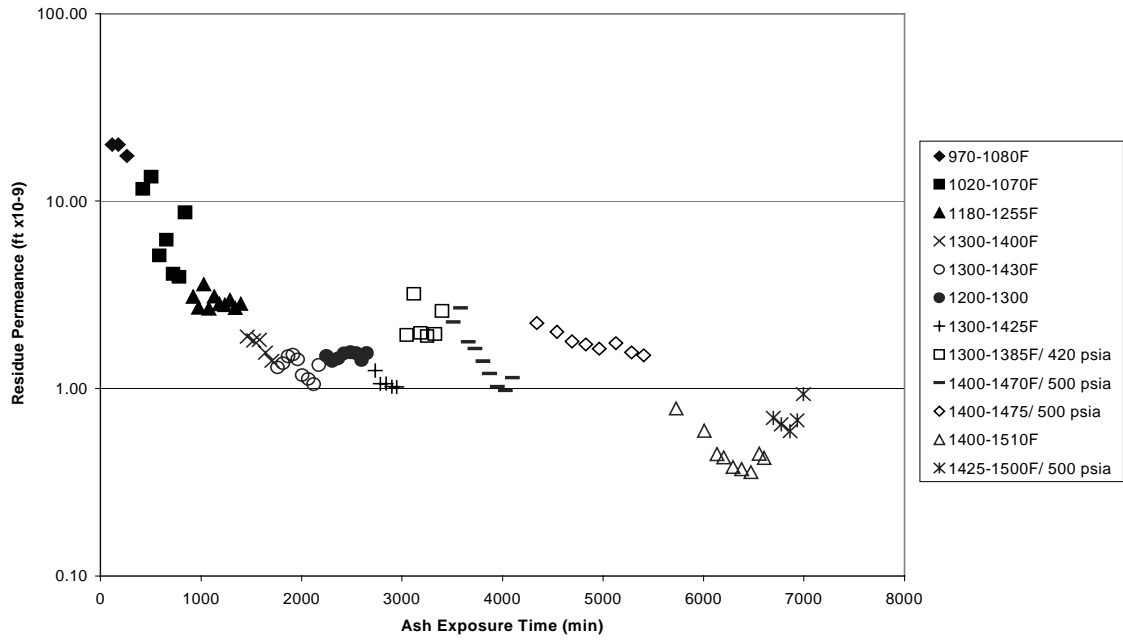
Figure 3.29 - Residue Permeance During McDermott 610 Inverted Candle Testing
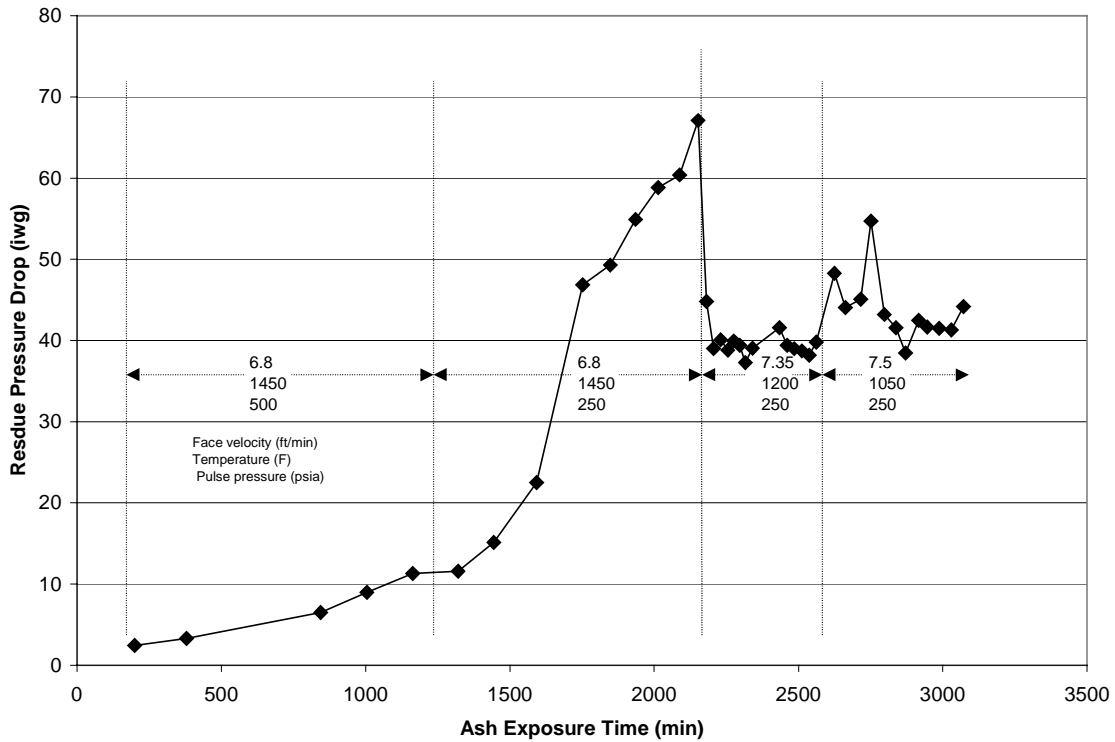
Figure 3.30 - Pall FeAl Inverted Candle Residue Pressure Drop
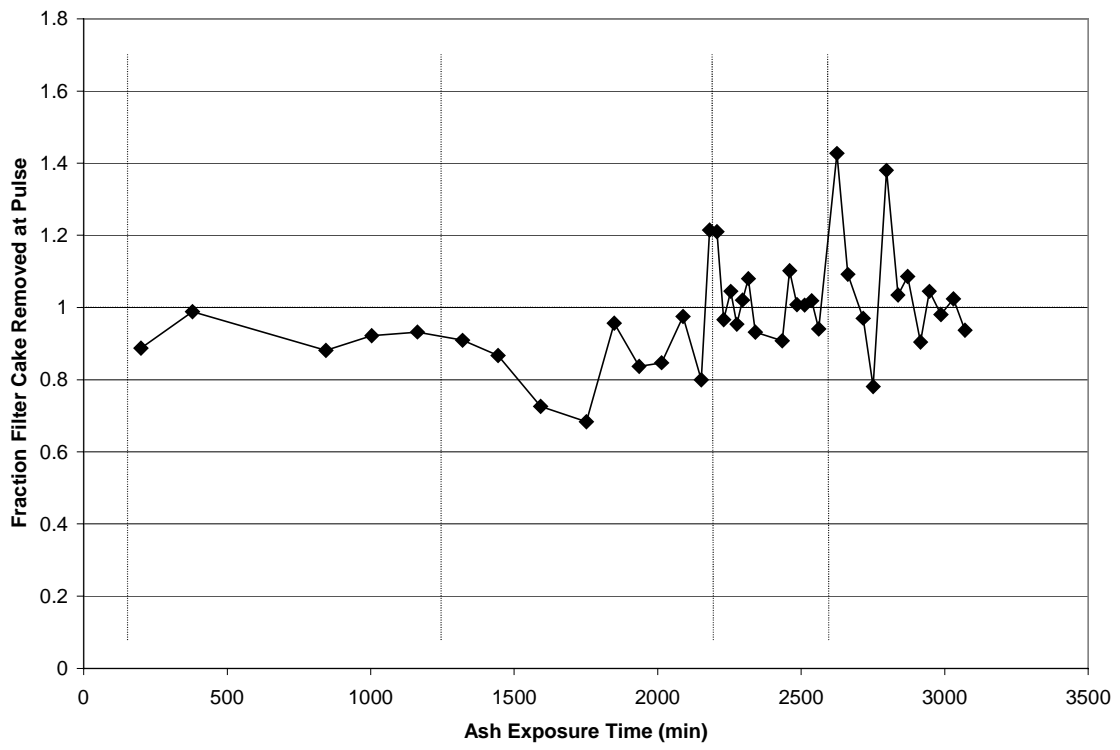
Figure 3.31 - Pall FeAl Inverted Candle Pressure Drop Recovery
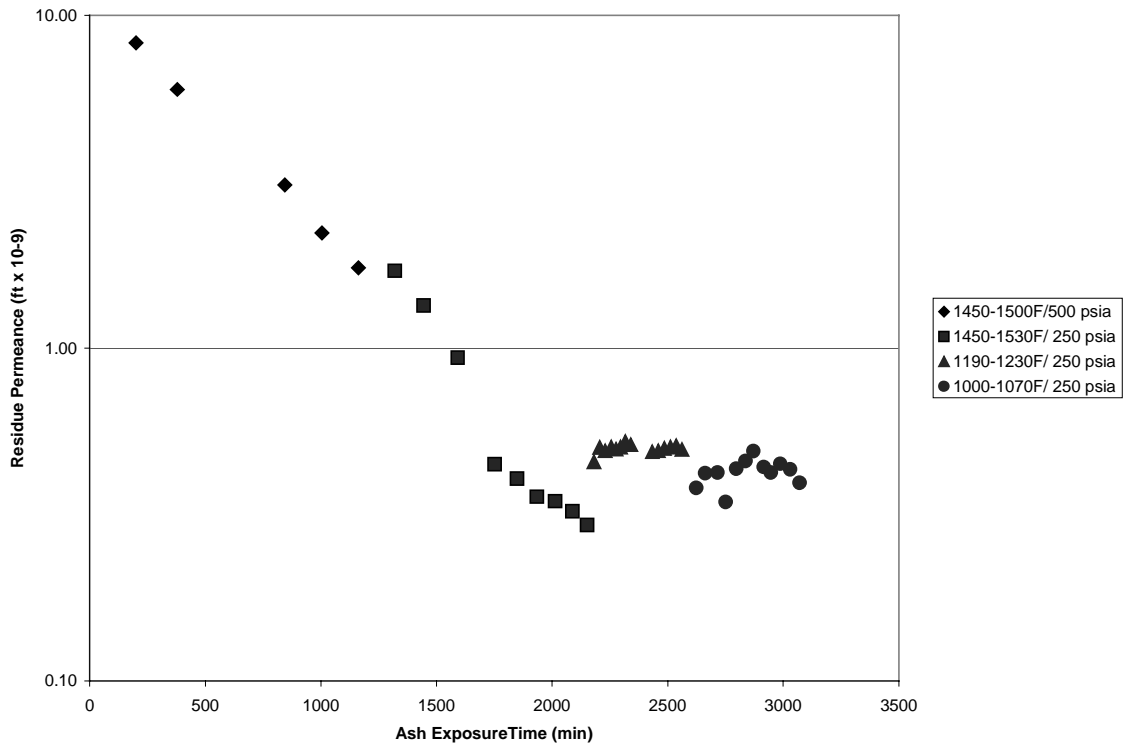
Figure 3.32 - Residue Permeance During Pall FeAl Inverted Candle Testing
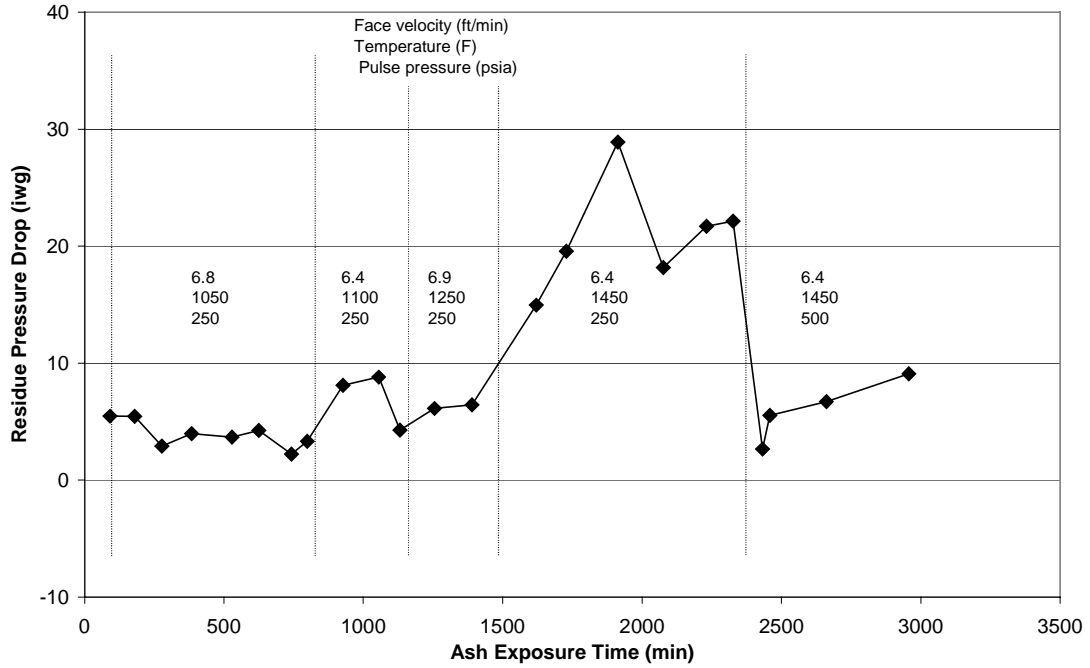
Figure 3.33- Standard Candle Residue Pressure Drop
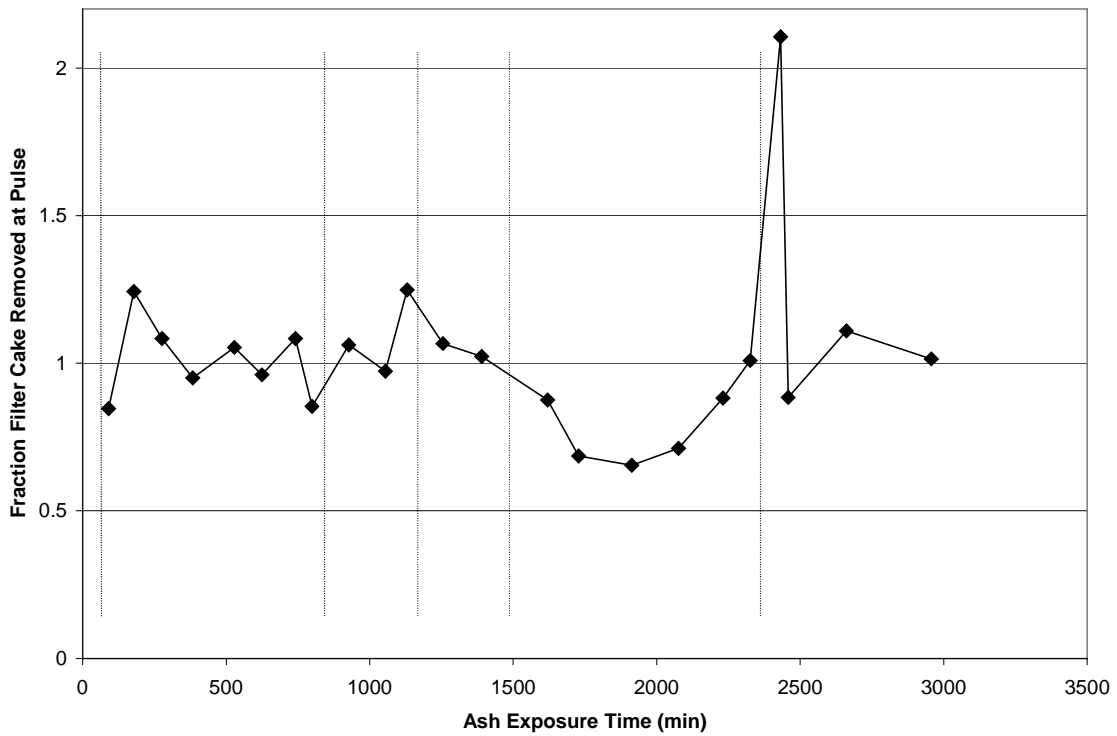
Figure 3.34 - Standard Candle Pressure Drop Recovery
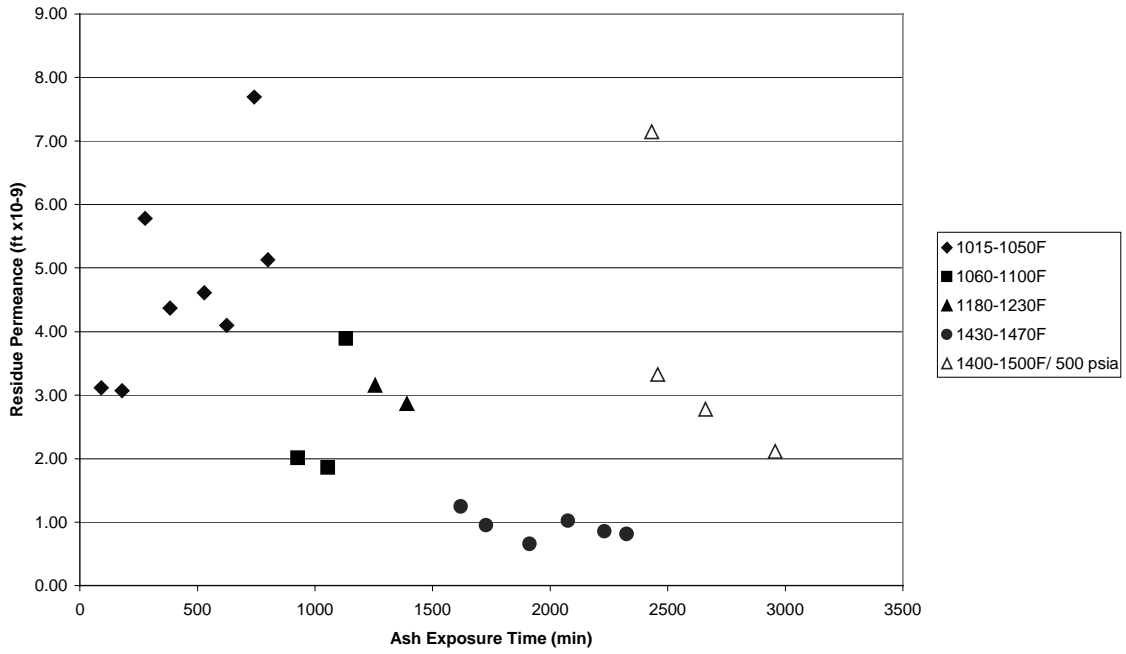
Figure 3.35 - Residue Permeance During Standard Candle Testing
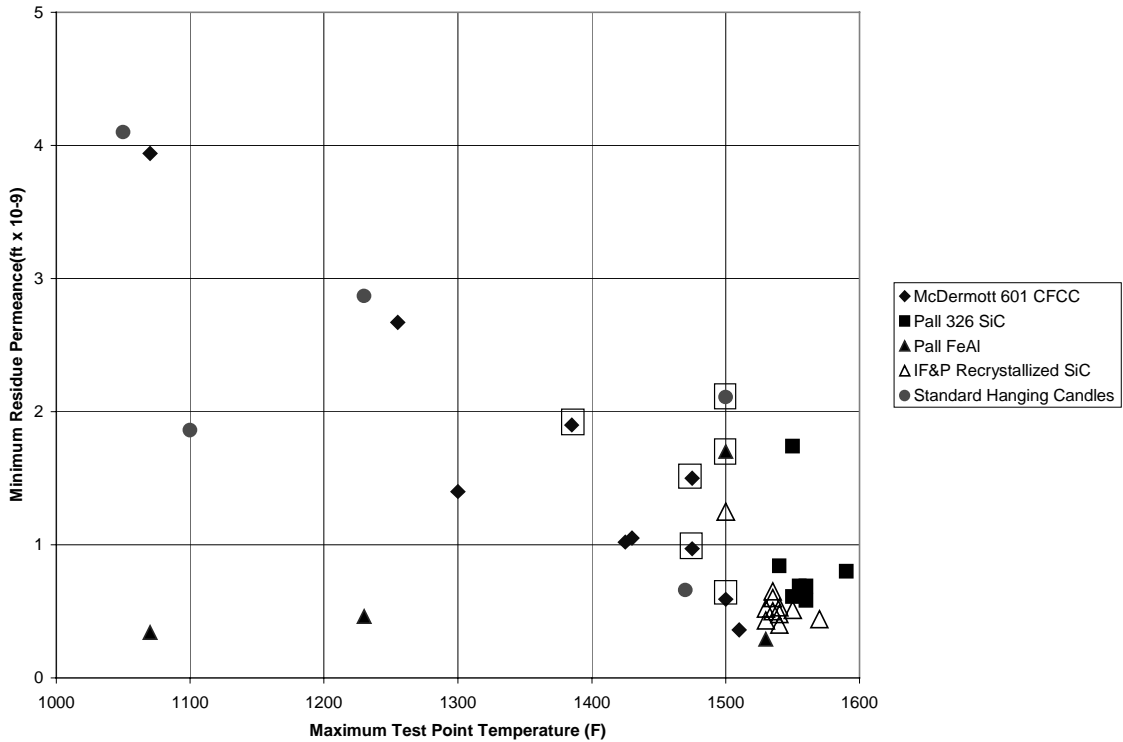
Figure 3.36 - Compiled Test Data Against Maximum Test Point Temperature

Figure 3.37 - Compiled Test Data Against Maximum Exposure Temperature

3.7 RESULTS AND DISCUSSION - INVERTED CANDLE COMMERCIAL FILTER SYSTEM COST AND PERFORMANCE UPDATE

A commercial, inverted candle hot gas filter evaluation for PFBC and IGCC applications was conducted in the Base Program and reported in the Base Program Final Report. The results of the Base Program commercial evaluation, and the test data reported in this document, clearly indicate that the thin-walled inverted candles, such as the McDermott 610 CFCC and Pall FeAl inverted candles, are the only practical inverted candle filter element candidates. To illustrate this point, the relative number of inverted candle filter elements required in a filter system for the same operating face velocity as the equivalent standard candle filter system, or, alternatively, the relative face velocity of the inverted candle filter system having the same number of filter elements as the equivalent standard candle filter system, are listed below as determined from the inside diameter of the inverted candle filter elements:

Filter System	Relative face velocity, or Relative number of filter elements
Standard candle system:	1.00
Coors and Ensto oxide-based inverted candle system:	1.65
Pall 326 SiC inverted candle system:	1.54
IF&P recrystallized SiC inverted candle system:	1.39
McDermott 610 CFCC inverted candle system:	1.21
Pall FeAl inverted candle system:	1.08

Presented here is an update of the commercial inverted candle hot gas filter evaluation. Based on the results of the inverted candle filter system testing, the commercial availability conclusions made in the Base Program change very little. An update of the commercial performance and cost estimates has been generated, but no new availability estimates have been made. With respect to availability, it is expected that the inverted candle hot gas filter system configuration has the potential to provide protection against ash bridging, filter element vibration, elongation and deformation, vessel overfilling, and various process upsets. The inverted candle hot gas filter system also protects against cascading filter element damage and ash nozzle plugging, or ash handling equipment damage by containing each filter element in the event of a filter fracture. The improvement in the hot gas filter availability is expected to be significant, especially for applications having difficult flyashes that are prone to ash bridging or deposition and/or having tendencies for process upsets.

Based on the Base Program evaluation results, for PFBC applications, the thin-walled, McDermott 610 CFCC inverted candle filter elements appear to be the best choice with respect to both performance and cost. No inside membrane is needed on the McDermott inverted candle filter element and its cost should be identical to that of the standard McDermott candle filter element. For PFBC applications, the hot gas filter system cost is a substantial portion of the total plant cost, and the hot gas filter system economics may be an issue. The use of inverted candle filter elements having 2 m length, coupled with the improved availability of the plant resulting from the inverted candle filter system configuration, would be expected to improve the overall barrier filter economics significantly. The McDermott inverted candle filter elements have the potential to be manufactured in 2 m lengths.

Based on the Base Program evaluation results, for IGCC applications, either the thin-walled McDermott or the thin-walled, Pall FeAl inverted candle filter elements would be best,

depending on the corrosive nature of the fuel gas. While only fabricated and tested in 1.5 m lengths, both of these inverted candle filter elements have high potential for fabrication as 2 m long inverted candle filter elements, providing the expectation for significant barrier filter cost advantage. The use of larger diameter inverted candles is not expected to be needed for the inverted candle filter system configuration to provide acceptable performance and economics.

In air-blown IGCC, the barrier filter system cost is a relatively small portion of the total plant cost, and in oxygen-blown IGCC the barrier filter system cost is even a smaller portion of the plant cost. Thus, in IGCC, the cost of the inverted candle filter system using 1.5 m long inverted candle filter elements should be acceptable, especially when the improved availability of the plant that results is considered.

It is evident from the testing that each inverted candle filter element should be housed in an individual containment pipe and should include a fail-safe/ regenerator. If the containment pipe has a flange at both the top and bottom, the inverted candle filter elements can be applied to the conventional SWPC candle cluster without lengthening the cluster or increasing the vessel length since the candles and containment pipes may be removed using the top flange ("top maintenance"). Alternatively, if bottom withdrawal of the inverted candle filter elements from the containment pipes is to be used ("bottom maintenance"), then the cluster and the vessel must both be increased in length to provide sufficient space under each plenum to allow the inverted candle filter element to be lowered from the containment pipe. In this case, the containment pipes are welded to the plenum, eliminating one set of flanges, and nuts & bolts for each filter element. This alternative arrangement provides maintenance advantages over the top maintenance scheme. Each plenum of containment pipes can also be surrounded by a complete containment cylinder to eliminate the accumulation of ash between the containment pipes.

The pressure vessel diameter can be reduced significantly because the shroud can be eliminated when using the inverted candle filter configuration. The vessel length is then also reduced because the shroud is eliminated, making the cluster length several feet shorter as well. The vessel length might also be reduced further because less excess ash storage capacity below the clusters is needed within the vessel to protect the filter elements from ash overfilling.

PFBC Application

The evaluation update for PFBC is based on a 314 MWe PFBC power plant hot gas filter system, and the following inlet operating conditions, as taken from the Base Program report:

- gas flow, m^3/s (acfm):   5,764 (203,539),
- gas temperature, °C (°F):   871 (1600),
- gas pressure, kPa (psia):   1296 (188),
- dust load, ppmw: 6,525.

The characteristics of a standard candle filter system design (using Pall 326 SiC candles) for this application are compared to Pall 326 SiC and McDermott 610 CFCC inverted candle filter system designs in Table 3.7. The types of inverted candles used, and their wall thicknesses are:

- Pall 326 SiC (7 mm wall thickness) with inside membrane added, 1.5 m long,
- McDermott 610 CFCC (5 mm wall thickness), 1.5 m long,
- McDermott 610 CFCC (5 mm wall thickness), 2.0 m long.

The Pall 326 SiC inverted candle having a 7 mm wall thickness and an inside membrane is a fictitious filter element, since the standard Pall 326 SiC candle has a 10 mm wall thickness, but it is assumed a feasible design. Top and bottom maintenance schemes are both considered. All of the filter system designs use the same number of parallel filter vessels, each holding the same number of filter clusters. The inverted candle filter vessels with 1.5 m long inverted candles support a greater number of filter elements than the standard filter system. The inverted candle cluster structure is larger in diameter, but shorter for top maintenance, and longer for bottom maintenance, than the standard candle cluster.

The standard candle filter vessel has a shroud that completely surrounds the top section of the clusters and promotes inlet gas flow upward initially. The shroud permits direct access to the cluster filter candles for inspection and maintenance through the vessel manways. The inverted candle filter vessel has no shroud, reducing the vessel diameter and length. It also has manways to service the internals. The vessel outer diameters and total weights are very similar for the filter systems. The vessels for the inverted candles using top maintenance are shorter than the standard candle filter vessel, and for bottom maintenance, are longer.

Table 3.7 - PFBC Filter Design Characteristics

	Standard Candle	Inverted Candle	Inverted Candle	Inverted Candle	Inverted Candle	Inverted Candle	Inverted Candle
Candle type	Pall 326 SiC	Pall 326 SiC	Pall 326 SiC	McDerm. CFCC	McDerm. CFCC	McDerm. CFCC	McDerm. CFCC
Candle length (m)	1.5	1.5	1.5	1.5	1.5	2.0	2.0
Maintenance type		Top	Bottom	Top	Bottom	Top	Bottom
Number of parallel vessels	8	8	8	8	8	8	8
Number clusters per vessel	5	5	5	5	5	5	5
Number candles per cluster	187	225	225	225	225	174	174
Total number candles	7480	9000	9000	9000	9000	6960	6960
Cluster diameter, m (ft)	1.02 (3.33)	1.11 (3.65)	1.11 (3.65)	1.11 (3.65)	1.11 (3.65)	1.11 (3.65)	1.11 (3.65)
Cluster length, m (ft)	10.2 (33.3)	9.3 (30.4)	12.3 (40.3)	9.3 (30.4)	12.3 (40.3)	9.1 (30.0)	13.7 (45.0)
Shroud type	Top shroud	None	None	None	None	None	None
Vessel OD, m (ft)	3.7 (12.2)	3.7 (12.1)	3.7 (12.1)	3.7 (12.1)	3.7 (12.1)	3.7 (12.1)	3.7 (12.1)
Vessel height, m (ft)	20.7 (68)	18.3 (60)	21.9 (72)	18.3 (60)	21.9 (72)	18.0 (59)	23.5 (77)
Vessel wall thickness, cm (in)	3.2 (1.25)	3.2 (1.25)	3.2 (1.25)	3.2 (1.25)	3.2 (1.25)	3.2 (1.25)	3.2 (1.25)
Refractory thickness, cm (in)	20 (8)	20 (8)	20 (8)	20 (8)	20 (8)	20 (8)	20 (8)
Vessel weight, Mg (tons)	147 (162)	134 (148)	153 (168)	134 (148)	153 (168)	134 (147)	161 (177)
Internals weight, Mg (tons)	36 (40)	45 (50)	48 (53)	44 (49)	47 (52)	42 (46)	46 (51)
Total filter weight, Mg (tons)	183 (202)	179 (198)	201 (221)	178 (197)	200 (220)	176 (193)	207 (228)

Figure 3.38 shows the general relation between the pulse cleaning frequency, the average filter pressure drop (the average of the trigger and baseline pressure drops), and the filter cake maximum thickness (thickness at the trigger pressure drop) for the filter systems considered in Table 3.7. It shows that at the low pulse cleaning rate, high pressure drop end of the graph, the inverted candle filter system must operate at a higher pulse gas frequency than the standard candle filter system, and the filter cakes will be slightly thinner than those of the standard candle filter, to maintain the same average pressure drop. At the high pulse frequency end of the graph, the system design differences dominate. The inverted candle filter systems can operate with a lower pressure drop than the standard candle filter system because the shroud pressure drop has been eliminated.
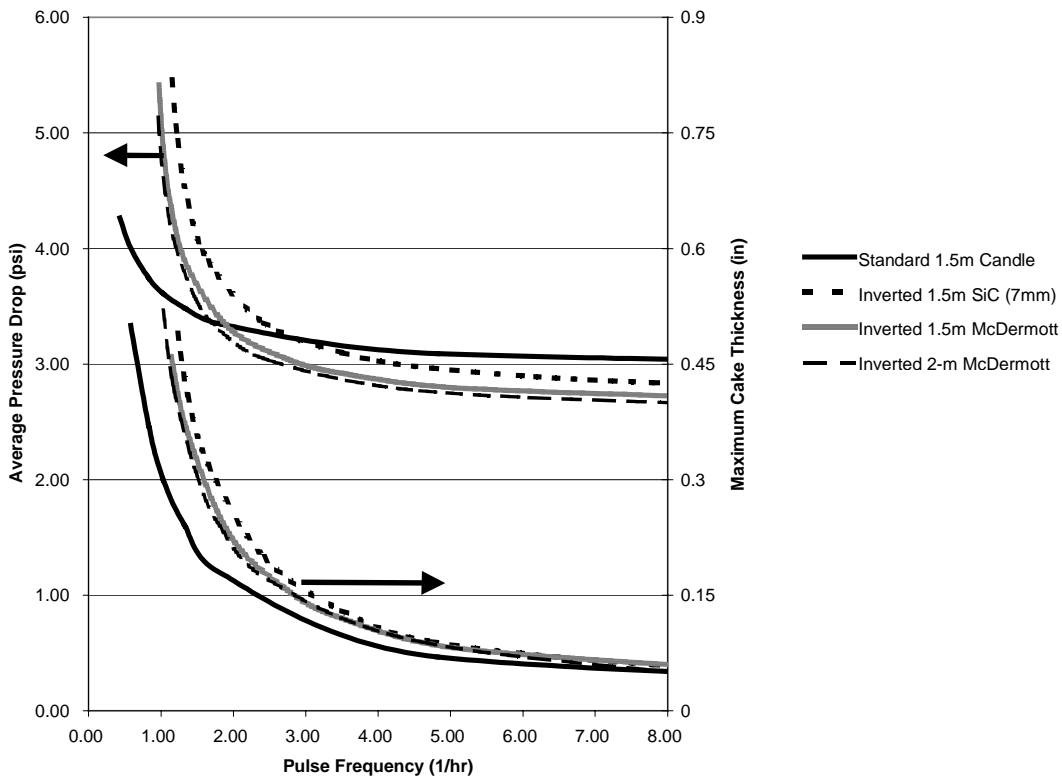
Figure 3.38 - Pressure Drop and Cake Thickness for PFBC Filters

The standard candle filter system performance is compared to the Pall SiC (7 mm wall) inverted candle and the McDermott 610 CFCC (5 mm wall) inverted candle filter system performance in Table 3.8. Filter element and ash characteristics measured in this program have been used to make these estimates, applying SWPC proprietary filter models. The face velocity is based on the dirty surface area of the respective candle type. The pressure drop includes the conditioned filter element, ash residue, filter cake, vessel gas inlet and outlet nozzles, fail-safe device, and other losses through the internals in the filter vessel. Assumptions for the pulse gas system are:

- pulse gas source pressure: 4137 kPa (600 psia)
- pulse gas type: air.

61

The Pall and McDermott inverted candle filter systems cannot achieve the same pressure drop as the standard candle filter system when designed with the same number of filter elements because their face velocities would be too high. They must operate with an increased number of filter elements, and Table 3.8 indicates that the face velocity is about the same for the McDermott inverted candle filter systems and the standard candle filter system, but the face velocity is higher for the Pall SiC inverted candle filter systems. Most performance results are identical for the top maintenance and bottom maintenance scheme and the values in Table 3.8 are not repeated if they do not change. The average pressure drops for the inverted candle filter systems are comparable to that of the standard candle filter system, and the pulse cleaning frequency is significantly greater. The pulse gas consumptions and compressor powers are also comparable. For the 2 m long McDermott CFCC inverted candle systems, pulse frequencies are lower than for the 1.5 m long inverted. The ash storage capacity of the inverted candle filter vessels is considerably larger than that of the standard candle filter vessel.

Table 3.8 - PFBC Application Filter Performance Characteristics

	Standard Candle	Inverted Candle	Inverted Candle	Inverted Candle	Inverted Candle	Inverted Candle	Inverted Candle
Candle type	Pall 326 SiC	Pall 326 SiC	Pall 326 SiC	McDerm. CFCC	McDerm. CFCC	McDerm. CFCC	McDerm. CFCC
Candle length (m)	1.5	1.5	1.5	1.5	1.5	2.0	2.0
Maintenance type		Top	Bottom	Top	Bottom	Top	Bottom
Face velocity, cm/s (ft/min)	4.8 (9.5)	5.2 (10.3)		4.8 (9.5)		4.7 (9.2)	
Trigger pressure drop, kPa (psi)	24.8 (3.6)	24.8 (3.6)		24.8 (3.6)		24.8 (3.6)	
Baseline pressure drop, kPa (psi)	23.4 (3.4)	23.4 (3.4)		22.8 (3.3)		23.4 (3.4)	
Pulse cleaning frequency, 1/hr	1.3	2.1		1.7		1.5	
Maximum cake thickness, cm (in)	0.61 (0.24)	0.58 (0.23)		0.66 (0.26)		0.76 (0.30)	
Pulse gas consumption, % of process gas	0.07	0.08		0.06		0.05	
Pulse gas compressor power, kW	42	46		35		28	
Ash storage capacity, hr	4.3	5.5	8.0	5.5	8.0	5.5	9.3

The operating conditions have been selected to result in an acceptable maximum filter cake thickness in the filter systems. The pulse gas consumption and compressor power uses are relatively small. Heat losses through the vessels, including mixing with the pulse gas are acceptable -- for all of the filter systems, the gas temperature drop across the filter vessel is 3-5ºC (6-10ºF) due both to vessel heat losses and cold pulse gas dilution. The ash storage time in the filter vessels, that is, the time before damage could occur to the lowest levels of candles in the filter vessel if ash drainage from the vessel was stopped, is relatively large. The lower pressure loss across the fail-safe devices in the inverted candle filter system results because of a larger number of filter elements, and this produces a lower, total pressure drop in the inverted candle filter system.

The delivered equipment costs, in end-1999-dollars, are listed in Table 3.9. The scope of equipment supply is the refractory-insulated filter "pressure vessels" (with shroud, tube sheet, metal liners, and maintenance items), the "filter elements" (with gasket sets, nuts & bolts, and fail-safe devices) the clusters, the pulse gas compressor system, and the pulse gas control skids. The assumed filter element costs are:

- Standard Pall 326 SiC candle, 1.5 m long -- $300,
- Pall 326 SiC (7 mm wall thickness) with inside membrane added, 1.5 m long -- $500,
- McDermott 610 CFCC (5 mm wall thickness), 1.5 m long -- $1200 ($300),
- McDermott 610 CFCC (5 mm wall thickness), 2.0 m long -- $1600 ($400).

Two cost levels are assumed for the McDermott inverted candles, the first representing the expected commercial cost of these elements in the near-term. The second represents the long-term cost expectation based on a healthy market and improved fabrication technologies, if production levels increase to several thousand per year.

Table 3.9 - PFBC Filter Cost Breakdowns

	Standard Candle	Inverted Candle	Inverted Candle	Inverted Candle	Inverted Candle	Inverted Candle	Inverted Candle
Candle type	Pall 326 SiC	Pall 326 SiC	Pall 326 SiC	McDerm. CFCC	McDerm. CFCC	McDerm. CFCC	McDerm. CFCC
Filter element length (m)	1.5	1.5	1.5	1.5	1.5	2.0	2.0
Filter element cost, $	300	500	500	1200 (300)	1200 (300)	1600 (400)	1600 (400)
Maintenance type		Top	Bottom	Top	Bottom	Top	Bottom
Pressure vessels	8,362	8,115	8,740	8,115	8,740	8,094	9,037
Filter elements	4,002	6,615	6,615	12,915 (4,815)	12,915 (4,815)	12,772 (4,420)	12,772 (4,420)
Clusters	8,448	10,150	10,507	10,150	10,507	8,506	9,048
Pulse gas compressor system	1,953	2,265	2,265	2,265	2,265	1,844	1,844
Pulse gas control skids	3,946	3,946	3,946	3,946	3,946	3,064	3,064
Total	26,711	31,091	32,073	37,391 (29,301)	38,373 (30,283)	34,280 (25,928)	35,765 (27,413)

The Pall 326 SiC (1.5 m long, 7 mm wall) inverted candle filter system cost with top maintenance is about 16% greater than the standard candle filter system cost, and represents an equipment cost of about 99 $/kW. With bottom maintenance, the system cost increases about 3%. The McDermott 610 CFCC (1.5 m long) inverted candle filter system cost with top maintenance and an inverted candle cost of $1200 is about 19% greater than the standard candle filter system. If the McDermott 610 CFCC inverted candle cost can be reduced to $300, the inverted candle filter system cost becomes only about 10% greater than the standard candle filter system cost. The use of 2 m long McDermott 610 CFCC has the potential to reduce the system cost by about 9%, and the resulting filter system cost can become comparable to that of the standard filter system if the 2 m long McDermott 610CFCC inverted candle cost can be reduced to $400. The greatly improved availability of the inverted candle filter system, according to the Base Program evaluation, is expected to provide for a significantly lower operating and life-cycle cost for the entire PFBC power plant, even with the slightly higher power plant capital investment resulting from the more expensive barrier filter system.

IGCC Application

The evaluation update for a 406 MWe, air-blown IGCC power plant filter system has the following operating conditions, as taken from the Base Program report:

- gas flow, m^3/s (acfm): 14.4 (30,414),
- gas temperature, °C (°F): 542 (1007),
- gas pressure, kPa (psia): 2620 (380),
- inlet dust load, ppmw: 9,864

The characteristics of a standard candle filter system design, using either Pall 326 SiC candles or Pall FeAl candles, for this application is compared to various inverted candle filter systems in Table 3.10. The inverted candles considered are: 1.5 m long Pall 326 SiC (7 mm wall), 1.5 m long Pall FeAl, 1.5 m long McDermott 610 CFCC, 2 m long Pall FeAl, 2 m long McDermott 610 CFCC. Both top maintenance and bottom maintenance designs are considered.

The filter system designs use the same number of parallel filter vessels, each holding the same number of filter clusters. The 1.5 m long inverted candle filter systems support greater numbers of filter elements than the standard filter system, and the cluster structure is larger in diameter, but shorter for top maintenance than the standard candle cluster. The standard candle filter vessels have a shroud that completely surrounds the top section of the clusters and promotes inlet gas flow upward initially. The top shroud permits direct access to the cluster filter candles for inspection and maintenance through the vessel manways. The inverted candle filter vessels have no shrouds, reducing their diameters, and also have manways to service the internals. The vessel dimensions and total weights are very similar for the filter systems. IGCC ash characteristics applied in the Base Program evaluation were applied to make the estimates in the table.

Table 3.10 - IGCC Filter Design Characteristics

	Standard Candle	Inverted Candle	Inverted Candle	Inverted Candle	Inverted Candle
Candle type	Pall 326 SiC, Pall FeAl	Pall 326 SiC, Pall FeAl, McDermott CFCC	Pall 326 SiC, Pall FeAl, McDermott CFCC	Pall FeAl, McDermott CFCC	Pall FeAl, McDermott CFCC
Candle length (m)	1.5	1.5	1.5	2.0	2.0
Maintenance type		Top	Bottom	Top	Bottom
Number of parallel vessels	2	2		2	
Number clusters per vessel	6	6		6	
Number candles per cluster	187	225		174	
Total number candles	2244	2700		2088	
Cluster diameter, m (ft)	1.02 (3.33)	1.13 (3.65)		1.13 (3.65)	
Cluster length, m (ft)	10.2 (33.3)	9.4 (30.4)	12.3 (40.3)	9.1 (30)	13.7 (45)
Shroud type	Top shroud	None	None	None	None
Vessel OD, m (ft)	3.7 (12.3)	3.9 (12.8)		3.9 (12.8)	
Vessel height, m (ft)	18.6 (61)	17.1 (56)	20.7 (68)	17.1 (56)	22.6 (74)
Vessel wall thickness, cm (in)	5.7 (2.25)	5.7 (2.25)		5.7 (2.25)	
Refractory thickness, cm (in)	10.2 (4.0)	10.2 (4.0)		10.2 (4.0)	
Vessel weight, Mg (tons)	152 (167)	144 (159)	170 (187)	143 (158)	182 (200)
Internals weight, Mg (tons)	41 (45)	54 (59)	58 (63)	54 (59)	58 (64)
Total filter weight, Mg (tons)	193 (212)	198 (218)	228 (250)	197 (217)	240 (264)

Both the McDermott and the Pall FeAl inverted candle filter systems could use the same number of filter elements as the standard candle design and operate with the same pressure drop as the standard candle filter system design by pulse cleaning more frequently. The pulse cleaning frequency can only be reduced by increasing the filter system pressure drop (not shown) or by increasing the number of filter elements to yield smaller face velocities. For IGCC, the consequences of operating with an increased filter system pressure drop may be very small, especially for an oxygen-blown gasifier application.

Figure 3.39 shows the relation between pulse cleaning frequency, the average pressure drops, and the filter cake maximum thickness for both types of filter systems. It shows that the inverted candle filter system must operate at a higher pulse gas frequency than the standard candle filter system, and the filter cake maximum thickness will be slightly lower. The maximum filter cake thickness must be selected to be sufficiently thick for good pulse cleaning, but not so thick that bridging might be initiated. The filter cakes differ in IGCC from those in PFBC due to their higher flow resistance and lower bulk density.
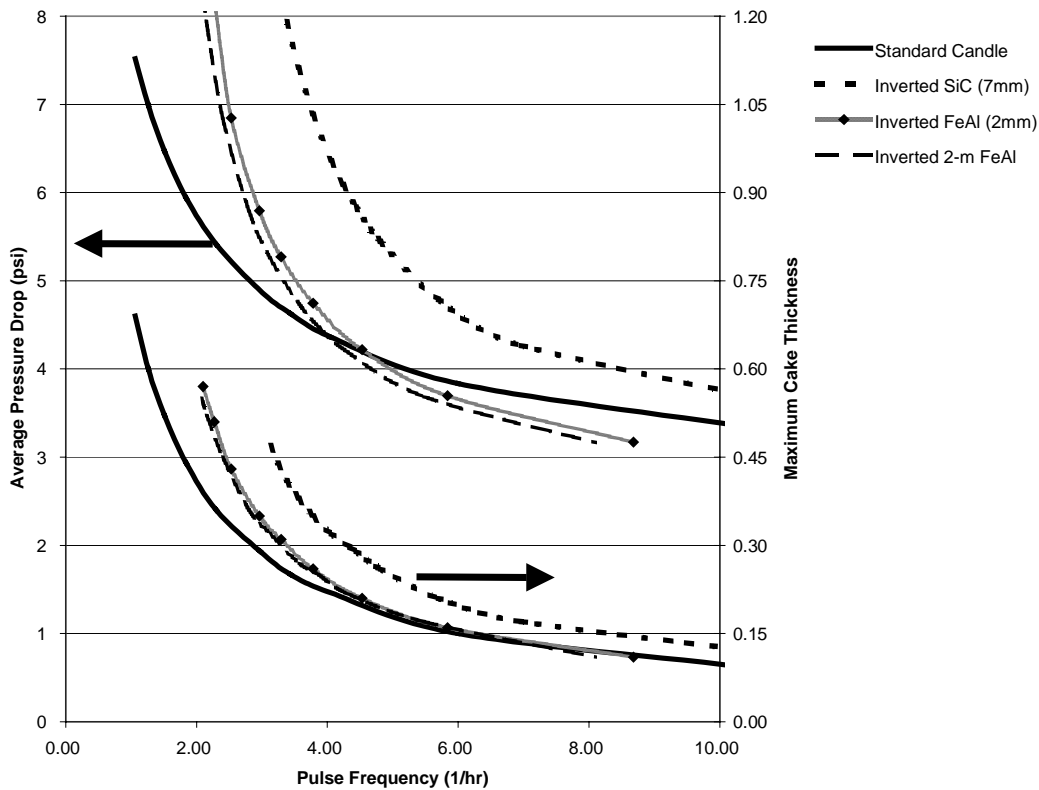
Figure 3.39 - Pressure Drops and Pulse Gas Consumption for IGCC Filters

The standard candle filter system performance is compared to the inverted candle filter systems performance in Table 3.11. The face velocity is based on the dirty surface area of the respective candle type, and the pressure drop includes the conditioned filter element, ash residue, filter cake, vessel gas inlet and outlet nozzles, fail-safe device, and other losses through the internals in the filter vessel. Note that the only performance difference between the top

maintenance and bottom maintenance schemes is the ash storage capacity of the vessels, and these are indicated in the last row of the table. Pulse gas system assumptions applied are:

- pulse gas source pressure: 5516 kPa (800 psia) for standard candles, 6206 kPa (900 psia) for inverted candles,
- pulse gas type: recycled syngas.

The Pall and McDermott inverted candle filter systems must operate with an increased number of filter elements, and Table 3.11 indicates that the face velocities are slightly lower for the McDermott and Pall FeAl inverted candle filter systems and the standard candle filter system, but the face velocity is slightly higher for the Pall SiC inverted candle filter systems. The performance results are identical for the top maintenance and bottom maintenance scheme and Table 3.11 does not distinguish between these except for the ash storage capacity performance. The average pressure drops for the inverted candle filter systems are comparable to that of the standard candle filter system, and the pulse cleaning frequency is significantly greater. The pulse gas consumptions and compressor powers are also larger for the inverted candle filter systems, but these have relatively small cost consequences. For the 2 m long McDermott CFCC and Pall FeAl inverted candle systems, pulse frequencies are slightly lower than for the 1.5 m long inverted candles. The ash storage capacity of the inverted candle filter vessels is considerably larger than that of the standard candle filter vessel. The gas temperature drop across the filter system is about the same for all of the systems, at 3 - 4°C (5 - 7°F).

Table 3.11 - IGCC Application Filter Performance Characteristics

	Standard Candle	Inverted Candle	Inverted Candle	Inverted Candle	Inverted Candle	Inverted Candle
Candle type	Pall SiC, Pall FeAl	Pall 326 SiC	Pall FeAl	Pall FeAl	McDermott CFCC	McDermott CFCC
Candle length (m)	1.5	1.5	1.5	2.0	1.5	2.0
Face velocity, cm/s (ft/min)	2.5 (4.9)	2.6 (5.2)	2.1 (4.2)	2.1 (4.1)	2.4 (4.7)	2.3 (4.6)
Trigger pressure drop, kPa (psi)	33.8 (4.9)	35.2 (5.1)	34.5 (5.0)	33.8 (4.9)	34.5 (5.0)	33.8 (4.9)
Baseline pressure drop, kPa (psi)	30.3 (4.4)	31.0 (4.5)	31.0 (4.5)	30.3 (4.4)	31.0 (4.5)	30.3 (4.4)
Pulse cleaning frequency, 1/hr	3.4	5.7	3.8	3.7	4.8	4.6
Maximum cake thickness, cm (in)	0.64 (0.25)	0.53 (0.21)	0.66 (0.26)	0.66 (0.26)	0.58 (0.23)	0.58 (0.23)
Pulse gas consumption, % of process gas	0.10	0.14	0.09	0.09	0.12	0.12
Pulse gas compressor power, kW	11	19	13	12	16	16
Ash storage capacity, hr (top /bottom maintenance)	2.2	2.5/ 3.6	2.5/ 3.6	2.5/ 4.1	2.5/ 3.6	2.5/ 4.1

The delivered equipment costs, in end-1999-dollars, are listed in Table 3.12. The scope of equipment is the refractory-insulated filter "pressure vessels" (with shroud, tube sheet, metal liners, and maintenance items), the "filter elements" (with gasket sets, nuts & bolts, and fail-safe devices), the clusters, the pulse gas compressor system, and the pulse gas control skids. The assumed filter element costs are:

- Standard Pall 326 SiC candle, 1.5 m long -- $300,
- Standard Pall FeAl candle, 1.5 m long -- $1500,
- Pall 326 SiC (7 mm wall thickness) with inside membrane added, 1.5 m long -- $500,
- Pall FeAl inverted candle, 1.5 m long -- $1500,
- Pall FeAl inverted candle, 2.0 m long -- $2000,
- McDermott 610 CFCC (5 mm wall thickness), 1.5 m long -- $1200 ($300),
- McDermott 610 CFCC (5 mm wall thickness), 2.0 m long -- $1600 ($400).

Two cost levels are assumed for the McDermott inverted candles, the first representing the expected commercial cost of these elements in the near-term. The second represents the long-term cost expectation based on a healthy market and improved fabrication technologies, if production levels increase to several thousand per year.

Table 3.12 - IGCC Filter Cost Breakdowns

	Standard Candle	Standard Candle	Inverted Candle	Inverted Candle	Inverted Candle	Inverted Candle
Candle type	Pall 326 SiC	Pall FeAl	Pall 326 SiC	Pall 326 SiC	Pall FeAl	Pall FeAl
Candle length (m)	1.5	1.5	1.5	1.5	1.5	1.5
Candle cost, $	300	1500	500	500	1500	1500
Maintenance type			Top	Bottom	Top	Bottom
Pressure vessels	2,356	2,356	2,298	2,546	2,298	2,546
Filter elements	1,201	3,893	1,985	1,985	4,685	4,685
Clusters	3,117	3,117	3,960	4,140	3,960	4,140
Pulse gas compressor system	657	657	762	762	762	762
Pulse gas control skids	1,163	1,163	1,163	1,163	1,163	1,163
Total	8,494	11,186	10,168	10,596	12,868	13,296

Table 3.12 - IGCC Filter Cost Breakdowns (continued)

	Inverted Candle	Inverted Candle	Inverted Candle	Inverted Candle	Inverted Candle	Inverted Candle
Candle type	Pall FeAl	Pall FeAl	McDerm. 610 CFCC	McDerm. 610 CFCC	McDerm. 610 CFCC	McDerm. 610 CFCC
Candle length (m)	2.0	2.0	1.5	1.5	2.0	2.0
Candle cost, $	2000	2000	1200 (300)	1200 (300)	1600 (400)	1600 (400)
Maintenance type	Top	Bottom	Top	Bottom	Top	Bottom
Pressure vessels	2,289	2,664	2,298	2,546	2,289	2,664
Filter elements	4,667	4,667	3,875 (1,445)	3,875 (1,445)	3,832 (1,326)	3,832 (1,326)
Clusters	3,394	3,666	3,960	4,140	3,394	3,666
Pulse gas compressor system	620	620	762	762	620	620
Pulse gas control skids	898	898	1,163	1,163	898	898
Total	11,868	12,515	12,058 (9,628)	12,486 (10,056)	11,033 (8,527)	11,680 (9,174)

The standard candle filter system cost using Pall FeAl candles is about 32% higher than the standard candle filter system cost using Pall 326 SiC candles and the more expensive

standard candles may be used in practice because they may provide higher availability for the filter system. Several of the inverted candle filter systems have the potential for lower-to-comparable cost than that of the standard candle filter system that uses Pall FeAl candles (Pall 326 (7 mm wall) with top and bottom maintenance; Pall FeAl with 2 m length and top maintenance; McDermott 610 CFCC with 2 m length, having a cost of $1600 each, and with top or bottom maintenance). The inverted candle filter system using McDermott inverted candles 2 m long and costing $300 has an estimated cost comparable to the standard candle filter system cost using Pall 326 SiC candles. The inverted candle filter system cost represents an equipment cost of only about 21 - 33 $/kW, a small percentage of the IGCC power plant cost. The greatly improved inverted candle filter system availability, according to the Base Program evaluation, will provide for a significantly lower operating and life-cycle cost for the entire IGCC power plant.

4. SHEET HOT GAS FILTER

Section 4 reviews the sheet hot gas filter engineering and test work completed in the program. It discusses the sheet filter element procurement, the test unit hardware development and fabrication, the cold flow and high-temperature testing, and the test data evaluation and interpretation.

4.1 SHEET FILTER ELEMENT PROCUREMENT

Before sheet filter element procurement activities could be initiated, an initial design evaluation of the sheet filter body and flange was conducted so that detailed specifications could be prepared. Ceramic and metal sheet filter flange design and body features (wall thickness, internal ribs, etc.) were assessed through finite element simulation of transient thermo-mechanical behavior. Detailed finite element simulations of sheet filter elements constructed from the various ceramic materials that are candidates for commercial development were completed. Designs with internal support ribs ranging in number from none to two were specified for the various materials. These analyses are presented in Appendix B of this report. The ceramic sheet filter flange design was based on the current, successful experience with standard ceramic candle filter elements, as well as on past test and design evaluations conducted on cross-flow filter element flanges (Lippert et al., 1993B).

Candidate ceramic and metal filter element vendors for the sheet filters were identified and discussions were held with them to identify issues and estimate the manufacturing feasibility of the sheet filters in the reference size conceived, 0.3 m x 0.3 m (1-ft x 1-ft). The specifications for the sheet filter were compiled and detailed drawings were prepared so that discussions with potential sheet filter manufacturers could proceed. The specification sheet filter wall thickness selected for all of the ceramic materials is 0.76 cm (0.3-inches), with the number of internal ribs depending on the specific ceramic material to be used. A drawing of a sheet filter having a single internal rib is shown in Figure 4.1. The single rib provides enough support for the sheet filter to withstand the maximum pressure and thermal stresses expected in operation. Note that the flange shape is much like the flange shape that has been in use with standard candle filter elements.

SWPC proprietary technical specifications were submitted to nine filter element suppliers, requesting a cost quotation and schedule for the manufacture of ten sheet filter elements. Sheet filter design concepts identified for review included (1) an open internal channel unit; (2) a single internal ribbed unit; and (3) a double internal ribbed unit. Materials selected included oxide-based ceramic monoliths, nonoxide-based ceramic monoliths, oxide-based ceramic composites, and intermetallics.

Figure 4.1 - Sheet Filter Element Design with Single Internal Rib

Return responses to the request for quote for ten sheet filter elements were obtained. Several vendors declined to bid due to the developmental nature of the effort. "Best effort" bids were obtained from some vendors, but were rejected because of their high cost and risk. Acceptable bids were obtained from IF&P REECER (open-channel, recrystallized SiC), Ensto (double-rib, mullite-bonded alumina), Specific Surface (double-rib, cordierite), and Blasch (double-rib, mullite-bonded alumina). The Blasch bid was initially rejected due to concern for their specific low-strength matrix, and orders were placed with IF&P, Ensto, and Specific Surface. Early in the fabrication period, Specific Surface indicated that they would be unable to obtain the required cordierite material for the sheet filter fabrication. Since the unique aspect of the Specific Surface sheet filter was its cordierite material, it was decided to replace this vendor with the Blasch double-ribbed sheet filter, representing a unique configuration meriting testing. During the fabrication period, Ensto had difficulties fabricating the sheet filter element and could not meet the program schedule or cost, so their efforts were halted.

After the remaining two sets of sheet filter elements were received, they were examined and room temperature gas flow resistances were measured. The dimensions of the Blasch and IF&P REECER sheet filter elements were acceptable. A photograph of the two sheet filter elements is shown in Figure 4.2. The flow resistances of both were below the SWPC candle

70

filter element gas flow resistance specification of 2.5 kPa at 0.05 m/s face velocity (10 iwg at 10 ft/min), with measurements of 1.3 kPa (5.25 iwg) and 0.3 kPa (1.2 iwg), respectively.

Figure 4.2 - IF&P REECER (black) and Blasch (white) Sheet Filter Elements

4.2 SHEET FILTER TEST HARDWARE

The sheet filter element is a more unusual and uncertain ceramic filter element design than the inverted candle filter element, having little fabrication and testing experience. Past experiences with the related cross-flow filter element raised concern that the flange, gasketing, holding mechanism, and fixturing to keep damaged sheet filter elements locked in position were critical to the success or failure of the sheet hot gas filter system. The sheet filter gasket and holder designs were reviewed based on standard candle filter element experience, past testing, and designs of cross-flow filter gaskets and holders. The sheet filter clamping-holder design was conceived for initial thermo-mechanical evaluation. The holder shape is based on the standard ceramic candle filter element holder design. The sheet filter fail-safe/regenerator design was reviewed and upgraded, but was not included in the testing. A drawing of the sheet filter element, with its clamping flange holder and its fail-safe device, is shown in Figure 4.3.
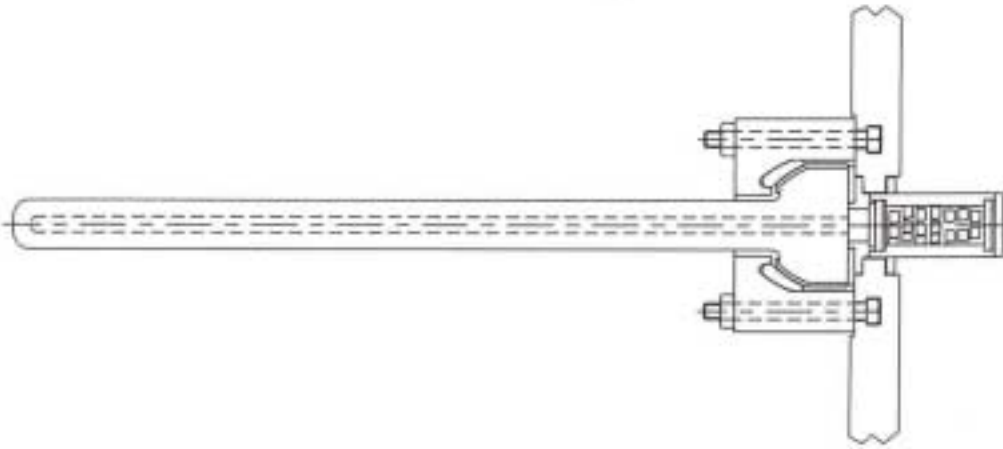
Figure 4.3 - Sheet Filter Element with Flanged Holder and Fail-safe

Fixture designs to keep the sheet filter element locked in position if it were damaged were also proposed and assessed. An initial "tray" configuration was selected due to its simplicity, limited interference with the sheet filter element surface areas, and its limited tendency to accumulate ash. Figure 4.4 illustrates the overall sheet filter element cluster configuration with a metal tray supporting each sheet filter element body. A metal wire is attached to the top to the cluster that supports the trays to minimize creep effects. The ability of the tray device to support a failed sheet filter element will depend on the nature of the failures that might be characteristic of the sheet filter element, and these can only be identified in high-temperature testing of prototype elements.

Prototype gaskets for the sheet filter elements were fabricated and received for evaluation, but the initial design was not acceptable. Discussions were held with the gasket supplier and identified the need for modification of the lower gasket, as well as suggestions for modification of the ceramic pad between the filter element side-wall and supporting metal ledge. Prototype gaskets were fabricated via die cutting multi-layers and limited stitching. The gasket utilized along the top of the flange and below the metal housing remained unchanged (i.e., lapped fabric with a seam). A preliminary mock-up of a Blasch sheet filter element with the gasket assembly and metal hold-down was acceptable.
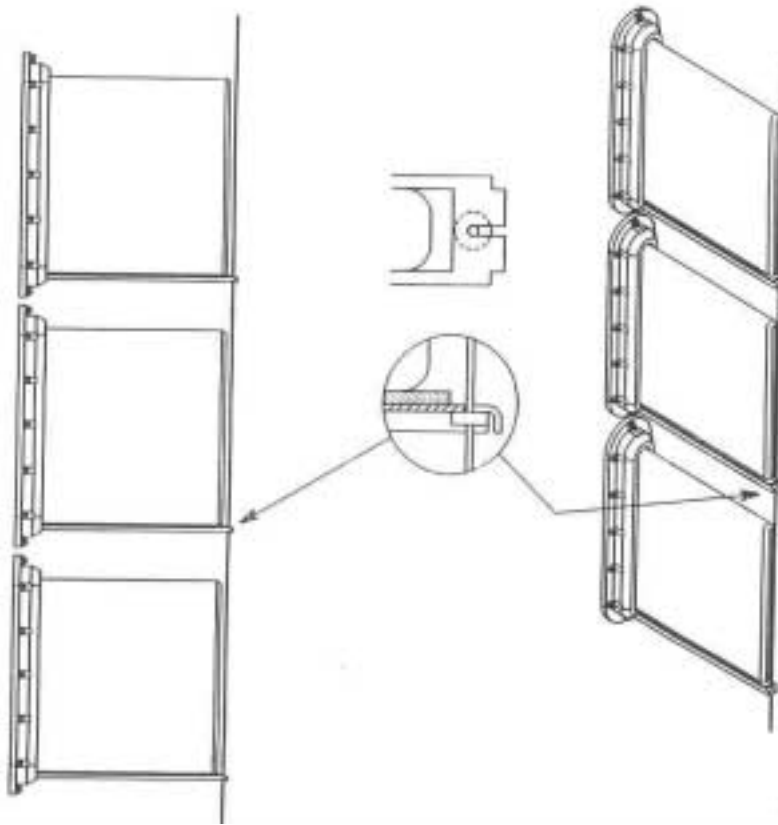
Figure 4.4 - Sheet Filter Element Retainer Tray Arrangement

Test hardware to hold two parallel sheet filter element clusters, with four sheet filter elements on each cluster, for testing in the cold flow test unit and in the HTHP test rig, was designed. The hardware was arranged to provide simulation of element-to-element, and cluster-to-cluster spacing and their impacts on pulse cleaning and ash bridging, duplicating key features expected in a commercial design. Detailed design of the sheet filter test hardware was completed and the equipment was fabricated. A photograph of the sheet filter element test clusters is shown in Figure 4.5. The photo shows the two clusters mounted in the cold flow unit tube sheet, and with the IF&P REECER recrystallized SiC sheet filter elements attached. The large, horizontal brace on the top of each cluster holds the support wire for the sheet filter retainer trays.

Figure 4.5 - Sheet Filter Test Clusters

4.3 EXPERIMENTAL - SHEET FILTER COLD FLOW TESTS

A set of cold flow tests to visually observe sheet filter element pulse cleaning, and filter cake buildup, and initiations of potential ash bridge accumulations were conducted in the ceramic barrier filter, Plexiglas, cold flow test rig. A set of eight sheet filter elements were installed in the test clusters fabricated for the program. Two independent plenums were used so that independent pulse cleaning of half of the sheet filter elements at a time could be completed.

The tests measured the sheet filter pressure drop and pulse cleaning performance at the reference PFBC design face velocity for the sheet filter of about 0.046 m/s (9 ft/min), as well as lower velocities representative of IGCC applications. One objective of the testing was to observe the accumulation and release of filter cake from the sheet filter elements to see if the mechanism of ash release was as expected, and to detect if there were any detrimental interactions between neighboring sheet filter elements. It was also a focus of the testing to demonstrate, under cold conditions, the short-term durability of the sheet filter elements.

High-speed photographic records of pulse cleaning were combined with pressure drop measurements to assess the performance. Test parameters included the level of ash load on the

sheet filter elements, and the pulse cleaning intensity. The cold flow nominal test conditions are listed in Table 4.1.

Table 4.1 - Sheet Filter Cold Flow Nominal Test Conditions

Temperature, °C (°F)	21 (70)
Pressure, kPa (atm)	122 - 203 (1.2-2.0)
Filter type	IF&P Recrystallized SiC Blasch Mullite-bonded Alumina
Number of filters installed	8
Face velocity, m/s (ft/min)	0.024 - 0.048 (4.7 - 9.4)
Gas flow, m^3/s (acfm)	0.034 - 0.071 (72 -151)
Ash type	Karhula Lakeland
Ash flow, kg/hr (lb/hr)	about 1.4 - 4.5 (3-10)
Ash flow (ppmw)	4,000 - 10,000

Description of the Testing

The sheet filter cold flow testing was initiated using the IF&P recrystallized SiC sheet filter elements, conducting five days of testing. A total of 34 kg (75 lb) of Lakeland flyash was fed during these tests. A series of tests were completed at a face velocity of about 0.046 m/s (9 ft/min) where a nominal 7.5 kPa (30 iwg) filter cake pressure drop was accumulated and then pulse cleaned at various pulse intensities. The pulse cleaning events were observed and video movies were taken of some of the events. The filter cake pulse cleaning performance was very good, with almost 100% pressure drop recovery at very low pulse intensities. Compared to standard candle filter element pulse cleaning, it appears that much lower pulse supply pressures could be applied with the sheet filter elements, with a significant reduction in pulse gas consumption resulting. Observations of the cleaning events showed that the filter cake was gently lifted horizotally from the filter surface as a sheet, and then this sheet of ash dropped as a single mass with little dust generation and re-entrainment. The pulse cleaning was seen to be uniform across the top and bottom sheet filter element locations on each plenum.

The testing was continued with thicker filter cakes and higher pressure drops. One IF&P recrystallized SiC sheet filter element collapsed during one of the filter cake accumulation sequences. Only one piece of the sheet filter element fell into the ash hopper. The outer, curved edges of the sheet filter element were not damaged and were held in place by the clamping holder. The other flat, fractured sections had been squeezed together from both sides, implying that the damage was done during forward air flow and not during pulse cleaning, and these fractured pieces were retained on the support tray. Pictures were taken, the broken sheet filter element was removed, and the pieces reassembled for further photographs. It is not known if the original sheet filter element had a defect or if the recrystallized SiC sheet filter elements were too weak for this service. Figure 4.6 shows a photograph of the broken sheet filter element as seen through the plexiglas vessel wall.

Figure 4.6 - Broken Sheet Filter Element in Cold Flow Test

The damaged IF&P recrystallized SiC sheet filter, after removal of the internals from the vessel and cleaning, is shown in Figure 4.7. The sheet filter elements are still mounted in their holders in this photograph. Here, the collapsed-nature of the sheet filter is clearly seen.

IF&P recrystallized SiC sheet filter element testing continued. The series of tests were at face velocities ranging from 0.024 to 0.048 m/s (4.7 to 9.4 ft/min), with the total pressure drop across the cold flow unit being limited such that thicker filter cake accumulations required lower face velocities. Trigger pressure drops in the testing ranged from 352 to 627 kPa (51 to 91 iwg), baseline pressure drops ranged from 159 to 276 kPa (23 to 40 iwg), and filter cake estimated thickness ranged from 0.20 to 1.37 cm (0.08 inches to 0.54 inches). Thick filter cakes were accumulated to see if any signs of potential ash bridging could be observed. The pulse cleaning events were observed and video records were made of some of these events. IF&P recrystallized SiC sheet filter element testing was terminated when another sheet filter element broke. The fractured sheet filter element looked very similar to the first, but more pieces dropping off of the holder. It is suspected that the recrystallized SiC material, having no internal ribs, is weaker than originally expected.

**Figure 4.7 - Damaged IF&P Recrystallized SiC Sheet Filter Element
in a Cold Flow Test**

The unit was disassembled and the Blasch Mullite-bonded Alumina sheet filter elements were installed. Cold flow testing continued with the Blasch Mullite sheet filter elements, conducting ten days of testing. A total of 133 kg (294 lb) of flyash was fed. Testing was completed, operating over a large range of variations in trigger pressure drop (filter cake thickness) and pulse pressure. The same kind of outstanding pulse cleaning performance was observed with the Blasch sheet filter elements and no sheet filter element breakage occurred. The internal ribs apparently provided sufficient strength for the Blasch sheet filter elements to withstand the pressure stresses. The Blasch sheet filter elements remained in the cold flow unit with filter cakes attached for several months. When they were removed and cleaned the surfaces of the sheet filter elements had a flaked appearance as though the surface had been pulled off in small patched (Figure 4.8).

Figure 4.8 - Damaged Surface of Blasch Sheet Filter Element after Cold Flow Tests

4.4 RESULTS AND DISCUSSION - INTERPRETATION OF SHEET FILTER COLD FLOW TESTING

The cold flow test results for both types of sheet filter elements are summarized in three figures. Figure 4.9 shows the quantity of pulse gas delivered in the sheet filter cold flow tests, expressed as the mass of pulse gas per sheet filter element. Over the range of pulse source pressures, 138 to 345 kPa (20 to 50 psig), the pulse gas delivery ranged from about 0.0045 to 0.0136 kg (0.01 to 0.03 lb) per sheet filter. The higher source pressure resulted in greater pulse gas delivery, although the fate of the pulse gas (delivered to the sheet filter elements or bypasses to the vessel head) is not known.
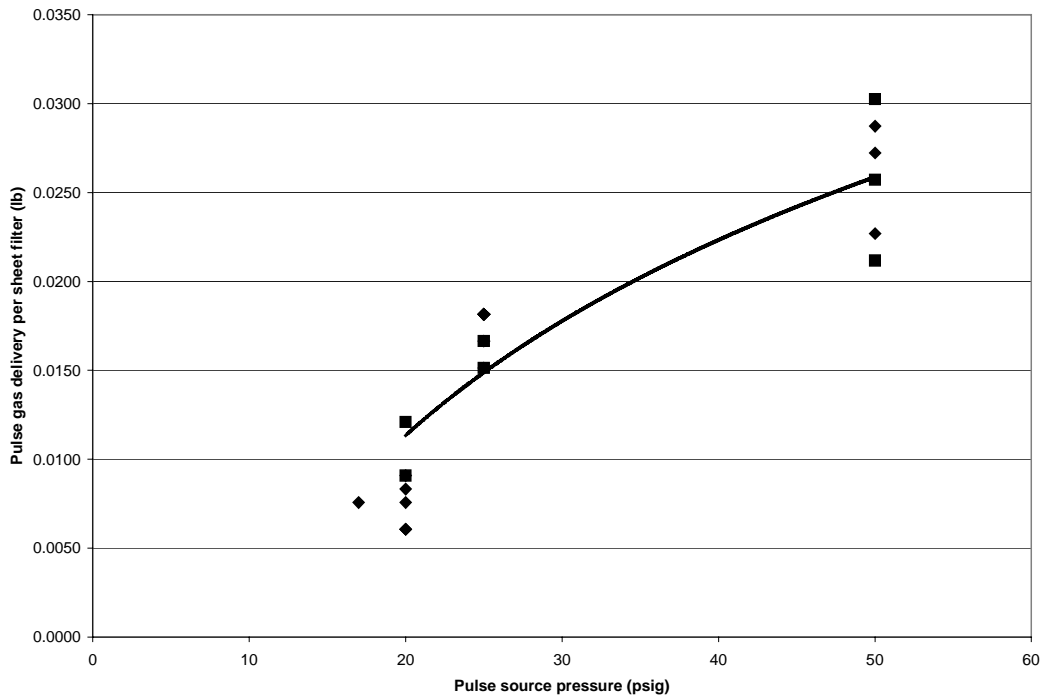
Figure 4.9 - Sheet Filter Cold Flow Test Pulse Gas Use

Figure 4.10 shows the pressure drop recovery measured in the tests as a function of the pulse gas source pressure. Little variation in the pressure drop recovery is shown over the range of pulse source pressures, and the recovery is very near unity. This implies that the sheet filter elements can be effectively cleaned with very low pulse intensity, conserving pulse gas and minimizing sheet filter element thermal shock.
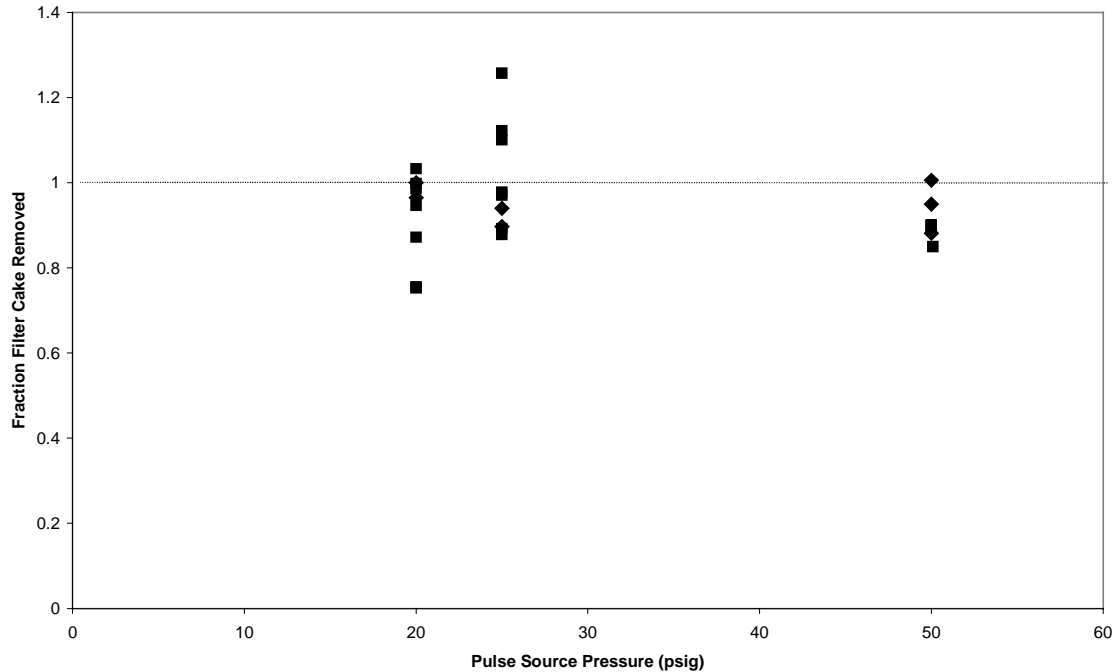
Figure 4.10 - Sheet Filter Cold Flow Pressure Drop recovery

Observations of the pulse cleaning events found that the entire sheet filter element, filter cake was relatively gently lifted from the filter element surface and then dropped as large agglomerate streams into the vessel hopper. The lower source pressure reduced the cake lift and minimized dust formation. In some cases the sheet filter elements pulse cleaning was repeated after the initial pulse clean and this resulted in further small, but measurable pressure drop recovery.

Figure 4.11 shows the total permeance of the two types of sheet filter elements (filter element and residue) as a function of the number of pulse events. Both sheet filter types showed a rapid decrease in permeance after several pulse cleanings and were quite similar in their behavior. The Blasch sheet filter elements were tested long enough to show a clear leveling off of the permeance at an acceptable value of about 25% of the clean element permeance.

The major conclusions from the cold flow sheet filter system testing are:

- The filter cake pulse cleaning performance was very good, with almost 100% pressure drop recovery at very low pulse intensities.

- Compared to standard candle filter system pulse cleaning, it appears that much lower pulse supply pressures could be applied with the sheet filter elements, with a significant reduction in pulse gas consumption resulting.
- The IF&P recrystallized SiC sheet filter elements were apparently too weak to hold up to the filtering pressure stresses in the tests, and two sheet filter elements were broken during the cold flow tests.
- The Blasch mullite sheet filter elements, with a pair of internal ribs, suffered no damage in the tests.
- The filter cake release phenomena appears relatively gentle and should be effective for limiting ash bridge formation that might result from released ash.
- Testing with filter cake thickness up to 12.7 mm (0.5-inch) showed no signs of ash bridge formation and resulted in no pulse cleaning difficulties.
- There appeared to be no detrimental interactions between neighboring sheet filter elements in the tests.
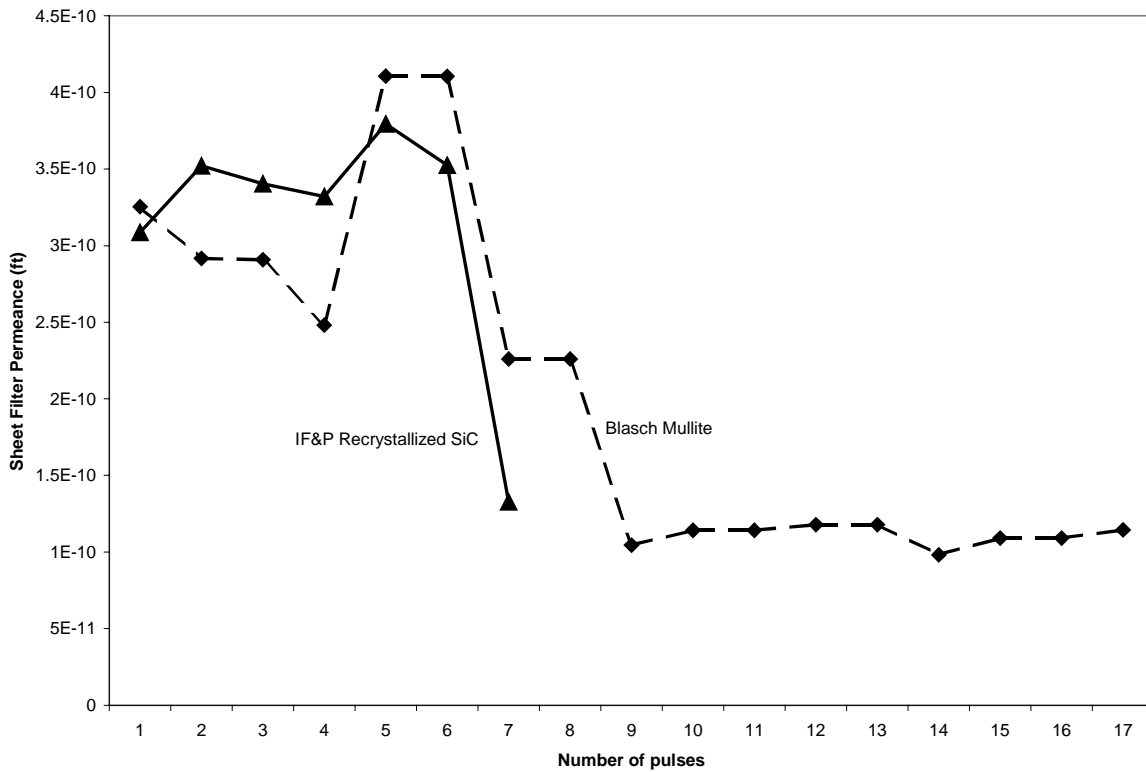
Figure 4.11 - Sheet Filter Cold Flow Total Permeance

4.5 EXPERIMENTAL - SHEET FILTER HIGH-TEMPERATURE TESTS

In the bench-scale, high-temperature test program, the overall operating performance of the Blasch sheet filter system was assessed in terms of:

- filtration efficiency of the sheet filter system,
- baseline pressure recovery and pulse cleaning requirement (gas quantity and pressure),
- effectiveness of dust cake removal along the filtration surface of the sheet filter elements,
- conditioned filter element pressure drop,
- reliability of the gasket seal and mounting configuration.
- elimination of ash bridges between adjacent sheet filter elements,
- retention of clean gasket seals,
- short-term durability of the filter body and flange (i.e., absence of crack formations; retention of the as-manufactured dimensional tolerances).

The Blasch sheet filter elements were fitted with high-temperature gasket sets and were installed in the high-temperature plenums. They were attached to the HTHP filter unit tube sheet as shown in Figure 4.12.

Figure 4.12 - Blasch Sheet Filter Elements Installed for HTHP Testing

A series of high-temperature tests with eight of the Blasch sheet filter elements was conducted in the existing high-temperature, high-pressure, barrier filter test rig. The tests addressed steady-state filtration performance of the sheet filter element array operated at relatively low-temperature PFBC conditions. Table 4.2 shows the high-temperature test matrix. It lists the test number and date, the nominal test temperature and face velocity, the trigger and

baseline pressure drops, the ash outlet concentration resulting from ash leaks in the system, and the hours of testing. Key comment are included on the condition of the equipment and the maximum filter cake thickness estimated for some of the tests.

Table 4.2 - Sheet Filter High-Temperature Test Matrix and Results

Test # (date)	Temp °C (°F)	Face velocity m/s (ft/min)	Trigger DP kPa (iwg)	Baseline DP kPa (iwg)	Ash leak (ppmw)	Test hours	Comments
1 (5/7)	538 (1000)	0.016 (3.2)			21-57	9.1	No pulses; tube sheet dust leak
2 (5/8)	"	"			up to 123	9.5	No pulses; tube sheet dust leak
3 (5/9)	"	"			100	5.8	No pulses; tube sheet dust leak
4 (5/10)	"	"	11 (44)	3 (12)	100	8.3	One pulse; tube sheet dust leak
5 (5/11)	"	"			NM	5.4	No pulses; tube sheet dust leak
6 (5/16)	"	"			normal	3.3	Tube sheet dust leak corrected; flame problems
7 (5/17)	"	0.017 (3.3)			normal	10.0	Dust feed problems
8 (5/18)	593 (1100)	0.030 (5.9)			normal	2.5	Dust feed problems
9 (5/29)	"	0.029 (5.7)			normal	5.0	Dust feed problems
10 (5/30)	"	0.033 (6.4)			NM	3.3	Dust feed fixed; pulse doesn't work; tube sheet dust leak
11 (6/6)	566 (1050)	0.030 (6.0)	19 (78)	9 (38)	20-30	8.3	6 pulses; cake up to 0.3 inch thick
12 (6/7)	"	0.016 (3.2)	18 (72)	4 (18)	20-30	9.2	2 pulses; cake up to 0.6 inch thick
13 (6/8)	538 (1000)	"	18 (73)	4 (17)	25	8.3	1 pulse; dust feed line rupture
14 (6/11)	"	"			NM	6.6	No pulse; dust feed line rupture
15 (6/12)	"	"	18 (72)	4 (16)	20-30	9.2	1 pulse
16 (6/13)	566 (1050)	"	17 (70)	5 (19)	50	9.2	2 pulses; dust feed line rupture; cake up to 0.6 inch thick
17 (6/14)	760 (1400)	0.020 (4.0)	18 (72)	8 (34)	50	8.3	1 pulse; cake up to 0.4 inch thick
18 (6/15)	"	"	21 (83)	10 (40) (7 with 2 pulses)	NM	5.0	2 pulses; cake up to 0.45 inch thick
19 (6/18)	"	"			500-700	3.3	No pulse; broken sheet filter
20 (6/21)	"	"	18 (72)	6 (25)	500	3.3	1 pulse; broken sheet filter
21 (7/9)	538 (1000)	0.029 (5.8)	20 (82)	10 (42)	100	8.3	5 pulses; cake up to 0.35 inch thick
22 (7/10)	"	0.030 (6.0)	21 (84)	11 (45)	100	6.7	5 pulses; cake up to 0.35 inch thick

NM: not measured

Twenty-two test runs were conducted. A relatively low pulse gas intensity was used in all of the test runs, with the source pressure only about 698 kPa (100 psi) about the vessel pressure. The same Karhula PFBC ash used in the inverted candle testing was used in the sheet

filter testing. All of the tests were performed at about 10-atmospheres vessel pressure and the inlet ash flow varied from 2,000 to 4,000 ppmw.

About 148 hours of testing was completed, where this is defined as the hours of ash feeding, with the unit at full test temperature and gas flow. Of the 22 test runs, 15 of them were disrupted by ash feed problems, flame problems, tube sheet ash leaks, or broken sheet filter elements. Only 4 test runs showed ash leakage at normal test facility background levels, all the others having significant ash leaks due to tube sheet seals, sheet filter gaskets, or damaged sheet filter elements. Due to a desire to test the sheet filter elements at severe conditions with thick filter cakes, only 26 pulse events were completed in the total campaign. Over the course of the testing, the sheet filter element flow resistance (average for the 8 filter elements in the unit) increased from about 1.5×10^9 ft^{-1} at their initial condition, to about 2.9×10^9 ft^{-1}. The only sheet filter element breaks (2 severely fractured sheets) occurred during the 4 tests operated at 760°C (1400°F). The sheet filters appeared to tolerate the 538-593°C (1000-1100°F) test conditions, at least without major fractures.

Test results from three of the better test runs are shown to illustrate the Blasch sheet filter behavior. Two curves are shown for Test Run 11 (6/6/2001), tested at nominally 538°C (1000°F). Figure 4.13 shows the pressure drop and face velocity profiles during test run 11, indicating 6 pulse cleaning events and good baseline pressure drop recovery. A relatively small dust leak was proceeding during this test. Figure 4.14 displays the estimated filter cake thickness based on an assumed value for the Karhula ash permeability. Note that the estimated cake thickness following each pulse event assumes that the residual cake has the same permeability as the fresh filter cake, and this is known not to be a valid assumption. Thus, the minimum cake thickness is expected to be less than this estimated value, with in turn means that the maximum cake thickness is overestimated.

Two curves are shown for Test Run 18 (6/15/2001), tested at nominally 760°C (1400°F). Figure 4.15 shows the pressure drop and face velocity profiles during test run 18, indicating 2 pulse cleaning events. The second pulse event consisted of two pulses in rapid succession, resulting in high baseline pressure drop recovery. Figure 4.16 displays the estimated filter cake thickness.

Finally, two curves are shown for Test Run 21 (7/9/2001), tested at nominally 538°C (1000°F), following the runs at 760°C (1400°F). Figure 4.17 shows the pressure drop and face velocity profiles during Test Run 21, indicating 5 pulse cleaning events, and the baseline pressure drop recovery looks excellent. A fairly large dust leak was proceeding during this test. Figure 4.18 displays the estimated filter cake thickness during the test run.
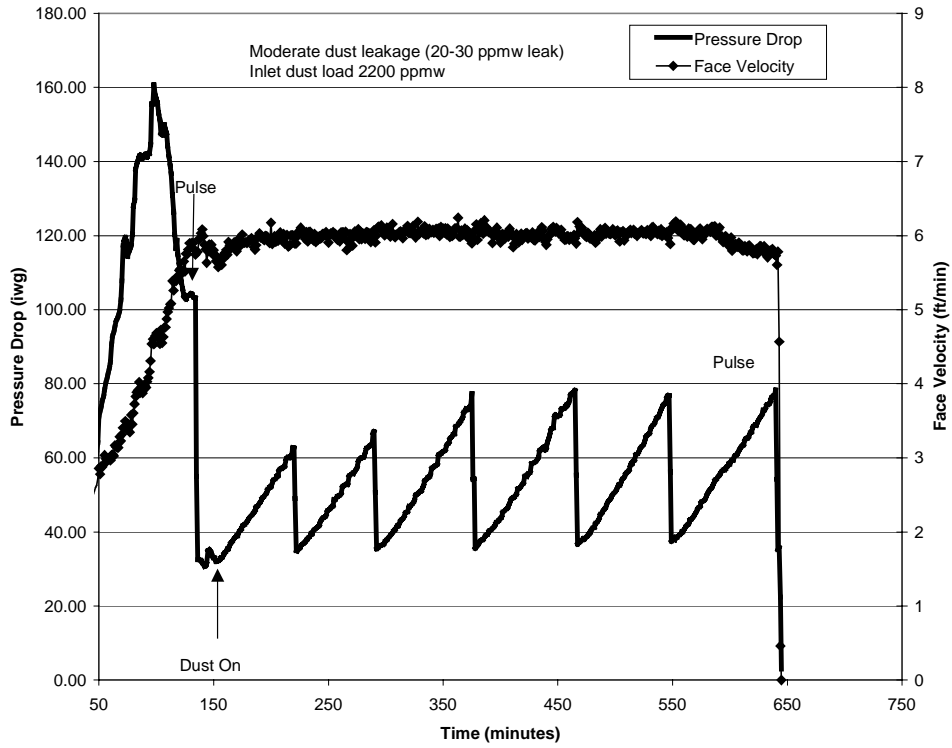
Figure 4.13 - Run 11 Pressure Drop and Face Velocity
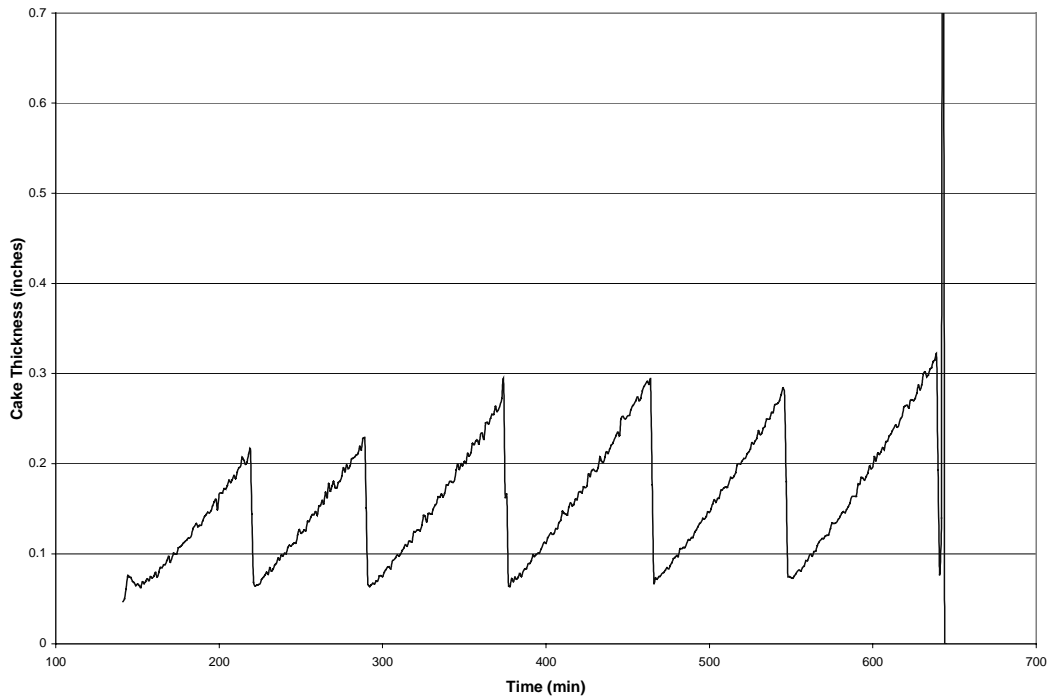
Figure 4.14 - Run 11 Estimated Filter Cake Thickness

84
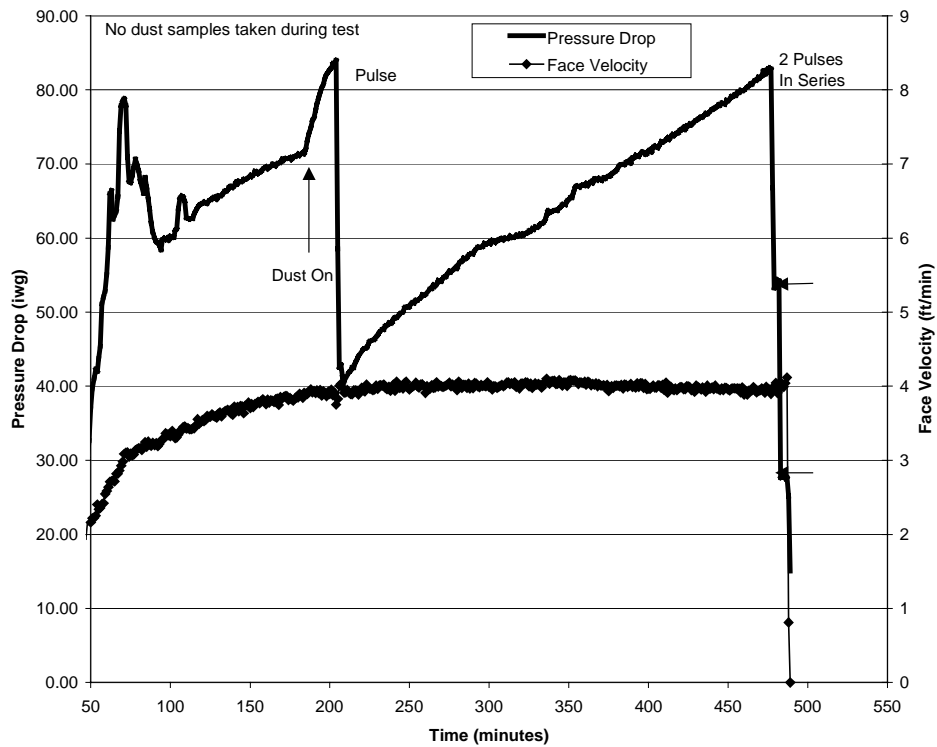
Figure 4.15 - Run 18 Pressure Drop and Face Velocity
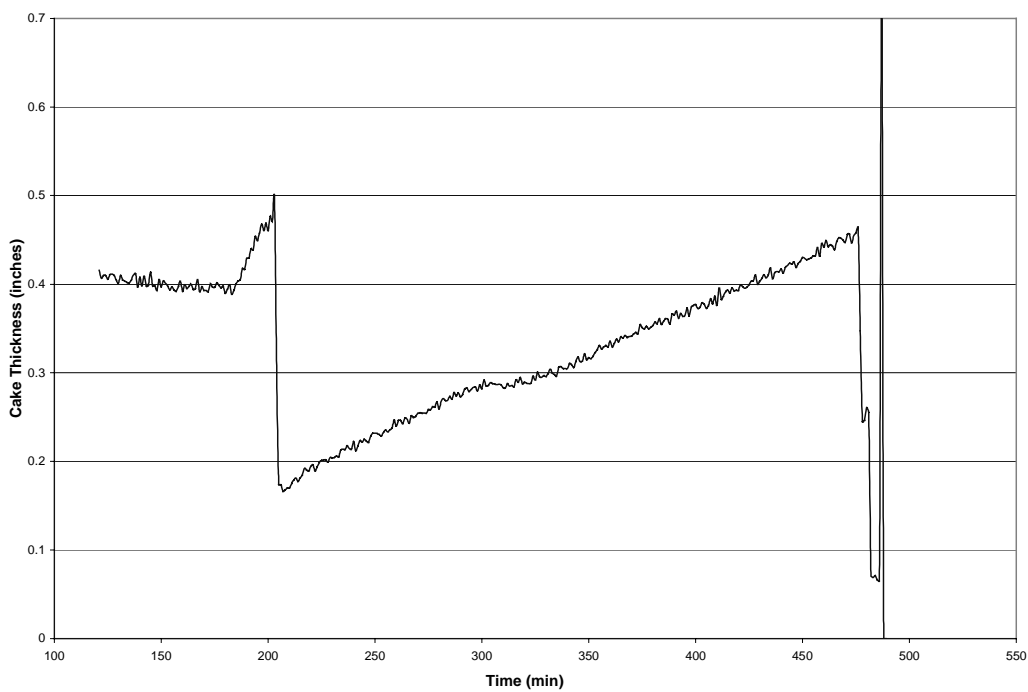
Figure 4.16 - Run 18 Estimated Filter Cake Thickness

85
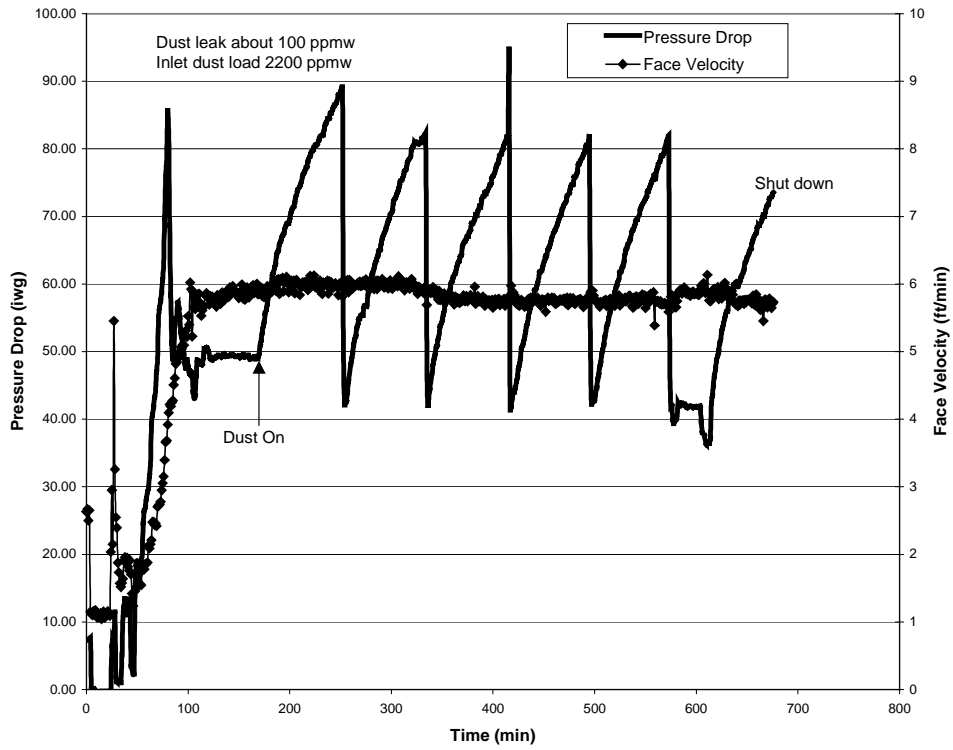
Figure 4.17 - Run 21 Pressure Drop and Face Velocity
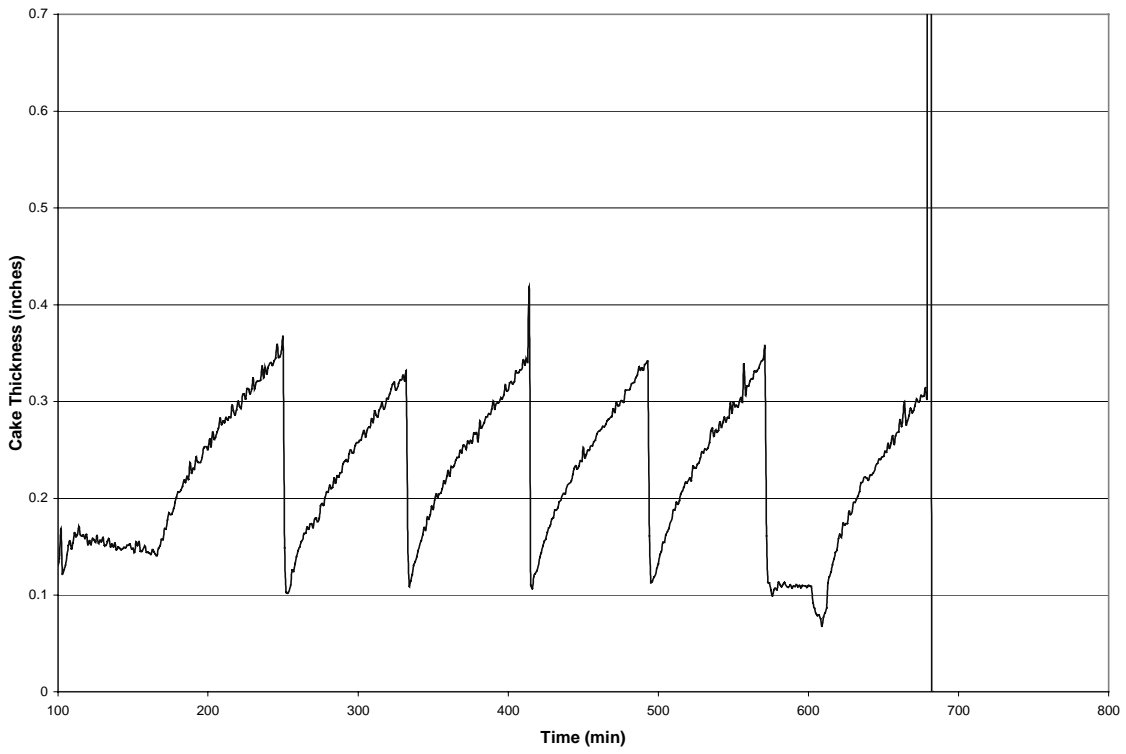
Figure 4.18 - Run 21 Estimated Filter Cake Thickness

86

HTHP testing was halted because of a suspected large leak. The unit was opened and the internals were lifted from the pressure vessel to find that one of the Blasch sheet filter elements had broken. It is shown in Figure 4.19. The break was on one side only and was along a horizontal line that corresponds to the bottom of one of the internal ribs. The broken piece had dropped off of the retainer tray.

Figure 4.19 - Broken Blasch Sheet Filter Element in HTHP Tests

Because extensive ash feeding had occurred on these sheet filter elements during this test sequence, examination showed thick filter cakes accumulated on the sheet filter elements, with deep piles of ash, of about 25 mm (1 inch), on the sheet filter tops and on nuts & bolts. Figure 4.20 shows photographs of the ash accumulation. The vertical, metal sections between parallel sets of sheet filter elements were very clean, as though they were regions of high velocity flow upward. This same behavior was seen in the cold flow tests. Some of the filter element surfaces had filter cakes with very wavy and lumpy ash formations, and it is not known if this is related to the rough appearance of the clean Blasch sheet filter elements or due to gas flow phenomena.

Figure 4.20 - Ash Accumulation on Sheet Filter Elements During HTHP Testing

Sheet Filter Post Test Examinations

The sheet filter test assembly was examined for signs of bridging between the filter elements and for patterns of pulse released ash. The sheet filter elements subjected to the high-temperature test conditions were examined. The pattern of ash accumulation on the filter elements was examined. Specific attention was given to the flange area of the elements to assure that the process and/or metal holder design had not induced the formation of cracks in this region of the filter element. In addition, the performance of the gasketing seals were evaluated after the tests.

At the end of the last ash accumulation test period in the sheet filter test program, one plenum was pulsed while the remaining plenum was left with its accumulated ash. When the pressure vessel had cooled, and the tube sheet and plenums were raised from the vessel, the two plenums were inspected. None of the eight sheet filter elements had broken. Observation of the plenum that had been pulse cleaned showed that only the two sheet filter elements in the bottom position had received significant cleaning. The two bottom sheet filter element had very thin filter cakes remaining while the two top sheet filter elements on this plenum had thick filter cakes of about 0.8 to 1.0 cm (0.3 to 0.4 inch) thickness. Figure 4.21 shows photographs of these bottom two sheet filter elements. The thick cakes had "sand dune" appearance at their surfaces. The plenum that was not pulsed (Figure 4.22) had uniformly thick filter cakes on both the top and bottom sets of sheet filter elements, looking much like the filter cakes on the top position of the plenum that had been pulse cleaned.

Similar behavior had previously been observed with cross-flow filters that were pulse cleaned as a vertical array, and the distribution of the pulse gas to the sheet filters would need to be induced to be more uniform by changes in the geometry of the sheet filter plenum for this to be a successful gas filtering system. Alternatively, had larger pulse gas source pressures been applied, the sheet filter plenums might have cleaned more effectively, but a larger plenum having numerous levels of sheet filter elements might not clean the elements uniformly. It should also be noted that both of the broken sheet filter elements from the previous runs at 760°C(1400°F) were in the bottom position on the plenum where pulse gas thermal shock would have been worst. As previously observed, in these tests, the metal surfaces of the plenum were very clean between neighboring sheet filter elements, apparently due to high gas flow in those regions, and there was a thick cap, about 2 cm (0.8 inches) in height, on top of each sheet filter element.

Figure 4.21 - Bottom Sheet Filter Elements on Pulsed Plenum

Following visual inspection of the ash accumulation and filter cakes in the test unit, all of the sheet filter elements were removed, cleaning and inspected. The six of the sheet filter elements that had been exposed to 760°C (1400°F) temperatures showed cracking at an almost identical location on the underside of the flange, as seen in Figure 4.23. This location corresponds to the highest point on each sheet filter element as they were installed in the plenums. This may be the point of the greatest flow of cold pulse gas, resulting in thermal shock and cracking. This cracking, that was very hard to see from the dirty-site of the sheet filter element, resulted in an ash leakage path around the gaskets and through the cracks. Significant ash accumulation was found within the two plenums and on top of the vessel tube sheet due to this leakage.

Figure 4.22 - Bottom Sheet Filter Elements on Non-pulsed Plenum
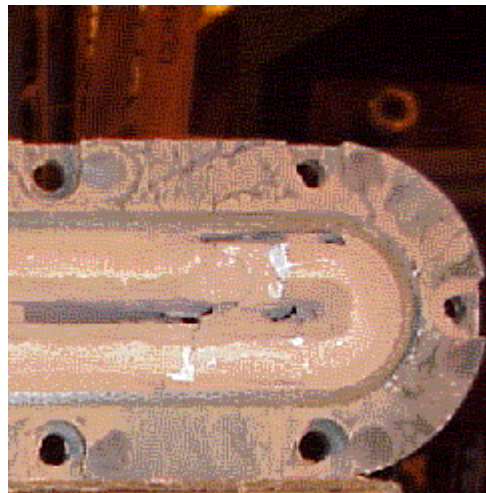
Figure 4.23 - Sheet Filter Element Cracking on the Underside of the Flange

4.6 RESULTS AND DISCUSSION - INTERPRETATION OF SHEET FILTER HIGH-TEMPERATURE TESTING

The Blasch sheet filter, high-temperature test data are assessed with respect both the recorded test performance data and the examinations made to the sheet filter internals following the test runs. The main factors are observations of the sheet filter system ash bridging potential and free-fall ash performance, observations of the retaining tray performance, the filter pulse cleaning performance, and the short-term durability of the filter elements.

Examination of the sheet filter internals following the test runs suggests that the sheet configuration should inherently minimize the potential for ash bridge formation, although large ash accumulations do appear on the top, horizontal edge of each sheet filter element. In a large filter system, with much longer sheet filter clusters, the volume of ash that will be discharged to fall between the channels of sheet filter elements will be much larger (as much as 20 times) than that occurring in the bench-scale testing, and this could result in ash accumulations and jamming not observed in the bench-scale tests.

The two broken sheet filter elements that occurred in the testing were almost completely held in place over the retaining tray, with only small sections dislodged. This behavior was largely due to the position of the horizontal breaks that occurred, the inward squeezing of the sheet plates, and the continued retention of the sheet filter flange in its holder, rather than being due to the retaining tray.

The pulse cleaning performance of the sheet filter system looks good based solely on the test data results, and the test data indicates that the increase in the sheet filter residue flow resistance is relatively small. In contrast, the examination of the sheet filter plenums at the end of the last test run suggests that the distribution of pulse gas is not good, and the bottom sheet filter elements tend to clean much more effectively than the top sheet filter elements. Thus, either the basic configuration of the plenums has to be modified to yield better pulse gas cleaning distribution, or higher pulse gas source pressures are needed to promote better distribution. The two sheet filter element levels in the bench-scale test plenums are not indicative of the behavior that might occur in a large cluster with as many as 30 to 40 sheet filter element levels.

The short-term durability of the Blasch sheet filter elements was not good when exposed to 760°C (1400°F) gas temperature under the severe thermal shock conditions in the tests. Two of the Blasch filter elements fractured, and cracking around the flange was found on all of the elements exposed to these conditions. The utilization of a fail-safe device to provide thermal regeneration of the pulse gas, and the restriction of the maximum operating temperature to about 538°C (1000°F) might result in durable Blasch sheet filter performance. Alternatively, construction of the sheet filter element from CFCC oxide-based ceramic, or non-oxide ceramics, or intermetallics might result in durable sheet filter performance.

It is clear that additional sheet filter element materials testing, and design and fabrication evolution is required. Small-scale testing of the sheet filter configuration, at a scale sufficiently large to expose potential large-scale ash behavior effects, is required before large-scale testing could be merited.

4.7 RESULTS AND DISCUSSION - SHEET FILTER COMMERCIAL COST AND PERFORMANCE UPDATE

Based on the results of the sheet filter testing, the commercial cost and performance, the commercial evaluation update is made assuming a durable sheet filter element exists, the sheet filter cluster can be effectively pulse cleaned using high pulse gas source pressures, and the configuration is resistance to ash bridging. It is also assumed that the sheet filter configuration protects the filter system from cascading filter element damage and ash nozzle plugging or ash handling equipment damage by holding each filter element in the event of a filter fracture. An update of the commercial performance and cost estimates has been generated, but no new availability estimates have been made. The use of larger sheet filter elements does not have the potential to improve barrier filter performance or economics, and the standard 0.3 x 0.3 m dimension is used in the evaluation.

It is clear from the testing that each sheet filter element should include a fail-safe/ regenerator. The sheet filter cluster design is significantly different from the conventional standard candle filter element cluster and detailed design and fabrication techniques will need to be devised to commercialize the configuration. The pressure vessel diameter can be reduced with some arrangements of the sheet filter clusters because they can overlap slightly. A shroud to protect the sheet filter elements from direct impingement by the inlet gas stream is needed, and a top shroud design is used that is similar to that used for standard candle filter elements. Maintenance on the sheet filter elements requires access to the internals through manways and the ability to rotate the clusters, or the addition of maintenance structures within the vessel, much as is done with the standard candle filter system.

PFBC Application

The evaluation update for PFBC applies a 314 MWe PFBC power plant hot gas filter system and the following operating conditions, as taken from the Base Program report:

- gas flow, m^3/s (acfm):   5,764 (203,539),
- gas temperature, °C (°F):   871 (1600),
- gas pressure, kPa (psia):   1296 (188),
- inlet dust load, ppmw: 6,525.

The characteristics of a standard candle hot gas filter system design for this application is compared to a sheet hot gas filter system design in Table 4.3. Both filter system designs use the same number of parallel filter vessels, the sheet filter vessel holding fewer filter clusters. The sheet filter system supports a greater number of filter elements than the standard candle filter system, and the cluster structure is larger in diameter and slightly longer. Because there are four clusters of sheet filter elements in the vessel, and because they can overlap slightly, the vessel diameter is smaller that for the standard candle filter system.

The standard candle filter vessels and sheet filter vessels both have shrouds that completely surround the top section of the clusters and promotes inlet gas flow upward initially. The shroud permits direct access to the cluster filter elements for inspection and maintenance through the vessel manways. The sheet filter vessels are more compact and lighter than those for the standard candle filter system.

Table 4.3 - PFBC Hot Gas Filter System Design Characteristics

	Standard Candle	Sheet Filter
Filter Element type	Pall 326 SiC	Unidentified
Number of parallel vessels	8	8
Number clusters per vessel	5	4
Number elements per cluster	187	326
Total number elements	7,480	10,432
Cluster diameter, m (ft)	1.02 (3.33)	1.09 (3.56)
Cluster length, m (ft)	10.2 (33.3)	12.0 (39.3)
Shroud type	Complete top shroud	Complete top shroud
Vessel OD, m (ft)	3.7 (12.2)	3.3 (10.8)
Vessel height, m (ft)	20.7 (68)	21.6 (71)
Vessel wall thickness, cm (in)	3.2 (1.25)	2.9 (1.13)
Refractory thickness, cm (in)	20 (8)	20 (8)
Vessel weight, Mg (tons)	147 (162)	128 (141)
Internals weight, Mg (tons)	36 (40)	29 (32)
Total filter weight, Mg (tons)	183 (202)	157 (173)

The standard candle filter system performance is compared to the sheet filter system performance in Table 4.4. Filter element and ash characteristics measured in this program have been used to make these estimates, applying SWPC proprietary filter models. The face velocity is based on the dirty surface area of the respective filter element type. The pressure drop includes the conditioned filter element, ash residue, filter cake, vessel gas inlet and outlet nozzles, fail-safe device, and other losses through the internals in the filter vessel.

Figure 4.24 shows the general relation between pulse cleaning frequency, the trigger and baseline pressure drops, and the pulse gas consumption rates for both type of filter systems. It shows that the sheet filter system must operate at a slightly higher pulse gas frequency than the standard candle filter system in most cases, but the pulse gas consumption rate is slightly lower. The figure does not include the other key performance variable, the maximum filter cake thickness, which must be selected to be sufficiently thick for good pulse cleaning, but not so thick that bridging might be initiated.

The sheet filter system cannot achieve the same pressure drop as the standard candle filter system when designed with the same number of filter elements because its face velocity would be too high. It must operate with an increased number of filter elements, and Table 4.4 indicates that the face velocity is about the same for both filter systems. The average pressure drop across the sheet filter system is slightly lower than that of the standard candle filter system, and the pulse cleaning frequency slightly greater.

These operating conditions have been selected to result in an acceptable maximum filter cake thickness in the two filter systems. The pulse gas consumption and compressor power use are both relatively small. Heat losses through the vessels, including mixing with the pulse gas, is acceptable. The ash storage time in the filter vessels, that is, the time before damage could occur to the lowest levels of filter elements in the vessel, if ash drainage was stopped, is relatively large. The distribution of pressure losses in the filter systems is also noted in Table 4.4, and the lower pressure loss across the fail-safe devices in the sheet filter, because of a larger number of filter elements, provides a lower pressure drop in the sheet filter system.

Table 4.4 - PFBC Application Hot Gas Filter System Performance Characteristics

	Standard Candle	Sheet Filter
Face velocity, m/s (ft/min)	0.048 (9.5)	0.050 (9.8)
Trigger pressure drop, kPa (psi)	24.8 (3.6)	24.1 (3.5)
Baseline pressure drop, kPa (psi)	23.4 (3.4)	22.8 (3.3)
Pulse gas type	air	air
Pulse gas source pressure, kPa (psia)	4137 (600)	3447 (500)
Pulse cleaning frequency, 1/hr	1.33	1.63
Maximum cake thickness, cm (in)	0.61 (0.24)	0.58 (0.23)
Pulse gas consumption, % of process gas	0.07	0.05
Pulse gas compressor power, kW	42	27
Gas temperature loss, °C (°F)	4 (8)	4 (7)
Ash storage capacity, hr	4.3	3.7
Cleaned system minimum pressure drop distribution, kPa (psi)		
gas inlet nozzle, shroud and outlet nozzle	3.59 (0.52)	4.4.1 (0.64)
conditioned filter elements	8.00 (1.16)	8.14 (1.18)
re-entrained filter cake	1.79 (0.26)	0.41 (0.06)
fail-safe devices	7.17 (1.04)	3.79 (0.55)
plenum & flow pipes	-0.69 (-0.10)	-0.28 (-0.04)
eductors	2.00 (0.29)	3.03 (0.44)
Total	21.86 (3.17)	19.51 (2.83)

The delivered equipment costs, in end-1999-dollars, are listed in Table 4.5. The scope of equipment supply is the insulated filter pressure vessels (with shroud, tube sheet, metal liners, and maintenance items), the filter elements (with gasket sets, nuts & bolts, and fail-safe devices) the clusters, the pulse gas compressor system, and the pulse gas control skids.

Table 4.5 - PFBC Hot Gas Filter System Cost Breakdowns

	Standard Candle (k$)	Sheet Filter (k$)
Pressure vessels	8,362	7,145
Filter elements	4,002	4,642
Clusters	8,448	8,277
Pulse gas compressor system	1,953	1,960
Pulse gas control skids	3,946	3,241
Total	26,711	25,265

The sheet filter system cost is about 5% less than the standard candle filter system cost, and represents an equipment cost of about 80 $/kW. This result is somewhat sensitive to the price of the sheet filter elements, with the filter elements representing less than 15% of the total filter system cost in Table 4.5. The evaluation assumed the sheet filter element price to be the same as the standard candle element on a per unit surface area basis. The improved availability of the sheet filter system, according to the Base Program evaluation, will provide for a lower

operating and life-cycle cost for the entire PFBC power plant, if this improved availability can be realized.
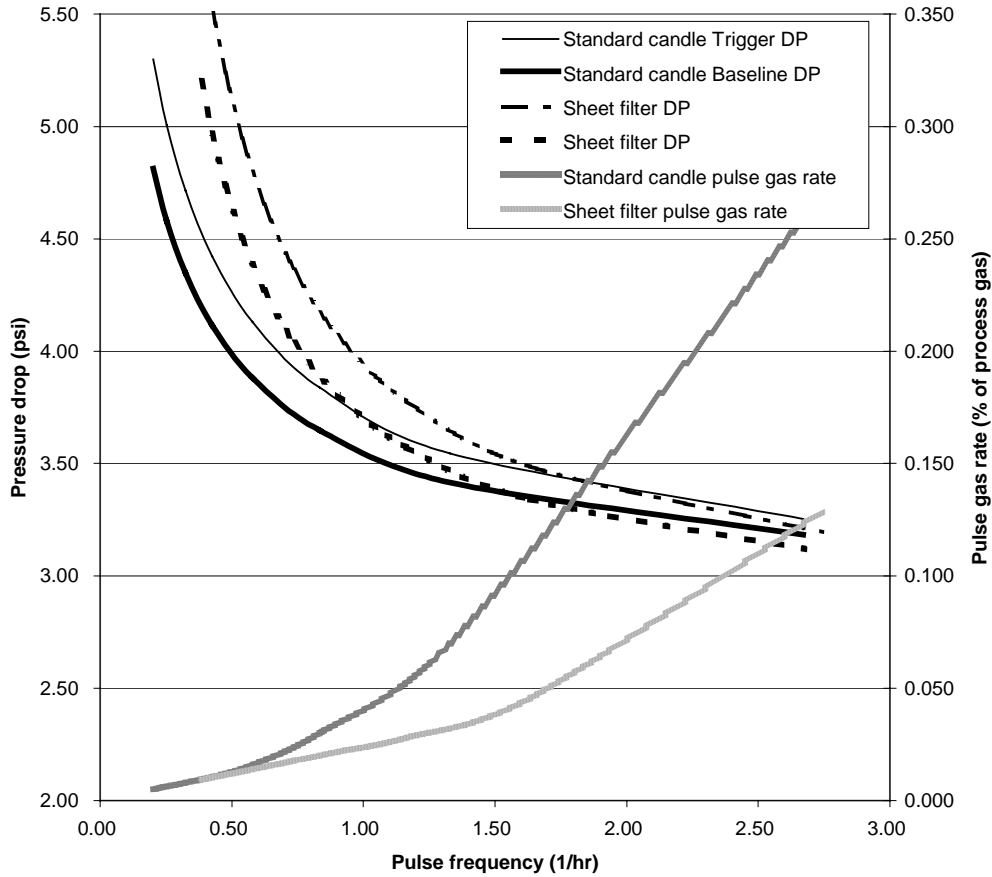
Figure 4.24 - Pressure Drop and Pulse Gas Consumption for PFBC Hot Gas Filter Systems

IGCC Application

The evaluation update for a 406 MWe, air-blown IGCC power plant filter system has the following operating conditions, as taken from the Base Program report:

- gas flow, m^3/s (acfm):   14.4 (30,414),
- gas temperature, °C (°F):   542 (1007),
- gas pressure, kPa (psia):   2620 (380),
- inlet dust load, ppmw: 19,727.

The characteristics of a standard candle hot gas filter system design for this application is compared to a sheet filter system designs in Table 4.6. Again, both filter system designs use the same number of parallel filter vessels, the sheet filter vessel holding fewer filter clusters. The sheet filter system supports a greater number of filter elements than the standard filter system,

and the cluster structure is larger in diameter and slightly longer. Both vessels use a shroud that completely surrounds the top section of the clusters and promotes inlet gas flow upward initially. The shroud permits direct access to the cluster filter elements for inspection and maintenance through the vessel manways. The vessel dimensions and total weight are very similar for the two filter systems. IGCC ash characteristics applied in the Base Program evaluation were applied to make the estimates in the table.

Table 4.6 - IGCC Hot Gas Filter System Design Characteristics

	Standard Candle	Sheet Filter
Element type	Pall 326 SiC	Unidentified
Number of parallel vessels	2	2
Number clusters per vessel	6	5
Number elements per cluster	187	320
Total number elements	2,244	3,200
Cluster diameter, m (ft)	1.02 (3.33)	1.09 (3.56)
Cluster length, m (ft)	10.2 (33.3)	11.6 (38.0)
Shroud type	Complete top shroud	Complete top shroud
Vessel OD, m (ft)	3.7 (12.3)	3.6 (11.9)
Vessel height, m (ft)	20.7 (60)	19.5 (64)
Vessel wall thickness, cm (in)	5.7 (2.25)	5.7 (2.25)
Refractory thickness, cm (in)	10 (4)	10 (4)
Vessel weight, Mg (tons)	151 (166)	153 (169)
Internals weight, Mg (tons)	41 (45)	36 (40)
Total filter weight, Mg (tons)	191 (211)	190 (209)

The standard candle filter system performance is compared to sheet filter system performance in Table 4.7. The face velocity is based on the dirty surface area of the respective filter element type, and the pressure drop includes the conditioned filter element, ash residue, filter cake, vessel gas inlet and outlet nozzles, fail-safe device, and other losses through the internals in the filter vessel. The pulse cleaning frequency can only be reduced by increasing the filter system pressure drop (not shown) or by increasing the number of filter elements to yield smaller face velocities. For IGCC, the consequences of operating with an increased filter system pressure drop may be very small, especially for an oxygen-blown gasifier application.

Figure 4.25 shows the relation between pulse cleaning frequency, the trigger and baseline pressure drops, and the pulse gas consumption rates for both type of filter systems in IGCC. It shows that the sheet filter system must operate at a higher pulse gas frequency than the standard candle filter system, but the pulse gas consumption rate may be slightly lower in some cases. The figure does not include the other key performance variable, the maximum filter cake thickness which must be selected to be sufficiently thick for good pulse cleaning, but not so thick that bridging might be initiated. The filter cakes differ in IGCC from those in PFBC due to their higher flow resistance and lower bulk density.

Table 4.7 - IGCC Application Hot Gas Filter System Performance Characteristics

	Standard Candle	Sheet Filter
Face velocity, m/s (ft/min)	0.024 (4.8)	0.024 (4.7)
Trigger pressure drop, kPa (psi)	39.3 (5.7)	39.3 (5.7)
Baseline pressure drop, kPa (psi)	35.2 (5.1)	34.5 (5.0)
Pulse gas type	recycle fuel gas	recycle fuel gas
Pulse gas source pressure, kPa (psia)	5516 (800)	4826 (700)
Pulse cleaning frequency, 1/hr	4.6	6.0
Maximum cake thickness, cm (in)	0.91 (0.36)	0.81 (0.32)
Pulse gas consumption, % of process gas	0.10	0.12
Pulse gas compressor power, kW	10	13
Gas temperature loss, °C (°F)	3 (6)	3 (6)
Ash storage capacity, hr	1.0	0.9
Cleaned system minimum pressure drop distribution, kPa (psi)		
gas inlet nozzle, shroud and outlet nozzle	9.51 (1.38)	9.51 (1.38)
conditioned filter elements	3.24 (0.47)	3.24 (0.47)
re-entrained filter cake	4.27 (0.62)	1.93 (0.28)
fail-safe devices	4.14 (0.60)	2.07 (0.30)
plenum & flow pipes	-0.41 (-0.06)	-0.21 (-0.03)
eductors	1.17 (0.17)	1.59 (0.23)
Total	21.92 (3.18)	18.13 (2.63)

The delivered equipment costs, in end-1999-dollars, are listed in Table 4.8. The scope of equipment is the insulated filter pressure vessels, with shroud, tube sheet, metal liners, and maintenance items; the filter elements, with gasket sets, nuts & bolts, and fail-safe devices; the clusters; the pulse gas compressor system, and the pulse gas control skids. The sheet filter system cost is about 1% greater than the standard candle filter system cost, and only represents an equipment cost of about 21 $/kW. The improved sheet filter system availability, according to the Base Program evaluation, will provide for a lower operating and life-cycle cost for the entire IGCC power plant

Table 4.8 - IGCC Hot Gas Filter System Cost Breakdowns

	Standard Candle (k$)	Sheet Filter (k$)
Pressure vessels	2,343	2,305
Filter elements	1,201	1,424
Clusters	3,117	3,035
Pulse gas compressor system	657	701
Pulse gas control skids	1,163	987
Total	8,371	8,452
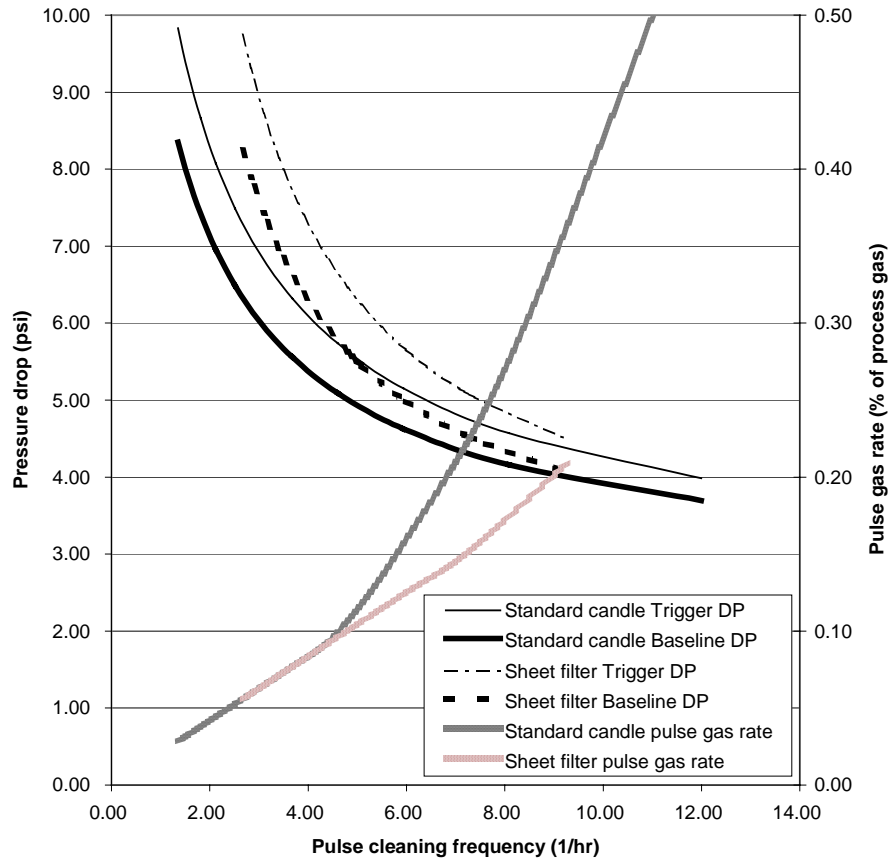
Figure 4.25 - Pressure Drops and Pulse Gas Consumption for IGCC Hot Gas Filter Systems

5. CONCLUSIONS AND RECOMMENDATIONS

Two advanced, hot gas, barrier filter concepts have been proposed by the Siemens Westinghouse Power Corporation to improve the reliability and availability of barrier filter systems in applications such as PFBC and IGCC power generation. The two hot gas, barrier filter concepts, the inverted candle filter system and the sheet filter system, were the focus of bench-scale cold flow and high-temperature testing, and commercial performance and cost evaluations to assess their feasibility as viable barrier filter systems.

Inverted Candle Filter System

The program results show that the inverted candle filter system has the potential to be a highly reliable, commercially successful, hot gas filter system. Some types of thin-walled, standard candle filter elements can be used directly as inverted candle filter elements, and the development of a new type of filter element is not required. Six types of inverted candle filter elements were procured and assessed in cold flow and high-temperature test campaigns. The thin-walled McDermott 610 CFCC inverted candle filter elements, and the thin-walled Pall iron aluminide inverted candle filter elements are the best candidates for the continued development of the inverted candle filter system based on the results of this program. Both of these inverted candles can be manufactured in lengths of 1.5 and 2 m. A hypothetical, clay-bonded SiC inverted candle, having 7 mm wall thickness, 1.5 m length, and inside membrane may also be a good candidate because of its potential low cost.

Depending on the commercial costs of the inverted candle elements, and the vessel maintenance configuration, the estimated capital cost of the inverted candle filter system ranges from 0 to 40% greater than the capital cost of the standard candle filter system in PFBC and IGCC applications. The availability, operating cost and life-cycle cost of the inverted candle filter system is expected to be superior to that of the standard candle filter system, and this will result in improved power plant cost-of-electricity.

The inverted candle filter system is recommended for continued development through larger-scale testing in a coal-fueled test facility. Testing under IGCC conditions is desirable because this clean-coal, power generation technology has great market potential, and inverted candle filter system testing in an IGCC environment has not been previously conducted. In response to this recommendation, 55 inverted candle containment pipes have been fabricated and shipped to the Southern Company Services, Power Systems Development Facility, in Wilsonville, AL, for future pilot testing on a barrier filter system exposed to syngas from a developing, transport gasifier.

Specific inverted candle filter testing and commercial evaluation conclusions are:
- dust penetration measured during most of the testing was at normal levels for standard candle filter elements, indicating no unusual leak paths existed during the tests,

- the inverted candles all were durable at the test conditions (high-temperature with severe thermal shock events), except the monolithic, oxide-based inverted candles (Coors and Ensto), which fractured,

- the inverted candle gaskets were taken directly from standard candle practice and were durable at the test conditions, showed no signs of significant ash leaks,

- plugging of the inverted candle bore, or excessive ash re-entrainment are not expected with inverted candles,

- the filter cake pressure drop behavior and pulse cleaning frequency was consistent with theoretical expectations - - that is, the pressure drop increases faster than it would using standard candle filter elements, and the pulse cleaning frequency is then greater,

- thin-walled inverted candles, having wall thickness of 5 mm or less, are desirable when using 60 mm OD candles,

- all of the inverted candles tested appear to have comparable performance, but the thin-walled McDermott 610 CFCC and Pall FeAl inverted candles provide the greatest performance and cost advantages,

- a pulse gas source pressure at least 2400 kPa (350 psi) above the filter vessel pressure, improves the cleaning performance, reduces the pulse cleaning frequency and ensures that a stable baseline pressure drop is achieved,

- the residue pressure drop is independent of the filter element geometry, and is influenced most strongly by the nature of the ash, the operating temperature, and the pulse cleaning source pressure,

- it may be desirable in some cases for the inverted candle ID to be larger than 50 mm (as large as 90 to 100 mm), especially for IGCC applications where the filter cakes are less permeable, in order to reduce the pulse cleaning frequency and promote pulse cleaning effectiveness.

- increased temperatures result in linear reduction in residue permeability and the associated need for more frequent pulse cleaning,

- broken inverted candles are retained within their containment pipes, and the cascading damage done to other filter elements in the standard candle filter system, with the potential plugging of the ash outlet nozzle, is eliminated.

With respect to availability, it is expected that the inverted candle filter configuration has the potential to provide protection against ash bridging, filter element vibration, elongation and deformation, vessel overfilling, and various process upsets. The inverted candles also protect the filter system from cascading filter element damage and ash nozzle plugging, or ash handling equipment damage by containing each filter element in the event of a filter fracture.

In PFBC applications, the thin-walled, McDermott inverted candle, and a hypothetical SiC inverted candle having 7 mm thick wall, appear to be the best choices with respect to both performance and cost. The hot gas filter system cost is a substantial portion of the total PFBC plant cost, and the hot gas filter economics may be an issue. For inverted candles having 1.5 m length, the inverted candle filter system cost is about 10 - 40% greater than the standard candle filter system cost, and represents an equipment cost of about 93 - 122 $/kW. The greatly improved availability of the inverted candle filter system will provide for a significantly lower operating and life-cycle cost for the entire PFBC power plant. The use of inverted candles having 2 m length, coupled with the improved availability of the inverted candle filter system, would improve PFBC power plant economics significantly. The McDermott inverted candles have the potential to be manufactured in 2 m lengths.

In air-blown IGCC, the barrier filter system is a relatively small portion of the total plant cost, and in oxygen-blown IGCC the filter system is even a smaller portion of the plant cost.

Thus, in IGCC, the cost of the filter system using 1.5 m long inverted candles would be acceptable, especially when the improved availability of the plant is considered. The standard candle filter system using Pall FeAl candles is estimated to be about 32% more expensive than a standard candle filter system using Pall SiC candles. For IGCC applications, either the thin-walled McDermott, the thin-walled, Pall FeAl inverted candles, or the hypothetical clay-bonded SiC inverted candles having 7 mm wall thickness would be best, depending on the corrosive nature of the fuel gas. For 1.5 m long inverted candles, the inverted candle filter system cost is about 14-56% greater than the cheapest standard candle filter system cost, but only represents an equipment cost of about 24-33 $/kW. The greatly improved inverted candle filter system availability will provide for a significantly lower operating and life-cycle cost for the entire IGCC power plant. Both the McDermott and Pall FeAl inverted candles have high potential for fabrication as 2 m long inverted candles, providing significant filter system cost advantage.

Sheet Filter System

The sheet filter system has not reached the same level of development as the inverted candle filter system, and it will require significantly more design development, filter element fabrication development, small-scale testing and evaluation before larger-scale testing could be recommended. Two types of sheet filter elements were procured and assessed in the program through cold flow and high-temperature testing. The Blasch, mullite-bonded alumina sheet filter element is the only candidate currently approaching qualification for continued development testing, although many other types of ceramic and metal sheet filter elements could be fabricated. The estimated capital cost of the sheet filter system is comparable to the capital cost of the standard candle hot gas filter system for both PFBC and IGCC applications, although this cost estimate is very uncertain because the commercial price of sheet filter element manufacturing has not been established. The sheet filter system, in principle, could result in a higher reliability and availability than the standard candle filter system, but not as high as that of the inverted candle filter system.

The major conclusions drawn for the sheet filter system are:

- the filter cake pulse cleaning performance is very good, with almost 100% pressure drop recovery at very low pulse intensities,

- compared to standard candle pulse cleaning, it appears that much lower pulse supply pressures could be applied with the sheet filters, with a significant reduction in pulse gas consumption resulting,

- the IF&P recrystallized SiC sheet filters were apparently too weak to hold up to the pressure stresses in the tests, and two sheet filters were broken during the cold flow tests, while the Blasch mullite sheet filters, with a pair of internal ribs, suffered no damage in these tests,

- the filter cake release phenomena appears relatively gentle and should be effective for limiting bridge formation that might result from released ash,

- testing with filter cake thickness up to 1.3 cm (0.5-inches) showed no signs of bridge formation and resulted in no pulse cleaning difficulties,

- there appeared to be no detrimental interactions between neighboring sheet filter elements in the tests,

- two fractured Blasch sheet filters resulted in HTHP testing at 760°C (1400°F),

- flanges on all of the Blasch sheet filter elements subjected to 760°C (1400°F) were cracked,

- the Blasch sheet filters apparently tolerated the bench-scale testing conducted at 538°C (1000°F),

- pulse cleaning distribution on the sheet filter plenums favored cleaning of the sheet filters located at the bottom position with the low pulse intensity conditions in the high-temperature tests.

6. REFERENCES

Alvin, M. A. et al., "Filter Component Assessment," paper presented at the Advanced Coal Based Power and Environmental Systems `97 Contractor's Review Meeting, Pittsburgh, PA, July 22-24, 1997 (Available at www.netl.doe.gov -- select publications, then Advanced Coal Based Power and Environmental Systems Conference, then Session 3A).

Alvin, M. A., "Assessment of Ceramic and Metal Filters in Advanced Power Systems," Proceedings of ASME Turbo Expo 2001, New Orleans, LA, June 2001.

Newby, R. A., G. J. Bruce, M. A. Alvin, T. E. Lippert, "Optimization of Advanced Filter Systems -- Base Contract Topical Report," Report to DOE/NETL under contract DE-AC26-97FT33007, April 1998.

Bishop, B., and N. Raskin, "CeraMem Filter Development Program," Proceedings of the Advanced Coal-Fired Power Systems '96 Review Meeting, 1996 (Available at www.netl.doe.gov -- select publications, then Advanced Coal Based Power Systems '96 Review Meeting).

Lippert, T. E., M. A. Alvin, and E. E. Smeltzer., "Subpilot Scale Gasifier Evaluation of Ceramic Cross Flow Filter," Final Report to DOE under Contract No. DE-AC21-88MC24021, August 1993.

Lippert, T. E., E E. Smeltzer, M. A. Alvin, and D. M. Bachovchin, "Long Term Durability Testing of Cross Flow Filter," Final Report to DOE under Contract No. DE-AC21-87MC24022, August 1993.

6. ACRONYMS AND ABREVIATIONS

CFCC: continuous fiber ceramic composite

DOE: U.S. Department of Energy

FeAl: iron aluminide

HTHP: high-temperature, high-pressure

ID: inner diameter

IF&P: Industrial Filter and Pump, Inc.

IGCC: integrated gasification combined cycle

OD: outer diameter

PFBC: pressurized fluidized bed combustion

SiC: silicon carbide

SWPC: Siemens Westinghouse Power Corporation

APPENDIX A - INVERTED CANDLE COLD FLOW TESTS -- TABULATED TEST CONDITIONS AND PERFORMANCE RESULTS

Note: values reported in this appendix are presented in English Engineering Units only.

A.1 Tests with 3 Inverted Candles and Forward Flow during Pulse Cleaning (Tests CI-1 through CI-12; CI-22 and CI23)

Table A1 - Test CI-1, 60-mm Inverted Candle Test Results

Test type: 3 Inverted Candles - Forward Flow During Pulse Cleaning					
Run Number:	**CI-1**				
Number of candles:	3				
Candle outer diameter (in):	2.36				
Candle wall thickness (in):	0.4				
Dirty-side mean face velocity (ft/min):	9.64				
Dirty-side filter surface area (ft^2):	1.88				
Candle element permeability (ft^2):	4.2E-11				
Residue layer permeability (ft^2):	1.00E-12				
Cake permeability (ft^2):	5.0E-12				
Gas viscosity (lb/ft-s):	1.24E-05				
Gas density (lb/ft^3):	0.075				
Cake bulk density (lb/ft^3):	30				
Ash fed (lb):	3.89				
Ash feed time (min):	43				
Calculated terms					
Filter radius (in):	0.78				
Air flow rate (lb/hr):	245.17				
Air mean velocity into candle bore (ft/s):	22.82				
Clean element DP (iwg):	7.63				
Ash feed rate (lb/hr):	5.43				
Feed dust loading (lb/lb gas; ppmw):	0.0221	22139			
Dust-to-filter element efficiency (%):	49.82				
Effective dust loading (lb/lb gas; ppmw):	0.0110	11030			
Pulse events					
	Cake Build	**Pulse 1**	**Pulse 2**	**Pulse 3**	**Pulse 4**
Initial DP (iwg):	8	39	24	17	13
Loaded DP (iwg):	39	24	17	13	12
Pulse air released (lb):		0.157	0.188	0.206	0.194
Pulse valve open time (sec):	0.3				
Pulse tank pressure (psig):	50				
Pulse delivery efficiency (%):	40				
Calculated performance terms					
Loaded cake thickness (in):	0.142	0.077	0.044	0.025	0.020
Loaded cake mass (lb):	0.646	0.366	0.215	0.122	0.099
Residue layer thickness (in):	0.000				0.020
Fraction remaining cake removed (%):		0.434	0.412	0.430	0.195
Fraction total initial cake removed (%)		0.434	0.233	0.143	0.037
Candle bore outlet pulse velocity (ft/s):		86.326	94.429	98.256	91.344
Pulse face velocity (ft/min):		29.631	35.482	38.879	36.614
Cake pulse DP (iwg):		95.287	58.891	36.298	18.991

106

Table A2 - Test CI-2, 60-mm Inverted Candle Test Results

Test type: 3 Inverted Candles - Forward Flow During Pulse Cleaning					
Run Number:	CI-2				
Number of candles:	3				
Candle outer diameter (in):	2.36				
Candle wall thickness (in):	0.4				
Dirty-side mean face velocity (ft/min):	9.56				
Dirty-side filter surface area (ft^2):	1.883898				
Candle element permeability (ft^2):	4.2E-11				
Residue layer permeability (ft^2):	1.00E-12				
Cake permeability (ft^2):	5.0E-12				
Gas viscosity (lb/ft-s):	1.24E-05				
Gas density (lb/ft^3):	0.075				
Cake bulk density (lb/ft^3):	30				
Ash fed (lb):	4.66				
Ash feed time (min):	50				
Calculated terms					
Filter radius (in):	0.78				
Air flow rate (lb/hr):	243.14				
Air mean velocity into candle bore (ft/s):	22.63				
Clean element DP (iwg):	7.56				
Ash feed rate (lb/hr):	5.59				
Feed dust loading (lb/lb gas; ppmw):	0.0230	22999.48			
Dust-to-filter element efficiency (%):	40.34				
Effective dust loading (lb/lb gas; ppmw):	0.0093	9277.94			
Pulse events					
	Cake Build	**Pulse 1**	**Pulse 2**	**Pulse 3**	**Pulse 4**
Initial DP (iwg):	12	42	26	16	13
Loaded DP (iwg):	42	26	16	13	12
Pulse air released (lb):		0.206	0.218	0.236	0.206
Pulse valve open time (sec):	0.3				
Pulse tank pressure (psig):	50				
Pulse delivery efficiency (%):	40				
Calculated performance terms					
Loaded cake thickness (in):	0.138	0.068	0.020	0.005	0.000
Loaded cake mass (lb):	0.627	0.323	0.098	0.025	0.000
Residue layer thickness (in):	0.004				0.004
Fraction remaining cake removed (%):		0.485	0.695	0.745	1.000
Fraction total initial cake removed (%)		0.485	0.358	0.117	0.040
Candle bore outlet pulse velocity (ft/s):		111.723	103.783	108.043	93.088
Pulse face velocity (ft/min):		38.879	41.144	44.541	38.879
Cake pulse DP (iwg):		122.006	60.253	18.636	4.067

Table A3 - Test CI-3, 60-mm Inverted Candle Test Results

Test type: 3 Inverted Candles - Forward Flow During Pulse Cleaning					
Run Number:		CI-3			
Number of candles:		3			
Candle outer diameter (in):		2.36			
Candle wall thickness (in):		0.4			
Dirty-side mean face velocity (ft/min):		9.6			
Dirty-side filter surface area (ft^2):		1.88			
Candle element permeability (ft^2):		4.2E-11			
Residue layer permeability (ft^2):		1.00E-12			
Cake permeability (ft^2):		5.0E-12			
Gas viscosity (lb/ft-s):		1.24E-05			
Gas density (lb/ft^3):		0.075			
Cake bulk density (lb/ft^3):		30			
Ash fed (lb):		4.54			
Ash feed time (min):		50			
Calculated terms					
Filter radius (in):		0.78			
Air flow rate (lb/hr):		244.15			
Air mean velocity into candle bore (ft/s):		22.72			
Clean element DP (iwg):		7.59			
Ash feed rate (lb/hr):		5.45			
Feed dust loading (lb/lb gas; ppmw):		0.0223	22314		
Dust-to-filter element efficiency (%):		42.61			
Effective dust loading (lb/lb gas; ppmw):		0.0095	9508		
Pulse events					
	Cake Build	**Pulse 1**	**Pulse 2**	**Pulse 3**	**Pulse 4**
Initial DP (iwg):	10	41	25	15	13
Loaded DP (iwg):	41	25	15	13	12
Pulse air released (lb):		0.23	0.218	0.218	0.218
Pulse valve open time (sec):	0.3				
Pulse tank pressure (psig):	50				
Pulse delivery efficiency (%):	40				
Calculated performance terms					
Loaded cake thickness (in):	0.142	0.072	0.025	0.015	0.010
Loaded cake mass (lb):	0.645	0.344	0.122	0.074	0.050
Residue layer thickness (in):	0.002				0.012
Fraction remaining cake removed (%):		0.466	0.645	0.392	0.329
Fraction total initial cake removed (%)		0.466	0.344	0.074	0.038
Candle bore outlet pulse velocity (ft/s):		125.603	104.558	101.878	100.564
Pulse face velocity (ft/min):		43.409	41.144	41.144	41.144
Cake pulse DP (iwg):		140.174	64.287	21.429	12.857

Table A4 - Test CI-4, 60-mm Inverted Candle Test Results

Test type: 3 Inverted Candles - Forward Flow During Pulse Cleaning					
Run Number:		**CI-4**			
Number of candles:		3			
Candle outer diameter (in):		2.36			
Candle wall thickness (in):		0.4			
Dirty-side mean face velocity (ft/min):		9.44			
Dirty-side filter surface area (ft^2):		1.88			
Candle element permeability (ft^2):		4.2E-11			
Residue layer permeability (ft^2):		1.00E-12			
Cake permeability (ft^2):		5.0E-12			
Gas viscosity (lb/ft-s):		1.24E-05			
Gas density (lb/ft^3):		0.075			
Cake bulk density (lb/ft^3):		30			
Ash fed (lb):		6.15			
Ash feed time (min):		64			
Calculated terms					
Filter radius (in):		0.78			
Air flow rate (lb/hr):		240.08			
Air mean velocity into candle bore (ft/s):		22.34			
Clean element DP (iwg):		7.47			
Ash feed rate (lb/hr):		5.77			
Feed dust loading (lb/lb gas; ppmw):		0.0240	24015		
Dust-to-filter element efficiency (%):		38.63			
Effective dust loading (lb/lb gas; ppmw):		0.0093	9276		
Pulse events					
	Cake Build	**Pulse 1**	**Pulse 2**	**Pulse 3**	**Pulse 4**
Initial DP (iwg):	13	53	26	14.5	12.5
Loaded DP (iwg):	53	26	14.5	12.5	11.5
Pulse air released (lb):		0.157	0.188	0.206	0.194
Pulse valve open time (sec):	0.3				
Pulse tank pressure (psig):	75				
Pulse delivery efficiency (%):	40				
Calculated performance terms					
Loaded cake thickness (in):	0.180	0.064	0.008	-0.003	-0.008
Loaded cake mass (lb):	0.792	0.304	0.038	-0.013	-0.039
Residue layer thickness (in):	0.006				-0.002
Fraction remaining cake removed (%):		0.616	0.876	1.338	-2.020
Fraction total initial cake removed (%)		0.616	0.337	0.064	0.033
Candle bore outlet pulse velocity (ft/s):		84.483	86.916	92.757	86.208
Pulse face velocity (ft/min):		29.631	35.482	38.879	36.614
Cake pulse DP (iwg):		125.556	48.863	6.178	-1.939

Table A5 - Test CI-5, 60-mm Inverted Candle Test Results

Test type: 3 Inverted Candles - Forward Flow During Pulse Cleaning					
Run Number:		**CI-5**			
Number of candles:		3			
Candle outer diameter (in):		2.36			
Candle wall thickness (in):		0.4			
Dirty-side mean face velocity (ft/min):		9.5			
Dirty-side filter surface area (ft^2):		1.88			
Candle element permeability (ft^2):		4.2E-11			
Residue layer permeability (ft^2):		1.00E-12			
Cake permeability (ft^2):		5.0E-12			
Gas viscosity (lb/ft-s):		1.24E-05			
Gas density (lb/ft^3):		0.075			
Cake bulk density (lb/ft^3):		30			
Ash fed (lb):		7.08			
Ash feed time (min):		74			
Calculated terms					
Filter radius (in):		0.78			
Air flow rate (lb/hr):		241.61			
Air mean velocity into candle bore (ft/s):		22.48			
Clean element DP (iwg):		7.51			
Ash feed rate (lb/hr):		5.74			
Feed dust loading (lb/lb gas; ppmw):		0.0238	23760		
Dust-to-filter element efficiency (%):		33.62			
Effective dust loading (lb/lb gas; ppmw):		0.0080	7987		
Pulse events					
	Cake Build	**Pulse 1**	**Pulse 2**	**Pulse 3**	**Pulse 4**
Initial DP (iwg):	10.5	50.5	24	15	14
Loaded DP (iwg):	50.5	24	15	14	12
Pulse air released (lb):		0.266	0.266	0.278	0.266
Pulse valve open time (sec):	0.3				
Pulse tank pressure (psig):	75				
Pulse delivery efficiency (%):	40				
Calculated performance terms					
Loaded cake thickness (in):	0.179	0.066	0.023	0.018	0.008
Loaded cake mass (lb):	0.793	0.315	0.111	0.087	0.038
Residue layer thickness (in):	0.003				0.011
Fraction remaining cake removed (%):		0.602	0.647	0.217	0.566
Fraction total initial cake removed (%)		0.602	0.257	0.030	0.062
Candle bore outlet pulse velocity (ft/s):		142.951	127.033	131.034	122.132
Pulse face velocity (ft/min):		50.203	50.203	52.468	50.203
Cake pulse DP (iwg):		211.382	71.341	24.853	18.496

Table A6 - Test CI-6, 60-mm Inverted Candle Test Results

Test type: 3 Inverted Candles - Forward Flow During Pulse Cleaning					
Run Number:	**CI-6**				
Number of candles:	3				
Candle outer diameter (in):	2.36				
Candle wall thickness (in):	0.4				
Dirty-side mean face velocity (ft/min):	9.5				
Dirty-side filter surface area (ft^2):	1.88				
Candle element permeability (ft^2):	4.2E-11				
Residue layer permeability (ft^2):	1.00E-12				
Cake permeability (ft^2):	5.0E-12				
Gas viscosity (lb/ft-s):	1.24E-05				
Gas density (lb/ft^3):	0.075				
Cake bulk density (lb/ft^3):	30				
Ash fed (lb):	6.47				
Ash feed time (min):	68				
Calculated terms					
Filter radius (in):	0.78				
Air flow rate (lb/hr):	241.61				
Air mean velocity into candle bore (ft/s):	22.48				
Clean element DP (iwg):	7.51				
Ash feed rate (lb/hr):	5.71				
Feed dust loading (lb/lb gas; ppmw):	0.0236	23628			
Dust-to-filter element efficiency (%):	36.79				
Effective dust loading (lb/lb gas; ppmw):	0.0087	8692			
Pulse events					
	Cake Build	**Pulse 1**	**Pulse 2**	**Pulse 3**	**Pulse 4**
Initial DP (iwg):	10.5	50.5	26	16	13.5
Loaded DP (iwg):	50.5	26	16	13.5	12.5
Pulse air released (lb):		0.242	0.278	0.278	0.252
Pulse valve open time (sec):	0.3				
Pulse tank pressure (psig):	75				
Pulse delivery efficiency (%):	40				
Calculated performance terms					
Loaded cake thickness (in):	0.179	0.075	0.028	0.015	0.010
Loaded cake mass (lb):	0.793	0.358	0.135	0.075	0.050
Residue layer thickness (in):	0.003				0.013
Fraction remaining cake removed (%):		0.549	0.622	0.446	0.329
Fraction total initial cake removed (%)		0.549	0.280	0.076	0.031
Candle bore outlet pulse velocity (ft/s):		133.510	134.517	130.178	116.465
Pulse face velocity (ft/min):		45.674	52.468	52.468	47.561
Cake pulse DP (iwg):		192.310	85.606	30.376	15.019

Table A7 - Test CI-7, 60-mm Inverted Candle Test Results

Test type: 3 Inverted Candles - Forward Flow During Pulse Cleaning					
Run Number:		CI-7			
Number of candles:		3			
Candle outer diameter (in):		2.36			
Candle wall thickness (in):		0.4			
Dirty-side mean face velocity (ft/min):		9.48			
Dirty-side filter surface area (ft^2):		1.88			
Candle element permeability (ft^2):		4.2E-11			
Residue layer permeability (ft^2):		1.00E-12			
Cake permeability (ft^2):		5.0E-12			
Gas viscosity (lb/ft-s):		1.24E-05			
Gas density (lb/ft^3):		0.075			
Cake bulk density (lb/ft^3):		30			
Ash fed (lb):		6.45			
Ash feed time (min):		68			
Calculated terms					
Filter radius (in):		0.78			
Air flow rate (lb/hr):		241.10			
Air mean velocity into candle bore (ft/s):		22.44			
Clean element DP (iwg):		7.50			
Ash feed rate (lb/hr):		5.69			
Feed dust loading (lb/lb gas; ppmw):		0.0236	23605		
Dust-to-filter element efficiency (%):		36.91			
Effective dust loading (lb/lb gas; ppmw):		0.0087	8713		
Pulse events					
	Cake Build	**Pulse 1**	**Pulse 2**	**Pulse 3**	**Pulse 4**
Initial DP (iwg):	11	51	24	16	14
Loaded DP (iwg):	51	24	16	14	13
Pulse air released (lb):		0.305	0.363	0.339	0.351
Pulse valve open time (sec):	0.3				
Pulse tank pressure (psig):	100				
Pulse delivery efficiency (%):	40				
Calculated performance terms					
Loaded cake thickness (in):	0.179	0.064	0.025	0.015	0.010
Loaded cake mass (lb):	0.794	0.305	0.123	0.075	0.050
Residue layer thickness (in):	0.004				0.014
Fraction remaining cake removed (%):		0.616	0.595	0.392	0.329
Fraction total initial cake removed (%)		0.616	0.229	0.061	0.031
Candle bore outlet pulse velocity (ft/s):		163.121	174.762	158.973	162.451
Pulse face velocity (ft/min):		57.564	68.510	63.981	66.246
Cake pulse DP (iwg):		242.885	93.949	33.745	20.964

Table A8 - Test CI-8, 60-mm Inverted Candle Test Results

Test type: 3 Inverted Candles - Forward Flow During Pulse Cleaning					
Run Number:		CI-8			
Number of candles:		3			
Candle outer diameter (in):		2.36			
Candle wall thickness (in):		0.4			
Dirty-side mean face velocity (ft/min):		9.46			
Dirty-side filter surface area (ft^2):		1.88			
Candle element permeability (ft^2):		4.2E-11			
Residue layer permeability (ft^2):		1.00E-12			
Cake permeability (ft^2):		5.0E-12			
Gas viscosity (lb/ft-s):		1.24E-05			
Gas density (lb/ft^3):		0.075			
Cake bulk density (lb/ft^3):		30			
Ash fed (lb):		6.24			
Ash feed time (min):		74			
Calculated terms					
Filter radius (in):		0.78			
Air flow rate (lb/hr):		240.59			
Air mean velocity into candle bore (ft/s):		22.39			
Clean element DP (iwg):		7.48			
Ash feed rate (lb/hr):		5.06			
Feed dust loading (lb/lb gas; ppmw):		0.0210	21029		
Dust-to-filter element efficiency (%):		37.75			
Effective dust loading (lb/lb gas; ppmw):		0.0079	7938		
Pulse events					
	Cake Build	**Pulse 1**	**Pulse 2**	**Pulse 3**	**Pulse 4**
Initial DP (iwg):	12	51.5	22.5	15.5	14
Loaded DP (iwg):	51.5	22.5	15.5	14	13
Pulse air released (lb):		0.375	0.327	0.327	0.315
Pulse valve open time (sec):	0.3				
Pulse tank pressure (psig):	100				
Pulse delivery efficiency (%):	40				
Calculated performance terms					
Loaded cake thickness (in):	0.178	0.052	0.018	0.010	0.005
Loaded cake mass (lb):	0.785	0.250	0.087	0.050	0.025
Residue layer thickness (in):	0.005				0.010
Fraction remaining cake removed (%):		0.682	0.651	0.423	0.497
Fraction total initial cake removed (%)		0.682	0.207	0.047	0.032
Candle bore outlet pulse velocity (ft/s):		194.655	154.788	151.760	144.278
Pulse face velocity (ft/min):		70.775	61.716	61.716	59.451
Cake pulse DP (iwg):		295.520	68.501	22.834	12.569

Table A9 - Test CI-9, 60-mm Inverted Candle Test Results

Test type: 3 Inverted Candles - Forward Flow During Pulse Cleaning					
Run Number:		**CI-9**			
Number of candles:		3			
Candle outer diameter (in):		2.36			
Candle wall thickness (in):		0.4			
Dirty-side mean face velocity (ft/min):		9.44			
Dirty-side filter surface area (ft^2):		1.88			
Candle element permeability (ft^2):		4.2E-11			
Residue layer permeability (ft^2):		1.00E-12			
Cake permeability (ft^2):		5.0E-12			
Gas viscosity (lb/ft-s):		1.24E-05			
Gas density (lb/ft^3):		0.075			
Cake bulk density (lb/ft^3):		30			
Ash fed (lb):		6.47			
Ash feed time (min):		69			
Calculated terms					
Filter radius (in):		0.78			
Air flow rate (lb/hr):		240.08			
Air mean velocity into candle bore (ft/s):		22.34			
Clean element DP (iwg):		7.47			
Ash feed rate (lb/hr):		5.63			
Feed dust loading (lb/lb gas; ppmw):		0.0234	23434		
Dust-to-filter element efficiency (%):		37.11			
Effective dust loading (lb/lb gas; ppmw):		0.0087	8697		
Pulse events					
	Cake Build	**Pulse 1**	**Pulse 2**	**Pulse 3**	**Pulse 4**
Initial DP (iwg):	12.5	53	25	17	15
Loaded DP (iwg):	53	25	17	15	14
Pulse air released (lb):		0.278	0.303	0.327	0.387
Pulse valve open time (sec):	0.3				
Pulse tank pressure (psig):	100				
Pulse delivery efficiency (%):	40				
Calculated performance terms					
Loaded cake thickness (in):	0.182	0.061	0.023	0.013	0.008
Loaded cake mass (lb):	0.800	0.294	0.111	0.063	0.038
Residue layer thickness (in):	0.005				0.013
Fraction remaining cake removed (%):		0.633	0.621	0.437	0.396
Fraction total initial cake removed (%)		0.633	0.228	0.061	0.031
Candle bore outlet pulse velocity (ft/s):		148.414	145.550	152.986	178.682
Pulse face velocity (ft/min):		52.468	57.186	61.716	73.040
Cake pulse DP (iwg):		225.101	75.723	29.420	19.343

Table A10 - Test CI-10, 60-mm Inverted Candle Test Results

Test type: 3 Inverted Candles - Forward Flow During Pulse Cleaning					
Run Number:		**CI-10**			
Number of candles:		3			
Candle outer diameter (in):		2.36			
Candle wall thickness (in):		0.4			
Dirty-side mean face velocity (ft/min):		9.19			
Dirty-side filter surface area (ft^2):		1.88			
Candle element permeability (ft^2):		4.2E-11			
Residue layer permeability (ft^2):		1.00E-12			
Cake permeability (ft^2):		5.0E-12			
Gas viscosity (lb/ft-s):		1.24E-05			
Gas density (lb/ft^3):		0.075			
Cake bulk density (lb/ft^3):		30			
Ash fed (lb):		15.42			
Ash feed time (min):		160			
Calculated terms					
Filter radius (in):		0.78			
Air flow rate (lb/hr):		233.73			
Air mean velocity into candle bore (ft/s):		21.75			
Clean element DP (iwg):		7.27			
Ash feed rate (lb/hr):		5.78			
Feed dust loading (lb/lb gas; ppmw):		0.0247	24741		
Dust-to-filter element efficiency (%):		24.06			
Effective dust loading (lb/lb gas; ppmw):		0.0060	5953		
Pulse events					
	Cake Build	**Pulse 1**	**Pulse 2**	**Pulse 3**	**Pulse 4**
Initial DP (iwg):	11	85.9	36	17	15
Loaded DP (iwg):	85.9	36	17	15	14
Pulse air released (lb):		0.327	0.351	0.424	0.375
Pulse valve open time (sec):	0.3				
Pulse tank pressure (psig):	100				
Pulse delivery efficiency (%):	40				
Calculated performance terms					
Loaded cake thickness (in):	0.309	0.121	0.031	0.021	0.016
Loaded cake mass (lb):	1.237	0.557	0.151	0.102	0.077
Residue layer thickness (in):	0.004				0.020
Fraction remaining cake removed (%):		0.549	0.728	0.324	0.245
Fraction total initial cake removed (%)		0.549	0.328	0.040	0.020
Candle bore outlet pulse velocity (ft/s):		207.091	171.804	201.983	176.235
Pulse face velocity (ft/min):		61.716	66.246	80.023	70.775
Cake pulse DP (iwg):		502.995	180.211	52.246	30.805

Table A11 - Test CI-11, 60-mm Inverted Candle Test Results

Test type: 3 Inverted Candles - Forward Flow During Pulse Cleaning					
Run Number:	**CI-11**				
Number of candles:	3				
Candle outer diameter (in):	2.36				
Candle wall thickness (in):	0.4				
Dirty-side mean face velocity (ft/min):	9.42				
Dirty-side filter surface area (ft^2):	1.88				
Candle element permeability (ft^2):	4.2E-11				
Residue layer permeability (ft^2):	1.00E-12				
Cake permeability (ft^2):	5.0E-12				
Gas viscosity (lb/ft-s):	1.24E-05				
Gas density (lb/ft^3):	0.075				
Cake bulk density (lb/ft^3):	30				
Ash fed (lb):	7.52				
Ash feed time (min):	79				
Calculated terms					
Filter radius (in):	0.78				
Air flow rate (lb/hr):	239.58				
Air mean velocity into candle bore (ft/s):	22.29				
Clean element DP (iwg):	7.45				
Ash feed rate (lb/hr):	5.71				
Feed dust loading (lb/lb gas; ppmw):	0.0238	23840			
Dust-to-filter element efficiency (%):	31.55				
Effective dust loading (lb/lb gas; ppmw):	0.0075	7522			
Pulse events					
	Cake Build	**Pulse 1**	**Pulse 2**	**Pulse 3**	**Pulse 4**
Initial DP (iwg):	14	54	24.5	16	15
Loaded DP (iwg):	54	24.5	16	15	15
Pulse air released (lb):		0.411	0.436	0.411	0.46
Pulse valve open time (sec):	0.3				
Pulse tank pressure (psig):	125				
Pulse delivery efficiency (%):	40				
Calculated performance terms					
Loaded cake thickness (in):	0.180	0.052	0.010	0.005	0.005
Loaded cake mass (lb):	0.791	0.250	0.050	0.025	0.025
Residue layer thickness (in):	0.007				0.012
Fraction remaining cake removed (%):		0.684	0.799	0.497	0.000
Fraction total initial cake removed (%)		0.684	0.252	0.032	0.000
Candle bore outlet pulse velocity (ft/s):		214.629	203.470	189.283	211.849
Pulse face velocity (ft/min):		77.570	82.288	77.570	86.818
Cake pulse DP (iwg):		329.383	91.722	16.469	9.216

Table A12 - Test CI-12, 60-mm Inverted Candle Test Results

Test type: 3 Inverted Candles - Forward Flow During Pulse Cleaning					
Run Number:		**CI-12**			
Number of candles:		3			
Candle outer diameter (in):		2.36			
Candle wall thickness (in):		0.4			
Dirty-side mean face velocity (ft/min):		9.23			
Dirty-side filter surface area (ft²):		$1.88			
Candle element permeability (ft²):		4.2E-11			
Residue layer permeability (ft²):		1.00E-12			
Cake permeability (ft²):		5.0E-12			
Gas viscosity (lb/ft-s):		1.24E-05			
Gas density (lb/ft³):		0.075			
Cake bulk density (lb/ft³):		30			
Ash fed (lb):		11.64			
Ash feed time (min):		121			
Calculated terms					
Filter radius (in):		0.78			
Air flow rate (lb/hr):		234.74			
Air mean velocity into candle bore (ft/s):		21.84			
Clean element DP (iwg):		7.30			
Ash feed rate (lb/hr):		5.77			
Feed dust loading (lb/lb gas; ppmw):		0.0246	24588		
Dust-to-filter element efficiency (%):		27.52			
Effective dust loading (lb/lb gas; ppmw):		0.0068	6767		
Pulse events					
	Cake Build	**Pulse 1**	**Pulse 2**	**Pulse 3**	**Pulse 4**
Initial DP (iwg):	14	74	27.5	17.5	15.5
Loaded DP (iwg):	74	27.5	17.5	15.5	15
Pulse air released (lb):		0.472	0.424	0.484	0.424
Pulse valve open time (sec):	0.3				
Pulse tank pressure (psig):	125				
Pulse delivery efficiency (%):	40				
Calculated performance terms					
Loaded cake thickness (in):	0.257	0.067	0.018	0.008	0.005
Loaded cake mass (lb):	1.068	0.320	0.089	0.039	0.026
Residue layer thickness (in):	0.007				0.012
Fraction remaining cake removed (%):		0.700	0.723	0.566	0.331
Fraction total initial cake removed (%)		0.700	0.217	0.047	0.012
Candle bore outlet pulse velocity (ft/s):		257.603	202.182	224.645	195.472
Pulse face velocity (ft/min):		89.082	80.023	91.347	80.023
Cake pulse DP (iwg):		579.084	117.044	34.639	13.005

Table A13 - Test CI-22, 60-mm Inverted Candle Test Results

Test type: 3 Inverted Candles - Forward Flow During Pulse Cleaning					
Run Number:	**CI-22**				
Number of candles:	3				
Candle outer diameter (in):	2.36				
Candle wall thickness (in):	0.4				
Dirty-side mean face velocity (ft/min):	8.85				
Dirty-side filter surface area (ft^2):	1.88				
Candle element permeability (ft^2):	4.2E-11				
Residue layer permeability (ft^2):	1.00E-12				
Cake permeability (ft^2):	5.0E-12				
Gas viscosity (lb/ft-s):	1.24E-05				
Gas density (lb/ft^3):	0.075				
Cake bulk density (lb/ft^3):	30				
Ash fed (lb):	7.09				
Ash feed time (min):	74				
Calculated terms					
Filter radius (in):	0.78				
Air flow rate (lb/hr):	225.08				
Air mean velocity into candle bore (ft/s):	20.95				
Clean element DP (iwg):	7.00				
Ash feed rate (lb/hr):	5.75				
Feed dust loading (lb/lb gas; ppmw):	0.0255	25,541			
Dust-to-filter element efficiency (%):	35.34				
Effective dust loading (lb/lb gas; ppmw):	0.0090	9,026			
Pulse events					
	Cake Build	**Pulse 1**	**Pulse 2**	**Pulse 3**	**Pulse 4**
Initial DP (iwg):	17	58	29.5	20.5	18
Loaded DP (iwg):	58	29.5	20.5	18	17
Pulse air released (lb):		0.424	0.387	0.448	0.448
Pulse valve open time (sec):	0.3				
Pulse tank pressure (psig):	125				
Pulse delivery efficiency (%):	40				
Calculated performance terms					
Loaded cake thickness (in):	0.193	0.065	0.019	0.013	0.005
Loaded cake mass (lb):	0.835	0.307	0.092	0.066	0.027
Residue layer thickness (in):	0.011				0.016
Fraction remaining cake removed (%):		0.632	0.702	0.281	0.596
Fraction total initial cake removed (%)		0.632	0.258	0.031	0.047
Candle bore outlet pulse velocity (ft/s):		232.291	186.785	213.204	208.748
Pulse face velocity (ft/min):		80.023	73.040	84.553	84.553
Cake pulse DP (iwg):		370.729	103.164	33.439	23.885

Table A14 - Test CI-23, 60-mm Inverted Candle Test Results

Test type: 3 Inverted Candles - Forward Flow During Pulse Cleaning					
Run Number:	**CI-23**				
Number of candles:	3				
Candle outer diameter (in):	2.36				
Candle wall thickness (in):	0.4				
Dirty-side mean face velocity (ft/min):	9.47				
Dirty-side filter surface area (ft^2):	$1.88				
Candle element permeability (ft^2):	4.2E-11				
Residue layer permeability (ft^2):	1.00E-12				
Cake permeability (ft^2):	5.0E-12				
Gas viscosity (lb/ft-s):	1.24E-05				
Gas density (lb/ft^3):	0.075				
Cake bulk density (lb/ft^3):	30				
Ash fed (lb):	7.07				
Ash feed time (min):	75				
Calculated terms					
Filter radius (in):	0.78				
Air flow rate (lb/hr):	240.85				
Air mean velocity into candle bore (ft/s):	22.41				
Clean element DP (iwg):	7.49				
Ash feed rate (lb/hr):	5.66				
Feed dust loading (lb/lb gas; ppmw):	0.0235	23484			
Dust-to-filter element efficiency (%):	33.62				
Effective dust loading (lb/lb gas; ppmw):	0.0079	7895			
Pulse events					
	Cake Build	**Pulse 1**	**Pulse 2**	**Pulse 3**	**Pulse 4**
Initial DP (iwg):	15.5	56			
Loaded DP (iwg):	56	27			
Pulse air released (lb):		0.363			
Pulse valve open time (sec):	0.3				
Pulse tank pressure (psig):	125				
Pulse delivery efficiency (%):	40				
Calculated performance terms					
Loaded cake thickness (in):	0.181	0.056			
Loaded cake mass (lb):	0.792	0.269			
Residue layer thickness (in):	0.008				
Fraction remaining cake removed (%):		0.660			
Fraction total initial cake removed (%)		0.660			
Candle bore outlet pulse velocity (ft/s):		192.654			
Pulse face velocity (ft/min):		68.510			
Cake pulse DP (iwg):		292.996			

A.2 Tests with 3 Normal Candles and Forward Flow during Pulse Cleaning (Tests CI-28 through CI-30)

Table A15 - Test CI-28, 60-mm Normal Candle Test Results

Test type: 3 Normal Candles - Forward Flow During Pulse Cleaning					
Run Number:	**CI-28**				
Number of candles:	3				
Candle outer diameter (in):	2.36				
Candle wall thickness (in):	0.4				
Dirty-side mean face velocity (ft/min):	6.33				
Dirty-side filter surface area (ft^2):	2.85				
Candle element permeability (ft^2):	4.2E-11				
Residue layer permeability (ft^2):	1.00E-12				
Cake permeability (ft^2):	5.0E-12				
Gas viscosity (lb/ft-s):	1.24E-05				
Gas density (lb/ft^3):	0.075				
Cake bulk density (lb/ft^3):	30				
Ash fed (lb):	17.23				
Ash feed time (min):	254				
Calculated terms					
Filter radius (in):	1.18				
Air flow rate (lb/hr):	243.55				
Clean element DP (iwg):	5.34				
Ash feed rate (lb/hr):	4.07				
Feed dust loading (lb/lb gas ppmw):	0.0167	16712			
Dust-to-filter element efficiency (%):	55.90				
Effective dust loading (lb/lb gas; ppmw):	0.0093	9341			
Pulse events					
	Cake Build	**Pulse 1**	**Pulse 2**	**Pulse 3**	**Pulse 4**
Initial DP (iwg):	17.5	58	28		
Loaded DP (iwg):	58	28	20		
Pulse air released (lb):		0.157	0.206		
Pulse valve open time (sec):	0.3				
Pulse tank pressure (psig):	50				
Pulse delivery efficiency (%):	40				
Calculated performance terms					
Loaded cake thickness (in):	0.361	0.085	0.020		
Loaded cake mass (lb):	3.210	0.677	0.153		
Residue layer thickness (in):	0.019				
Fraction remaining cake removed (%):		0.789	0.774		
Fraction total cake removed (%):		0.789	0.163		
Pulse face velocity (ft/min):		19.587	25.700		
Cake pulse DP (iwg):		125.318	42.630		

Table A16 - Test CI-29, 60-mm Normal Candle Test Results

Test type: 3 Normal Candles - Forward Flow During Pulse Cleaning					
Run Number:	**CI-29**				
Number of candles:	3				
Candle outer diameter (in):	2.36				
Candle wall thickness (in):	0.4				
Dirty-side mean face velocity (ft/min):	5.8				
Dirty-side filter surface area (ft^2):	2.85				
Candle element permeability (ft^2):	4.2E-11				
Residue layer permeability (ft^2):	1.00E-12				
Cake permeability (ft^2):	5.0E-12				
Gas viscosity (lb/ft-s):	1.24E-05				
Gas density (lb/ft^3):	0.075				
Cake bulk density (lb/ft^3):	30				
Ash fed (lb):	19.71				
Ash feed time (min):	205				
Calculated terms					
Filter radius (in):	1.18				
Air flow rate (lb/hr):	223.16				
Clean element DP (iwg):	4.89				
Ash feed rate (lb/hr):	5.77				
Feed dust loading (lb/lb gas ppmw):	0.0259	25851			
Dust-to-filter element efficiency (%):	50.95				
Effective dust loading (lb/lb gas; ppmw):	0.0132	13172			
Pulse events					

	Cake Build	Pulse 1	Pulse 2	Pulse 3	Pulse 4
Initial DP (iwg):	20	58	21		
Loaded DP (iwg):	58	21	18		
Pulse air released (lb):		0.242	0.242		
Pulse valve open time (sec):	0.3				
Pulse tank pressure (psig):	75				
Pulse delivery efficiency (%):	40				
Calculated performance terms					
Loaded cake thickness (in):	0.373	0.009	-0.017		
Loaded cake mass (lb):	3.348	0.067	-0.131		
Residue layer thickness (in):	0.026				
Fraction remaining cake removed (%):		0.980	2.958		
Fraction total cake removed (%):		0.980	0.059		
Pulse face velocity (ft/min):		30.191	30.191		
Cake pulse DP (iwg):		197.803	5.205		

Table A17 - Test CI-30, 60-mm Normal Candle Test Results

Test type: 3 Normal Candles - Forward Flow During Pulse Cleaning					
Run Number:		**CI-30**			
Number of candles:		3			
Candle outer diameter (in):		2.36			
Candle wall thickness (in):		0.4			
Dirty-side mean face velocity (ft/min):		5.56			
Dirty-side filter surface area (ft^2):		2.85			
Candle element permeability (ft^2):		4.2E-11			
Residue layer permeability (ft^2):		1.00E-12			
Cake permeability (ft^2):		5.0E-12			
Gas viscosity (lb/ft-s):		1.24E-05			
Gas density (lb/ft^3):		0.075			
Cake bulk density (lb/ft^3):		30			
Ash fed (lb):		16.5			
Ash feed time (min):		178			
Calculated terms					
Filter radius (in):		1.18			
Air flow rate (lb/hr):		213.92			
Clean element DP (iwg):		4.69			
Ash feed rate (lb/hr):		5.56			
Feed dust loading (lb/lb gas ppmw):		0.0260	25,999		
Dust-to-filter element efficiency (%):		66.50			
Effective dust loading (lb/lb gas; ppmw):		0.0173	17,290		
Pulse events					
	Cake Build	**Pulse 1**	**Pulse 2**	**Pulse 3**	**Pulse 4**
Initial DP (iwg):	19	58	19		
Loaded DP (iwg):	58	19	16		
Pulse air released (lb):		0.302	0.351		
Pulse valve open time (sec):	0.3				
Pulse tank pressure (psig):	100				
Pulse delivery efficiency (%):	40				
Calculated performance terms					
Loaded cake thickness (in):	0.404	0.000	-0.026		
Loaded cake mass (lb):	3.657	0.000	-0.203		
Residue layer thickness (in):	0.025				
Fraction remaining cake removed (%):		1.000	#DIV/0!		
Fraction total cake removed (%):		1.000	0.056		
Pulse face velocity (ft/min):		37.676	43.789		
Cake pulse DP (iwg):		264.277	0.000		

A.3 Test with 3 Inverted Candles and No Forward Flow during Pulse Cleaning (Test CI-21)

Table A18 - Test CI-21, 60-mm Inverted Candle Test Results

Test type: 3 Inverted Candles and No forward flow During Pulse					
Run Number:		**CI-21**			
Number of candles:		3			
Candle outer diameter (in):		2.36			
Candle wall thickness (in):		0.4			
Dirty-side mean face velocity (ft/min):		8.88			
Dirty-side filter surface area (ft^2):		1.88			
Candle element permeability (ft^2):		4.2E-11			
Residue layer permeability (ft^2):		1.00E-12			
Cake permeability (ft^2):		5.0E-12			
Gas viscosity (lb/ft-s):		1.24E-05			
Gas density (lb/ft^3):		0.075			
Cake bulk density (lb/ft^3):		30			
Ash fed (lb):		7.02			
Ash feed time (min):		75			
Calculated terms					
Filter radius (in):		0.78			
Air flow rate (lb/hr):		225.84			
Air mean velocity into candle bore (ft/s):		21.02			
Clean element DP (iwg):		7.02			
Ash feed rate (lb/hr):		5.62			
Feed dust loading (lb/lb gas; ppmw):		0.0249	24867		
Dust-to-filter element efficiency (%):		34.86			
Effective dust loading (lb/lb gas; ppmw):		0.0087	8669		
Pulse events					
	Cake Build	**Pulse 1**	**Pulse 2**	**Pulse 3**	**Pulse 4**
Initial DP (iwg):	18	58			
Loaded DP (iwg):	58	16			
Pulse air released (lb):		0.424			
Pulse valve open time (sec):	0.3				
Pulse tank pressure (psig):	125				
Pulse delivery efficiency (%):	40				
Calculated performance terms					
Loaded cake thickness (in):	0.188	-0.011			
Loaded cake mass (lb):	0.816	-0.054			
Residue layer thickness (in):	0.012				
Fraction remaining cake removed (%):		1.066			
Fraction total initial cake removed (%)		1.066			
Candle bore outlet pulse velocity (ft/s):					
Pulse face velocity (ft/min):		80.023			
Cake pulse DP (iwg):		360.465			

A.4 Tests with 3 Simulated 110-mm Inverted Candles and Forward Flow during Pulse Cleaning (Tests CI-31through CI33)

Table A19 - Test CI-31, Simulated 110-mm Inverted Candle Test Results

Test type: 110-mm Inverted Candle Simulation					
Run Number:	CI-31				
Number of candles:	3				
Candle outer diameter (in):	2.36				
Candle wall thickness (in):	0.4				
Dirty-side mean face velocity (ft/min):	10.3				
Dirty-side filter surface area (ft^2):	0.75				
Candle element permeability (ft^2):	4.2E-11				
Residue layer permeability (ft^2):	1.00E-12				
Cake permeability (ft^2):	5.0E-12				
Gas viscosity (lb/ft-s):	1.24E-05				
Gas density (lb/ft^3):	0.075				
Cake bulk density (lb/ft^3):	30				
Ash fed (lb):	3.96				
Ash feed time (min):	45				
Calculated terms					
Filter radius (in):	0.78				
Air flow rate (lb/hr):	104.78				
Air mean velocity into candle bore (ft/s):	9.75				
Clean element DP (iwg):	8.15				
Ash feed rate (lb/hr):	5.28				
Feed dust loading (lb/lb gas; ppmw):	0.0504	50390			
Dust-to-filter element efficiency (%):	21.97				
Effective dust loading (lb/lb gas; ppmw):	0.0111	11069			
Pulse events					
	Cake Build	**Pulse 1**	**Pulse 2**	**Pulse 3**	**Pulse 4**
Initial DP (iwg):	23	63	32		
Loaded DP (iwg):	63	32	21		
Pulse air released (lb):		0.266	0.315		
Pulse valve open time (sec):	0.3				
Pulse tank pressure (psig):	75				
Pulse delivery efficiency (%):	40				
Calculated performance terms					
Loaded cake thickness (in):	0.165	0.041	-0.009		
Loaded cake mass (lb):	0.290	0.078	-0.019		
Residue layer thickness (in):	0.014				
Fraction remaining cake removed (%):		0.731	1.237		
Fraction total initial cake removed (%)		0.731	0.333		
Candle bore outlet pulse velocity (ft/s):		137.334	142.367		
Pulse face velocity (ft/min):		125.508	148.628		
Cake pulse DP (iwg):		487.410	129.869		

Table A20 - Test CI-32, Simulated110-mm Inverted Candle Test Results

Test type: 110-mm Inverted Candle Simulation					
Run Number:		**CI-32**			
Number of candles:		3			
Candle outer diameter (in):		2.36			
Candle wall thickness (in):		0.4			
Dirty-side mean face velocity (ft/min):		10.35			
Dirty-side filter surface area (ft^2):		0.75			
Candle element permeability (ft^2):		4.2E-11			
Residue layer permeability (ft^2):		1.00E-12			
Cake permeability (ft^2):		5.0E-12			
Gas viscosity (lb/ft-s):		1.24E-05			
Gas density (lb/ft^3):		0.075			
Cake bulk density (lb/ft^3):		30			
Ash fed (lb):		4.52			
Ash feed time (min):		44			
Calculated terms					
Filter radius (in):		0.78			
Air flow rate (lb/hr):		105.29			
Air mean velocity into candle bore (ft/s):		9.80			
Clean element DP (iwg):		8.19			
Ash feed rate (lb/hr):		6.16			
Feed dust loading (lb/lb gas; ppmw):		0.0585	58539		
Dust-to-filter element efficiency (%):		19.64			
Effective dust loading (lb/lb gas; ppmw):		0.0115	11499		
Pulse events					
	Cake Build	**Pulse 1**	**Pulse 2**	**Pulse 3**	**Pulse 4**
Initial DP (iwg):	21	62			
Loaded DP (iwg):	62	27			
Pulse air released (lb):		0.363			
Pulse valve open time (sec):	0.3				
Pulse tank pressure (psig):	100				
Pulse delivery efficiency (%):	40				
Calculated performance terms					
Loaded cake thickness (in):	0.168	0.027			
Loaded cake mass (lb):	0.296	0.053			
Residue layer thickness (in):	0.012				
Fraction remaining cake removed (%):		0.821			
Fraction total initial cake removed (%)		0.821			
Candle bore outlet pulse velocity (ft/s):		179.754			
Pulse face velocity (ft/min):		171.276			
Cake pulse DP (iwg):		678.485			

Table A21 - Test CI-33, Simulated 110-mm Inverted Candle Test Results

Test type: 110-mm Inverted Candle Simulation					
Run Number:		**CI-33**			
Number of candles:		3			
Candle outer diameter (in):		2.36			
Candle wall thickness (in):		0.4			
Dirty-side mean face velocity (ft/min):		10.55			
Dirty-side filter surface area (ft^2):		0.75			
Candle element permeability (ft^2):		4.2E-11			
Residue layer permeability (ft^2):		1.00E-12			
Cake permeability (ft^2):		5.0E-12			
Gas viscosity (lb/ft-s):		1.24E-05			
Gas density (lb/ft^3):		0.075			
Cake bulk density (lb/ft^3):		30			
Ash fed (lb):		3.19			
Ash feed time (min):		36			
Calculated terms					
Filter radius (in):		0.78			
Air flow rate (lb/hr):		107.33			
Air mean velocity into candle bore (ft/s):		9.99			
Clean element DP (iwg):		8.34			
Ash feed rate (lb/hr):		5.32			
Feed dust loading (lb/lb gas; ppmw):		0.0495	49538		
Dust-to-filter element efficiency (%):		26.99			
Effective dust loading (lb/lb gas; ppmw):		0.0134	13370		
Pulse events					
	Cake Build	**Pulse 1**	**Pulse 2**	**Pulse 3**	**Pulse 4**
Initial DP (iwg):	20	60	26.5		
Loaded DP (iwg):	60	26.5	22		
Pulse air released (lb):		0.363	0.339		
Pulse valve open time (sec):	0.3				
Pulse tank pressure (psig):	100				
Pulse delivery efficiency (%):	40				
Calculated performance terms					
Loaded cake thickness (in):	0.162	0.029	0.009		
Loaded cake mass (lb):	0.287	0.056	0.013		
Residue layer thickness (in):	0.011				
Fraction remaining cake removed (%):		0.804	0.763		
Fraction total initial cake removed (%)		0.804	0.150		
Candle bore outlet pulse velocity (ft/s):		179.973	159.373		
Pulse face velocity (ft/min):		171.276	159.952		
Cake pulse DP (iwg):		649.388	98.549		

APPENDIX B - SHEET FILTER THERMO-MECHANICAL DESIGN EVALUATIONS

Note: values reported in this appendix are presented in English Engineering Units only.

B1 - Sheet Filter Geometry

Review of the rationale for specifications for sheet filter geometry is presented below based on the pressure and thermal stress calculations completed.

Filter Flange Design

The sheet filter flange design will be analogous to the standard ceramic candle flange design configuration. The specific choice of sheet filter flange geometry will be left to the discretion of the manufacturers, based on fabrication considerations and cost, because the effect of the different designs evaluated on stresses is small.

Number of Ribs and Wall Thickness

To evaluate the effect of the pressure loads on the sheet filter walls, it is necessary to compare the stresses with the material strengths below:

Maximum tensile strength of materials (psi)

Material	Range	Minimum
Pall	4019 ± 576	3443
Blasch	544 ± 121	423
McDermott	1008 ± 228	780

For wall thickness and rib spacing, the pressure loads may be evaluated by using plate equations. The equations have the form

$$\text{Max } \sigma = \beta\, q\, b^2 / t^2$$

where b is the width, t is the thickness, β is a function of the plate aspect ratio, and q is the pressure. Since the sheet filter plate is 12 inches wide and 0.75 inches deep, with radiused ends, the effective width of the plate is 11.25 inches. Table B1 shows the stresses for various rib numbers and various wall thicknesses. A pulse pressure of 5 psi was assumed, representing the maximum pressure drop across the sheet filter wall during a pulse cleaning event.

Table B1 - Sheet Filter Wall Stresses (psi) Due to a 5 psi Pulse Pressure

Wall Thickness	0.125 inches	0.1875 inches	0.25 inches	0.4 inches
no rib	16584	7371	4146	1620
1 rib	5034	2237	1259	492
2 ribs	2241	996	560	219
3 ribs	1263	561	316	123
4 ribs	809	360	202	79

Given a thick enough wall and enough ribs, the stresses from the pulse may be reduced to an acceptable level for any of the materials. The stresses for a 0.25 inch thick wall with 3 ribs are below the tensile strengths for all of the materials, and this is selected as the design specification.

Thermal Stresses

The thermal stress evaluations were made using transient 2D plate models, with an assumed pulse gas temperature difference of 600°F, with the initial temperature of the filter at 1600°F. To model the effect of the pulse on the temperature in the filter wall, the cooling was modeled as a convection load. The convection coefficient was calculated to accommodate the increased surface area of the porous material.

The assumed pulse used for the analysis is 0.25 pounds of air in 0.5 seconds, per sheet filter. With an assumption of three ribs (which reduce the face area), the flow is calculated as follows:

Flow surface area:	$2 \times 11.5 \times (11.25 - 3 \times 0.25) + 2 \pi \, 0.75 \, (11.5) = 296 \text{ in}^2$
Flow per area:	$0.25 \text{ lb} / 313 \text{ in}^2 = 0.000845 \text{ lb/in}^2$
Flow rate:	$0.000799 / 0.5 = 0.00169 \text{ lb/in}^2 \text{ sec}$

If all of the pulse air is heated to the initial filter temperature, the energy transferred (per square inch) is:

$$q = m \, C_p \, \Delta T \, dt \; = \; 0.00169 \text{ lb/sec} \, (0.263 \text{ Btu/lb°F}) \, (600°F) \, (0.5 \text{sec}) \; = \; 0.133 \text{ Btu}$$

The assumption (made for modeling convenience) that the energy transfer is made at the inner face of the filter results in the following:

$$q = h \, A \, dT \, dt$$
$$h = 0.133 \text{ Btu} / (1 \text{ in}^2 \times 600°F \times 0.5 \text{sec}) = 0.000443 \text{ Btu/in}^2°F \text{ sec}$$
$$= 230 \text{ Btu/ft}^2 \, °F \text{ hr}$$

In the analysis, the convection load is applied for 0.5 seconds, and then reduced to about 1% of the initial value for another 0.5 seconds, and the maximum stress is calculated at 0.1 second increments. Table B2 shows the maximum stresses which occur in the sheet filters during the pulse event. Pall and Blasch filters are evaluated for two wall thicknesses. Since the cooling is a function of the surface temperature, after the initial runs were made, the inner face temperatures were checked and found to cause a 20% lower difference in temperature. Therefore, an analysis was made for each material using a 20% higher convection coefficient to increase the heat transfer. Since the heat transfer occurs at the face of the model, the stresses listed should represent the upper limit of what would occur in the filter, since the airflow would tend to move some of the heat transfer into the filter wall, making the gradient less steep.

Table B2 - Maximum Thermal Stress (psi) Resulting from Pulse Cleaning

Filter mtl.	Wall thick. (inch)	Heat transfer coeff	Time step (sec)									
			0.1	0.2	0.3	0.4	0.5	0.6	0.7	0.8	0.9	1.0
Pall	0.25	Base	416	1030	1356	1592	1775	1604	1248	1054	919	837
	0.4	Base	418	1005	1348	1633	1854	1755	1433	1245	1109	1023
	0.25	1.2 x Base	495	1217	1591	1857	2071	1868	1448	1222	1065	968
Blasch	0.25	Base	346	965	1449	1844	2186	2245	2042	1878	1725	1603
	0.4	Base	360	991	1468	1849	2170	2192	1986	1835	1733	1656
	0.25	1.2 x Base	519	1351	1896	2327	2643	2658	2427	2238	2065	1923

The thermal conductivity of the Blasch filter material is about 5 BTU in/hr ft^2 °F while the Pall thermal conductivity is about 38 BTU in/hr ft^2 °F. Analyses were not performed for the McDermott material since the modulus of elasticity and Poisson's ratios have not been verified. However, since the McDermott material has a higher coefficient of thermal expansion than the other filter materials and an extremely low thermal conductivity, it would be expected that the thermal stresses would be higher in the McDermott filter material.

The stresses in the Blasch filter material exceed the tensile strength of the material, while the Pall thermal stresses do not. These results indicate that the Blasch material, if used in sheet filter form, will require application of pulse gas heat regeneration, such as is provided by the SWPC fail-safe device. Further testing and analysis to prove the compatibility of the Blasch material, in sheet filter form, with hot gas filtration systems is needed.

Conclusions

The pulse cleaning thermal stresses appear to be more restrictive than the stresses from the pulse cleaning pressure. The pressure stresses can be significantly reduced by adding internal ribs and increasing wall thickness. The thermal stresses are not easily reduced by modifying the sheet filter design, but analogous ceramic candle testing indicates that thermal stress damage may not be significant. The clay-bonded, non-oxide, Pall material would have the least severe stresses and the largest design margin. The design specification to the sheet filter manufacturers will be 0.3" wall thickness with three internal ribs, and general guidelines will be provided for the flange geometry.

B2 - Thermo-mechanical Evaluation

A general sheet filter design with body features and flange, as shown in Figure B1, has been prepared for initial thermomechanical evaluation. The flange shape is based on the convex ceramic candle flange that has been relatively free from the type of mechanical failure observed with previous cross-flow filter testing. The evaluations performed have compared the relative stress behavior of different filter clamping geometries and the relative performance of different ceramic materials.
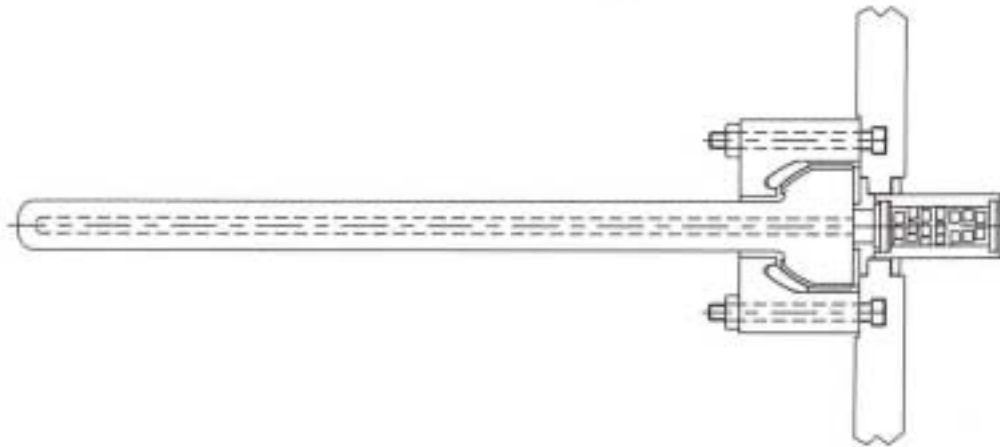
Figure B1 - Sheet Filter Element and Clamping Features

Two-Dimensional Comparison

For the initial comparison, the sheet filter geometry was evaluated for stresses by using the same material properties with 2D representations of the filter, gasket, and bracket. The filter was treated as having no ribs, contact elements were used in several locations to allow sliding of different components, and the bracket was held against the wall by a force. While the 2D section treats the filter as though the sheet filter were infinitely long, the model is considerably less complex than a 3D model, and allows relative comparison of the flange geometrical differences.

The material properties used in the 2D analyses were as follow:

Filter	Young's Modulus		5.7e6
	Poisson's Ratio	.3	
	Coeff. Of Therm. Exp.	2.8e-6 in/in/°F	
	Thermal Conductivity		7.33e-5 Btu/sec-in-°F
Steel	Young's Modulus		28e6
	Poisson's Ratio	.29	
	Coeff. Of Therm. Exp.	9.9e-6 in/in/°F	
	Thermal Conductivity		2.18e-4 Btu/sec-in-°F
Gasket	Young's Modulus		2.e6
	Poisson's Ratio	.3	
	Coeff. Of Therm. Exp.	2.8e-6 in/in/°F	
	Thermal Conductivity		7.33e-5 Btu/sec-in-°F

The material properties of the gasket were treated as though they were for a weaker filter material.

Three flange geometries were selected that represent differing transition shapes at the critical flange-to-body interface, as shown in Figure B2. For mechanical modeling purposes, the gasket geometries were simplified and the total length of each filter was set at 12.75 inches.

| | A) | | B) | | C) |
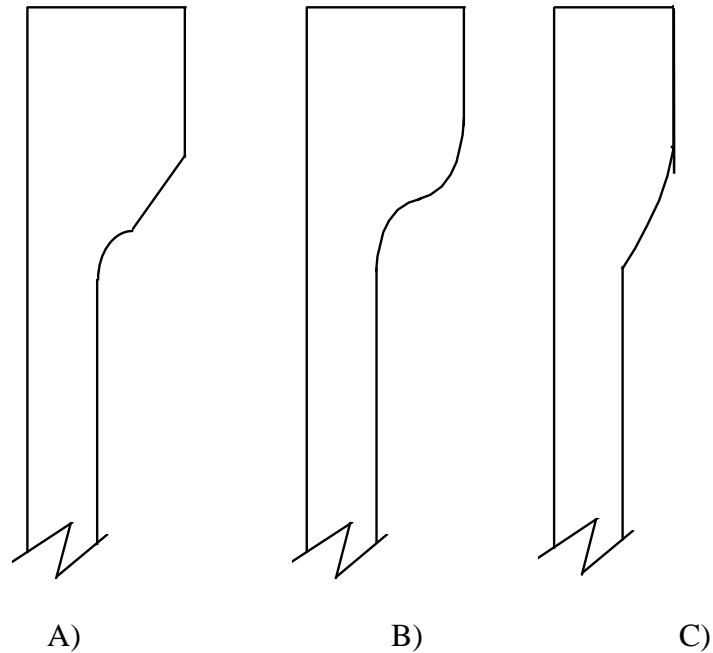
Figure B2- Alternative Sheet Filter Flange Designs

The stresses with a 5 psi load on the inside of the filter, at ambient temperature, are listed in Table B3 for direct comparison. The maximum stresses in the filter occur away from the clamped end, so to allow comparison of the ends, stresses were compared for the entire length of the filter, the top 6 inches, and for the top 3 inches.

For the preceding cases, many of the stresses exceed the compressive and tensile strengths of most of the filter materials. This is not necessarily a concern in this evaluation since the geometries include no ribs, which will reduce the stresses significantly. The purpose of the evaluation is to compare the relative effects of modifications to the clamped end.

Table B3 - Relative Stresses for Three Sheet Filter Flange Designs

	Design A			Design B			Design C		
	Full length	Top 6 inches	Top 3 inches	Full length	Top 6 inches	Top 3 inches	Full length	Top 6 inches	Top 3 inches
S1, min	0	0	0	0	0	0	0	0	0
S1, max	13790	4182	3076	11714	4422	3011	11921	4573	3192
S2,min	-68	-68	-68	-57	-58	-58	-46	-46	-46
S2,max	2843	4	4	2395	44	44	2445	94	94
S3,min	-8029	-4177	-3071	-6707	-4417	-3006	-6793	-4568	-3244
S3,max	0	0	0	0	0	0	0	0	0
Sx, min	-6809	-282	-282	-5782	-105	-105	-5885	-104	-104
Sx, max	12735	17	17	10860	47	47	11048	105	105
Sy, min	-8028	-4177	-3071	-6706	-4417	-3006	-6793	-4568	-3244
Sy, max	9903	4182	3076	8330	4422	3011	8779	4573	3192

The minimum tensile and compressive stresses occur in design B, but are comparable to the stresses in design C. Assuming that one of these designs will be used and that design C is easier to manufacture, additional evaluations were made using flange design C.

Table B4 gives the results for pulse stresses at ambient, 1000°F and 1600°F in design C, for each of the 3 ceramic materials being evaluated, with the assumption that the pulse gas temperature is approximately the same as the process gas temperature. The stresses in the table are for the top 3 inches of the filter.

Table B4 - Pulse Stresses with Flange C Design and Three Ceramic Materials

	Pall			Blasch			McDermott		
Stress	ambient	1000°F	1600°F	ambient	1000°	1600°	ambient	1000°	1600°
S1, min	0	0	0	0	0	0	-640	-638	-637
S1, max	3186	3264	3288	3026	3082	3121	3160	3148	3226
S2, min	-55	-20	-35	-81	-286	-465	-844	-841	-1159
S2, max	99	83	74	107	129	159	1041	1037	1156
S3, min	-3236	-3314	-3337	3079	-3134	-3182	-2740	-2730	-4183
S3, max	0	0	0	0	0	0	997	993	992
Sx, min	-103	-134	-211	-173	-606	-992	-771	-1524	-2496
Sx, max	112	105	171	138	761	1235	1399	1617	2668
Sy, min	-3236	-3314	-3337	-3079	-3134	-3172	-2609	-2601	-2749
Sy, max	3186	3264	3288	3026	3082	3121	2757	2750	3120

The material properties used were:

	Pall 326	Blasch	McDermott
Young's Modulus (psi)	5.e6	2.15e6	1.61e6
Poisson's Ratio	0.16	0.18	0.99
Coeff. Of Therm. Exp. (in/in/°F)	2.7e-6	3.6e-6	4.1e-6
Thermal Conductivity (Btu/sec-in-°F)	7.36e-5	7.36e-5	3.3e-6

Evaluation of thermal growth differences

Since the gasket material properties and behavior are unknown, the effect of the thermal growth was evaluated in several ways:

1) The relative growth of the filter and the bracket was calculated. This gives a difference against which the growth and recovery from compression of the gasket may be compared.
2) A closed system was analyzed, with assumed material properties for the gasket, comparing the differences in stresses at different temperatures.
3) For the assumption that the gasket is keeping the bracket away from the wall, the temperature at which the bolt pre-load becomes zero was calculated, along with the growth beyond that temperature.

Relative Growth

Table B5 shows the thermal growth at 1000°F, using the thermal coefficients of expansion of 9.9e-6, 2.6e-6, 3.2e-6, and 3.8e-6 in/in/°F for 304 stainless, Pall 326, Blasch, and McDermott, respectively, with the three different flange geometries.

Table B5 - Thermal Growth at 1000°F

Design	Filter material.	ΔL (bracket)	ΔL (filter)	Difference
A	Pall	0.012706	0.002519	0.010058
A	Blasch	0.012706	0.0031	0.008895
A	McDermott	0.012706	0.003681	0.007733
B	Pall	0.012429	0.002731	0.008924
B	Blasch	0.012429	0.003361	0.007664
B	McDermott	0.012429	0.003991	0.006403
C	Pall	0.012337	0.014386	0.009187
C	Blasch	0.012337	0.014386	0.007988
C	McDermott	0.012337	0.014386	0.006788

Table B6 lists the growth at 1600°F, assuming a 70°F ambient, and using the thermal coefficients of expansion of 10.5e-6, 2.7e-6, 3.6e-6, and 4.1e-6 in/in/°F for 304 stainless, Pall 326, Blasch, and McDermott, respectively.

Table B6 - Thermal Growth at 1600°F

Design	Filter material	ΔL (bracket)	ΔL (filter)	Difference
A	Pall	0.02217	0.004303	0.017867
A	Blasch	0.02217	0.005737	0.016433
A	McDermott	0.02217	0.006534	0.015636
B	Pall	0.021688	0.004666	0.017022
B	Blasch	0.021688	0.006221	0.015467
B	McDermott	0.021688	0.007085	0.014603
C	Pall	0.021527	0.004441	0.017086
C	Blasch	0.021527	0.005921	0.015606
C	McDermott	0.021527	0.006743	0.014784

As can be seen in the tables, the potential gap is greatest for the Pall filters, with a difference of up to 0.018 inches in the thermal growth of the inner bracket length and the filter top length. These numbers would only result in gaps of this size if the gasket materials did not grow thermally or had no recovery from compression. If the expected growth and recovery is at least 0.018 inches, there should be no gap.

136

Thermal Stresses

In the evaluation of the thermal stresses, the finite element model was setup to use contact elements and springs to maintain the appropriate component positions. The results for the models which include pulse pressure are in the previous section. The following results show the effects of just the thermal differences, with results at 1000°F and at 1600°F. The stresses in Table B7 are for the top three inches of the sheet filter, to focus on the differences due to the material and to avoid the issues associated with the ribs

Table B7- Sheet Filter Stresses in Top 3-inches

	Pall		Blasch		McDermott	
Stress	1000°F	1600°F	1000°	1600°	1000°	1600°
S1, min	0	0	0	0	-288	-477
S1, max	299	489	1320	2172	1957	3214
S2, min	-21	-34	-281	-462	-704	-1161
S2, max	45	74	51	84	705	1161
S3, min	-212	-348	-1198	-1972	-2538	-4188
S3, max	0	0	0	0	572	942
Sx, min	-126	-207	-602	-990	-1631	-2676
Sx, max	104	171	748	1230	1598	2629
Sy, min	-107	-176	-1037	-1706	-1453	-2422
Sy, max	256	421	624	1026	1866	3066

Loss of Pre-load

A torque of 20 in-lb is typically applied to bolts during fixturing of filter elements. The 20 in-lb on the bolts can be evaluated as a deflection in the bolt, using the equation

$$\delta = P\,L\,/\,A\,E$$

Since the torque calculations showed that the force is 400 lb for 20 in-lb torque, the elongation of the bolt is:

$$\delta = 400 \text{ lb x .75 in} / (\pi\, .1887^2 \text{ in}^2 \text{ x 28e6 psi})$$

$$= .000096 \text{ inches}$$

This deflection corresponds to a temperature change of 13°F, from

$$\delta = \alpha\,L\,\Delta T$$

As a relative change in growth, the elongation of 0.000338 inches is about 1% of the differential growth for the Pall filter, design A, indicating that the preload will be lost relatively quickly as the system is heated.

Evaluation of Results

The Pall 326 as-manufactured material has strength which is more favorable than the other two materials considered, and for the most part, the stresses from the thermal and pulse

loads do not exceed the Pall 326 limits. The exception is the burst pressure, which is exceeded in the pulse conditions. The Blasch and McDermott materials exceed the compressive, tensile, and hoop strengths for both thermal and pulse conditions. They also fail to meet the burst strength.

While more complete modeling may, with the inclusion of ribs, tend to reduce the stresses, the improvements are likely to be relative, and the Pall filter material is the most promising. Although the thermal growth difference is greater with the Pall, this difference is within 3 mils.

Three-Dimensional Evaluation of Clamping

Based on the information from the two-dimensional model, a three-dimensional model was built to allow further comparison of the stresses for various conditions. To simplify the model and reduce the number of elements, the filter was represented by a combination of solid and shell elements.

The geometry of flange design C was used in the construction of the 3-D model. The initial model did not include any ribs, so that the results could be compared with the results of the 2-D model. Using Pall material properties, the full length 3-D filter model evaluated at ambient temperatures had the following stress ranges, with the maximum values generally occurring at the bottom of the filter or at the radius at the top:

S_1 0 to 13027 psi
S_2 -1089 to 2382 psi
S_3 -4099 to 1451 psi
S_x -3381 to 12976 psi

The stresses at the top of the filter, near the middle of the filter, should compare most closely to the top three inches of the 2-D filter model's stresses. The stress ranges for this region in the 3-D evaluation were as follow:

S_1 -7 to 3125 psi
S_2 -1089 to 330 psi
S_3 -5685 to 0 psi
S_y -2073 to 1637 psi

The S_1 for the 2-D model, with a range of 0 to 3186, compares well with that of the 3-D model. The S_2 and the S_3 values, however, are considerably higher for the 3-D model, although the S_y values are lower for the 3-D model. The most extreme values in S_2 and S_3 occur at the transition between solid and shell elements, and may be due to the model rather than to the actual loads in the filter.

Note on model: The number of elements used result in over 2 gigabytes of disk usage (more than half the hard disk space) during the analysis. While smaller elements would be better, the model is limited somewhat by the computer. Still, a relative evaluation may be made using the coarse model, and trouble areas may be modeled separately for more accurate evaluation. In these cases the results from the coarse model can provide information which allows appropriate constraints and loads to be placed on the finer model without requiring the complete model.

With a rib-less model analyzed, the next step was to analyze a model with ribs. The model used the assumption that 3 ribs would be used in the filter. The results of the analysis for the full length filter had the following stress ranges for the Pall material model:

S_1 -52 to 647 psi
S_2 -113 to 356 psi
S_3 -554 to 112 psi

For the top 3 inches of the filter, this time including the rounded end, the stress ranges are as follow:

S_1 -13 to 624 psi *
S_2 -113 to 356 psi *
S_3 -519 to 112 psi

*The S_1 maximum stresses occur where modeling anomalies are affecting the results, more accurate modeling may give a maximum more on the order of 400 -450 psi. The S_2 tensile peak is also occurring at one of these locations.

As a result of the 3-D modeling, the stresses in the filters are sufficiently reduced by the effects of the ribs that the material limits are more easily avoided. The stresses in the flange are low, and, with the ribs in place, the limiting stresses are along the ribs, and may be calculated using plate equations. The equations are in the form

Max $\sigma = - \beta \, q \, b^2 / t^2$

where b is the width, t is the thickness, β is a function of the plate aspect ratio, and q is the pressure.

As can be seen, the stresses from the pressure are independent of the material properties, so the stresses calculated may be directly compared to the allowable stresses for the material.

Conclusions

The sheet filter stresses, using the three alternative flange shapes identified, are not too sensitive to the flange shape, and the flange shape selection should be made based on ease of manufacturing. The Pall 326 material sheet filter preliminary design, with wall thickness of 0.3" and three internal ribs, appears to be acceptable from this evaluation. Similar evaluations performed to estimate acceptable design features for the other two ceramic materials (Blasch, and McDermott) have shown that with the internal ribs (2) the material properties are not critical, and the same plate thickness (0.3") should be sufficient with respect to pulse pressure stresses.